



MULTIPERIOD MODELLING PLANNING AND PRODUCTIVITY AND ENERGY EFFICIENT ASSESSMENT OF AN INDUSTRIAL GASES FACILITY

David Fernández Linares

ADVERTIMENT. L'accés als continguts d'aquesta tesi doctoral i la seva utilització ha de respectar els drets de la persona autora. Pot ser utilitzada per a consulta o estudi personal, així com en activitats o materials d'investigació i docència en els termes establerts a l'art. 32 del Text Refós de la Llei de Propietat Intel·lectual (RDL 1/1996). Per altres utilitzacions es requereix l'autorització prèvia i expressa de la persona autora. En qualsevol cas, en la utilització dels seus continguts caldrà indicar de forma clara el nom i cognoms de la persona autora i el títol de la tesi doctoral. No s'autoritza la seva reproducció o altres formes d'explotació efectuades amb finalitats de lucre ni la seva comunicació pública des d'un lloc aliè al servei TDX. Tampoc s'autoritza la presentació del seu contingut en una finestra o marc aliè a TDX (framing). Aquesta reserva de drets afecta tant als continguts de la tesi com als seus resums i índexs.

ADVERTENCIA. El acceso a los contenidos de esta tesis doctoral y su utilización debe respetar los derechos de la persona autora. Puede ser utilizada para consulta o estudio personal, así como en actividades o materiales de investigación y docencia en los términos establecidos en el art. 32 del Texto Refundido de la Ley de Propiedad Intelectual (RDL 1/1996). Para otros usos se requiere la autorización previa y expresa de la persona autora. En cualquier caso, en la utilización de sus contenidos se deberá indicar de forma clara el nombre y apellidos de la persona autora y el título de la tesis doctoral. No se autoriza su reproducción u otras formas de explotación efectuadas con fines lucrativos ni su comunicación pública desde un sitio ajeno al servicio TDR. Tampoco se autoriza la presentación de su contenido en una ventana o marco ajeno a TDR (framing). Esta reserva de derechos afecta tanto al contenido de la tesis como a sus resúmenes e índices.

WARNING. Access to the contents of this doctoral thesis and its use must respect the rights of the author. It can be used for reference or private study, as well as research and learning activities or materials in the terms established by the 32nd article of the Spanish Consolidated Copyright Act (RDL 1/1996). Express and previous authorization of the author is required for any other uses. In any case, when using its content, full name of the author and title of the thesis must be clearly indicated. Reproduction or other forms of for profit use or public communication from outside TDX service is not allowed. Presentation of its content in a window or frame external to TDX (framing) is not authorized either. These rights affect both the content of the thesis and its abstracts and indexes.

Multiperiod modelling planning and productivity and energy efficient assessment of an industrial gases facility

David Fernández Linares



DOCTORAL THESIS

2018

UNIVERSITAT ROVIRA I VIRGILI
MULTIPERIOD MODELLING PLANNING AND PRODUCTIVITY AND ENERGY EFFICIENT ASSESSMENT OF AN INDUSTRIAL GASES
FACILITY

David Fernández Linares

UNIVERSITAT ROVIRA I VIRGILI
MULTIPERIOD MODELLING PLANNING AND PRODUCTIVITY AND ENERGY EFFICIENT ASSESSMENT OF AN INDUSTRIAL GASES
FACILITY

David Fernández Linares

UNIVERSITAT ROVIRA I VIRGILI
MULTIPERIOD MODELLING PLANNING AND PRODUCTIVITY AND ENERGY EFFICIENT ASSESSMENT OF AN INDUSTRIAL GASES
FACILITY

David Fernández Linares

David Fernández Linares

Multiperiod modelling planning and productivity and energy efficient assessment of an industrial gases facility

Doctoral Thesis

Supervised by:

Dr. Laureano Jiménez Esteller

Dr. Carlos Pozo Fernández

Dr. Gonzalo Guillén Gosálbez



DEPARTMENT OF CHEMICAL
ENGINEERING

MESSER IBÉRICA DE GASES S.A.U.

SUSCAPE Research Group



UNIVERSITAT
ROVIRA I VIRGILI

TARRAGONA

2018

UNIVERSITAT ROVIRA I VIRGILI
MULTIPERIOD MODELLING PLANNING AND PRODUCTIVITY AND ENERGY EFFICIENT ASSESSMENT OF AN INDUSTRIAL GASES
FACILITY

David Fernández Linares



ESCOLA TÈCNICA SUPERIOR D'ENGINYERIA QUÍMICA
DEPARTAMENT D'ENGINYERIA QUÍMICA

Av. Països Catalans, 26

Campus Sescelades

43007 Tarragona (Spain)

<http://www.etseq.urv.es/deq/>

I STATE that the present study, entitled “Multiperiod modelling planning and productivity and energy efficient assessment of an industrial gases facility” and presented by David Fernández Linares for the award of the degree of Doctor, has been carried out under our supervision at the Department of Chemical Engineering of this university.

Tarragona, 18th July 2018

Doctoral Thesis Supervisor/s

Dr. Laureano Jiménez

Esteller

Dr. Carlos Pozo

Fernández

Dr. Gonzalo Guillén

Gosálbez

Aquesta tesi s'ha realitzat amb el suport de la Secretaria d'Universitats i

Recerca del Departament d'Empresa i Coneixement de la

Generalitat de Catalunya



Generalitat de Catalunya
Departament d'Economia i Coneixement
Secretaria d'Universitats i Recerca

Agradecimientos

Para empezar, quisiera expresar mi más sincero agradecimiento a todas las personas que han estado presentes durante el desarrollo de esta tesis. Aunque muchas de ellas no estén aquí citadas explícitamente, agradezco su ayuda, dedicación y apoyo, ya que de una forma u otra han contribuido a la realización de esta tesis.

Asimismo, quiero dar las gracias a mis supervisores de tesis: Dr. Laureano Jiménez Esteller, Dr. Gonzalo Guillén Gosálbez y Dr. Carlos Pozo Fernández. Ellos me ofrecieron la posibilidad de realizar este trabajo de doctorado y me han orientado y aconsejado constantemente. Me han demostrado su gran profesionalidad y agradezco todo el conocimiento que me han transmitido durante este tiempo. También doy las gracias al Sr. Rubén Folgado Girón, mi supervisor por parte de la empresa y la persona que me animó a realizar este doctorado industrial. Del mismo modo, quiero agradecerle a él y a José Manuel Montoro, toda la confianza que han depositado en mí desde que empecé a trabajar en Messer Ibérica de Gases S.A.U., permitiendo mi desarrollo profesional dentro de la empresa. Al mismo tiempo, quiero expresar mi gratitud a todo el personal de Messer Ibérica de Gases S.A.U. que me ha ayudado y apoyado durante el desarrollo de la tesis. Especialmente a mis compañeros del área de producción por su soporte y compañerismo durante todo este tiempo. Agradezco también la colaboración de todos los miembros del grupo de investigación SUSCAPE de la Universitat Rovira i Virgili. A pesar de no haber podido estar muy presente en su día a día, he podido aprender mucho de sus conocimientos.

Esta tesis va dedicada especialmente a mi familia. Primeramente a mis padres, Enrique y Rosario, por inculcarme desde pequeño los valores de la perseverancia y el esfuerzo y por estar presentes en todo momento. También a mi hermano Daniel, que me ha ayudado a no bajar nunca los brazos. Gracias también a mis abuelos por el ejemplo y el cariño que me dan, y a mis tías Elena y Petri por la energía positiva que

siempre me han transmitido. Por último, doy las gracias a mi novia Olivia por estar a mi lado en los momentos buenos y malos, y por hacer que el camino hasta este día haya sido mucho más fácil.

A todos vosotros muchas gracias.

Summary

Climate change, air pollution and non-renewable resources depletion are the main threats facing humanity in the 21st century. The growth of energy demand and the continuous technological development of society are surpassing the environmental limits of our planet. Without adequate measures, this situation can lead to serious problems that could cause irreversible damages to the environment and the well-being of humanity.

The industrial sector is the largest energy consumer, with about one-third of global energy demand. Globally, the use of energy represents the largest source of greenhouse gas emissions, which are linked to burning fossil fuels to produce energy. In Europe, the energy processes are the largest emitters of greenhouse gases, being responsible for 78% of total European emissions in 2015 (European Environment Agency, 2017). There is an evident relationship between electric power consumption and climatic change (Ghulam *et al.*, 2014), thus the challenge of mitigating climate change will not only imply changes in regulations, lifestyles and consumption habits, but also the industrial sector will play a crucial role. In this sense, the current use of energy in industry can be improved creating great opportunities for energy savings and, simultaneously, reduce its environmental impact.

Energy efficiency stands as a new competitiveness factor in the industry, and goes through the transition of the model based on greater consumption and dependence of resources to another whose priority is the reduction of the energy needed to produce goods and services. In this sense, it is essential to obtain information derived from research and scientific analysis that allows developing solutions focused on the reduction of energy costs. This thesis has dealt with the needs of a segment of the industry, specifically the production of industrial gases, by creating tools based on mathematical optimization models which allow much more agile and effective operational decision makings as well as the detection of areas for energy improvement.

In this line, energy management should be regarded as an investment that will be amortized with energy savings, reduction of polluting emissions, lower consumption of hydrocarbons and improvement of industrial processes. With this contribution, we will try to address all these aspects proposing new tools to encourage and move towards a more efficient industry that allows a more sustainable future.

Two main contributions are derived from this thesis. On the one hand, it creates a multiperiod optimization tool that allows to obtain the optimal operational configuration (from the economic and energetic point of view) of an industrial gas manufacturing process, taking into account all the variables that affect the system. On the other hand, a methodology named Data Envelopment Analysis is used to compare different industrial gas production units, identifying inefficiency sources and making recommendations to adopt the best practices.

Summarizing, this thesis offers a set of practical and effective tools that support the decision making process in industrial activities and allows the identification of opportunities for energy improvement. Contributions extracted from this thesis, although may seem minuscule in the face of the great challenge of curbing the environmental threat, will help move towards a more efficient industrial sector in which the decline in energy demand is going to become a structural phenomenon.

Resumen

El cambio climático, la contaminación atmosférica y el agotamiento de recursos no renovables son las principales amenazas a las que se enfrenta la humanidad en el siglo XXI. El crecimiento de la demanda energética y el continuo desarrollo tecnológico de la sociedad está sobrepasando los límites medioambientales de nuestro planeta. Sin las medidas adecuadas, esta situación puede derivar en graves problemas que podrían ocasionar daños irreversibles para el medioambiente y el bienestar de la humanidad.

El sector industrial es el mayor consumidor de energía, con alrededor de un tercio de la demanda energética global. A nivel mundial, el uso de la energía representa la mayor fuente de emisiones de gases de efecto invernadero, ya que éstas están vinculadas a la quema de combustibles fósiles para producir energía. En Europa, los procesos energéticos son los mayores emisores de gases de efecto invernadero, siendo responsables del 78% del total de emisiones europeas en 2015 (European Environment Agency, 2017). Existe una relación evidente entre el consumo de energía eléctrico y el cambio climático (Ghulam *et al.*, 2014), por lo que el reto de mitigar el cambio climático comportará, no sólo modificaciones en normativas, estilos de vida y hábitos de consumo, si no que el sector industrial tenga también una labor crucial. En este sentido, el uso actual de la energía en la industria es mejorable, ofreciendo grandes oportunidades de ahorro energético y reduciendo, además, su impacto medioambiental.

La eficiencia energética se erige como un nuevo factor de competitividad en la industria que pasa por lograr la transición del modelo actual, basado en un mayor consumo y dependencia de los recursos, a otro cuya prioridad sea la reducción de la energía necesaria para producir bienes y servicios. Para esto, es básico obtener información derivada de la investigación y el análisis científico que permita desarrollar soluciones con un nuevo paradigma que esté enfocado a la reducción de costes energéticos. Esta tesis ha tratado las necesidades de un segmento de la industria, concretamente la producción de gases industriales, mediante la creación de

herramientas basadas en modelos matemáticos de optimización que permiten una toma de decisiones operativas de una forma ágil y eficaz, así como la detección de posibilidades de mejora energética.

En esta línea, la gestión energética debe considerarse como una inversión que se amortizará con los ahorros de energía, la reducción de emisiones contaminantes, el menor consumo de hidrocarburos y la mejora de los procesos industriales. Con esta contribución se intenta abordar todos estos aspectos proponiendo nuevas herramientas para incentivar y avanzar hacia una industria más eficiente que permita un futuro más sostenible.

De esta tesis se derivan dos contribuciones principales. Por un lado se crea una herramienta de optimización multiperiodo que permite obtener la configuración operacional óptima (desde el punto de vista económico y energético) de un proceso de fabricación de gases industriales, teniendo en cuenta todas las variables que afectan al sistema. Por otro lado, se usa una metodología de análisis envolvente de datos (Data Envelopment Analysis) para el estudio de diferentes unidades de producción de gases industriales. Esta metodología permite comparar las plantas entre sí, evaluar sus parámetros y realizar recomendaciones para aumentar su eficiencia.

En resumen, esta tesis ofrece un conjunto de herramientas prácticas y eficaces que apoyan al proceso de toma de decisiones en actividades industriales y permite la identificación de oportunidades de mejora energética. Las contribuciones extraídas de esta tesis, aunque pueden parecer minúsculas frente al gran desafío de frenar la amenaza medioambiental, ayudan a avanzar hacia un sector industrial más eficiente dentro de un modelo industrial en el que el descenso de la demanda energética va a convertirse en un fenómeno estructural.

Contents

1. Introduction	1
1.1. Background and motivation.....	1
1.2. Objectives	6
1.3. Industrial gases	7
1.3.1. Brief history.....	9
1.3.2. Air Separation Process	11
1.4. Decision making tools	22
1.5. Mathematical programming	24
1.5.1. Objective optimization problems	25
1.5.1. Multiperiod optimization problems.....	29
1.5.2. Data Envelopment Analysis	30
1.5.3. Malmquist Productivity Index.....	37
1.6. Outline: problems addressed	41
1.6.1. Multiperiod optimization (Article 1, Chapter 2)	41
1.6.2. Data Envelopment Analysis and Malmquist Productivity for efficiency assessment (Article 2, Chapter 3)	42
1.7. Conclusions	43
1.8. Future work	44
1.9. Nomenclature	46
1.10. References	48
2. Optimal operation planning in industrial gases production.....	57
2.1. Introduction	57

2.2. Problem Statement.....	62
2.2.1. Process Description	62
2.2.2. Problem Definition	65
2.3. Mathematical Formulation: Deterministic Model	66
2.3.1. Mass-balance constraints.....	66
2.3.2. Capacity constrains.....	68
2.3.3. Utility consumption.....	75
2.3.4. Objective function	79
2.4. Case studies	82
2.4.1. Case study 1: Electrical periods	83
2.4.2. Case study 2: Demand variability.....	89
2.5. Conclusions	94
2.6. Nomenclature	95
2.7. References	101
3. Data Envelopment Analysis and Malmquist Productivity Index for efficiency assessment	109
3.1. Introduction	109
3.2. Methodology.....	113
3.2.1. Fundamentals of DEA.....	113
3.2.2. Fundamentals of Malmquist Productivity Index	119
3.3. Case study: industrial air separation units	126
3.3.1. Results and discussion.....	132
3.4. Conclusions	144
4. Appendix	157
4.1. Short CV.....	157

4.2. List of publications	159
4.2.1. Indexed journals	159
4.2.2. Other publications	159
4.3. Conferences	160
4.3.1. Oral communications	160
4.3.2. Poster presentations	160

Chapter 1.

Introduction

UNIVERSITAT ROVIRA I VIRGILI
MULTIPERIOD MODELLING PLANNING AND PRODUCTIVITY AND ENERGY EFFICIENT ASSESSMENT OF AN INDUSTRIAL GASES
FACILITY

David Fernández Linares

1. Introduction

1.1. Background and motivation

The world is currently faced with challenges in all three dimensions of sustainable development: economic, social and environmental. Millions of people are still living in extreme poverty, income inequality among countries is steadily growing and unsustainable consumption and production patterns have resulted in high economic and social costs and may endanger humans welfare. The satisfaction of the “Triple Bottom Line” aspects (Savitz and Weber, 2006) will require global actions to further economic and social progress while strengthening environmental protection. The efforts to address sustainability will be crucial and would benefit both the society and the environment by identifying proactive pathways towards sustainability. In this framework, research based information facing such problems may play a major role in decision and policy-making support to accelerate the effective shift toward a sustainable development.

Industrial energy use accounts for 40% of global electrical usage (Enerdata, 2017) and is a substantial contributor to CO₂ emissions causing global warming (EIA, 2017). The possibilities for improving the energy efficiency of industrial facilities are notorious, even in mature industries and technologies. Energy use in industry differs from energy use in commercial and residential sectors, since industrial sites are very large individual energy users which may change production volumes, schedules and the type of manufactured product many times during the useful life of the factory. Furthermore, industries are striving to improve the efficiency of their processes, which has led to the reduction of the energy use per unit of economic output in nearly 20% between 2000 and 2016 (IEA, 2017).

This thesis points towards one of the main structural transformation needed to reconnect the human development to sustained progress (Rockström *et al.*, 2013), the *energy transformation* (Riahi *et al.*, 2012; Tester *et al.*, 2005, Van Vuuren *et al.*, 2012). In essence, energy transformation supports the shift towards an environmentally

friendly economy to prevent exceeding the Earth limits, which would result in an irreversible situation threatening human well-being and the environment equilibrium (Rockström *et al.*, 2009 and Steffen *et al.*, 2015).

Specifically, this thesis is focused in the cryogenic air separation technology, which is currently the only practical technology available for mass-production of air products such as oxygen, nitrogen and argon (Smith and Klosek, 2001). A high number of industries such as steel, petrochemical, metallurgy, medical or food demand large amounts of these air products. Inherent to its operation, cryogenic air separation plants are in general energy intensive, with the power input being the main factor on which the ultimate production cost will depend. Experience has shown that relatively small improvements in energy efficiency on these plants generally result in significant reduction of production cost. This dissertation discusses the means for effective energy management at these plants aimed at ultimately minimizing the energy consumption. Furthermore, this would not only bring down the electrical cost per amount of product obtained, but also reduce the overall environmental impacts (*e.g.*, CO₂ and greenhouse gas emissions) derived from the lower usage of energy resources.

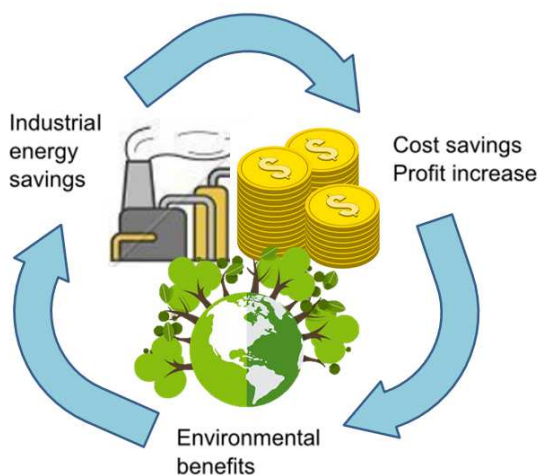


Figure 1.1. Industrial energy savings bring cost savings (profit increase in companies) and environmental benefits.

This thesis aims to give decision and policy makers methods and tools to improve the energy efficiency in energy-intensive consumers and, in this way, contribute to the

global energy transformation required for a more sustainable world. Note that in the present contribution no environmental criterion has been considered explicitly, yet they have been implicitly addressed through energy management, since the cost in these processes is energy driven.

This thesis has been done within the framework of the “Industrial Doctorates Plan” developed by the Generalitat de Catalunya with the aim of contributing to the industry competitiveness. The essential element of the industrial doctorate process is that the research project is carried out within a company (in this case Messer Ibérica de Gases S.A.U), where the doctoral student further develops its research in collaboration with a university (in this case Universitat Rovira i Virgili). Therefore, the industrial doctorate act as a bridge for knowledge transfer between industry and university. In this context, the mathematical models posed in the following sections represent real facilities and, thus, their formulation allows to optimize existing industrial activities and provide solutions for plant managers and/or decision makers. Results are presented in such a way that the confidential agreement is not violated.

Despite there is a large number of approaches to solve the emerging problems, mathematical optimization/programming appears as an effective tool to find the best solution to them. For this reason, it has been widely used to aid decision-making in many scientific or engineering problems. Mathematical programming allows solving real problems by building a model based on equations, which are later solved with the proper solver alternatives.

In the cryogenic air separation field, the complexity of optimally managing this kind of facilities is very high due to the interactions between process variables (*e.g.*, flow rates, levels, quality requirements, etc.), utilities and product prices, fluctuations in customers’ product demand, electricity varying prices, etc. In order to deal with this complexity, we developed a tailored multiperiod model, taking the form of a mixed-integer linear programming (MILP) problem, which was applied to the Messer plant located in Tarragona. This model allows to determine the optimal production schedule of an industrial cryogenic air separation process so as to maximize the net profit by minimizing energy consumption [1]. In the context of cryogenic air separation, some tools were presented to determine the optimal operating schedule depending on the

power costs (Ierapetritou *et al.*, 2002), as well as depending on demand, contractual obligations and variable electricity pricing (Zhu *et al.*, 2011). These works simplify the models to keep a manageable size by means of reductions in the number of periods and abbreviating the linear models, and they also assume non-realistic product demand and power pricing. The work of this thesis [1], extends previous proposals increasing the granularity in the modeling of the electricity price pattern in order to account for hourly variations considering electricity markets peculiarities, and including real demand levels (both for gas and for liquid) when optimizing the production schedule. Furthermore, the network boundaries of the air separation process are amplified by including the complete system: production, compression, liquefaction, storage and delivery. The model formulation is further complemented with the possibility to purchase a certain amount of product from an external supplier by means of economical and power pricing contracts, thereby offering the possibility to achieve significant reductions in operational costs if properly managed. Finally, the model also takes into account idle times occurring during equipment start-ups (until the desired product loads and purities are reached).

The proposed model [1] allows to optimize the *operation* of a given facility, yet it cannot identify other inefficiency sources arising for instance from its *design*. Therefore, additional tools are required to identify further inefficiency sources in air separation units. To this end, we also present the application of a standard mathematical programming method (Data Envelopment Analysis) to compare the relative performance of a set of Air Separation Units (ASUs) according to energy efficiency and productivity criteria [2]. The dataset considered in this case study includes a great number of Messer plants worldwide. As demonstrated in this thesis, this tool provides insight on how to improve the efficiency of inefficient facilities by identifying inefficiency sources and reference facilities that could be used for benchmarking. Figure 1.2 summarizes the work done in this thesis.

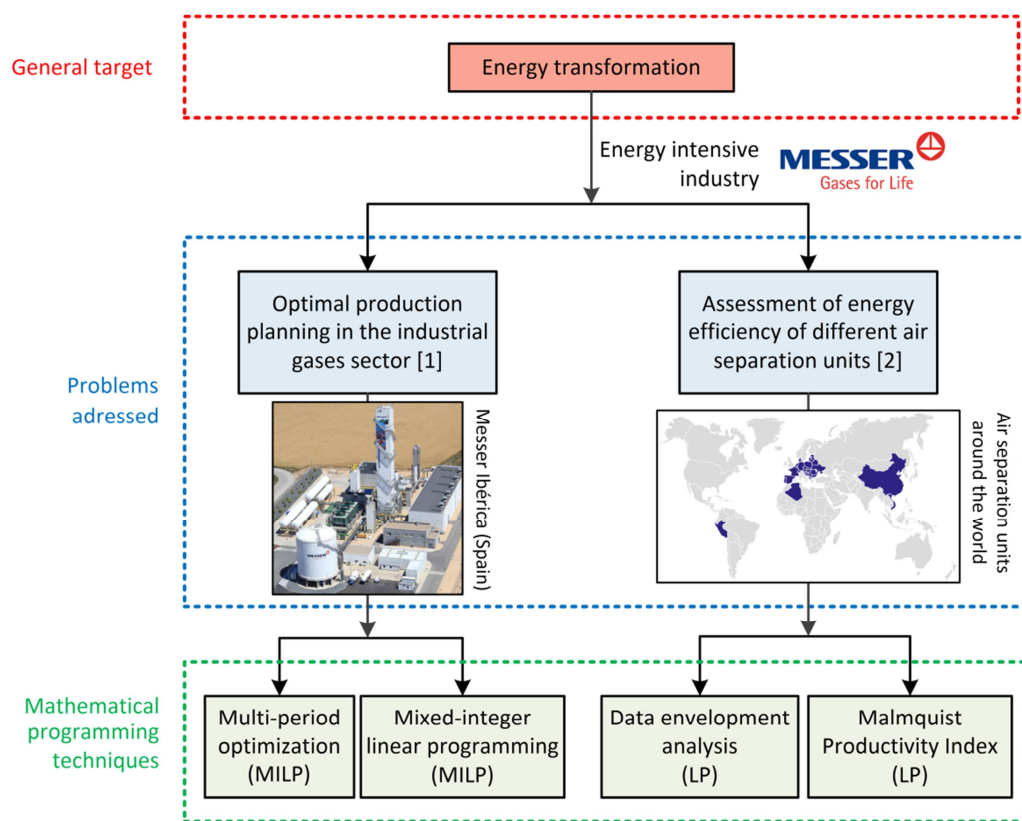


Figure 1.2. Thesis roadmap.

This PhD thesis is divided in three main chapters. Chapter 1 introduces the problems addressed, the main objectives to achieve and a general background of the mathematical programming techniques used. The main conclusions, future work and references are presented as well. Chapters 2 and 3 describe in further detail the two decision-aided tools used to solve each particular problem. Specifically, Chapter 2 presents the multi-period optimization tool developed to increase the final profit (which implies energy savings) in an energy-intensive process producing industrial gases, while Chapter 3 presents the application of Data Envelopment Analysis for the assessment of the energy efficiency of several air separations units. Finally, Chapter 4 presents a brief curriculum vitae of the PhD student, the main contributions published during the thesis period as well as the works that have been presented in oral communications.

1.2. Objectives

As previously described, the aim of this thesis is to contribute in the efficient use of energy resources in industry as well as to identify opportunities to reduce their energy consumption and boost their competitiveness, while simultaneously reducing their environmental impact. To this end, the main goal is to develop mathematical programming tools to solve real problems in an industrial framework related with process management. These tools will find alternatives and improvements in the industrial process that can result in significant economic and environmental benefits which could be hard to identify otherwise by using standard heuristics or rules of thumb.

Several particular objectives are identified as necessary to achieve the overall goal:

- To formulate a deterministic multi-period optimization model capable of determining the operation of the air separation network (*i.e.*, equipment startup and shutdown times, stream flow rates, product purchases to external suppliers, etc.) that optimizes its economic performance. This model has to improve current models in several areas such as scope, granularity, consideration of idle times, etc. to be more realistic. This tool will assist engineers in their daily activities by effectively optimizing production planning, energy rules, sales and product stocks, while simultaneously considering external constraints and dynamic market conditions.
- To apply a Data Envelopment Analysis (DEA) model to assess the performance of a set of air separation units with the aim of identifying the best ones according to energy efficiency and productivity criteria and define improvement targets for those found inefficient.
- To apply the Malmquist Productivity Index (MPI) to analyze the temporal evolution of the efficiency scores of the air separation units to provide insight on efficiency changes and detect those plants showing larger improvements in the recent past.
- To demonstrate the capabilities of the tools and methodology developed through their application to existing plants.

1.3. Industrial gases

The term industrial gases refers to all gases produced at large scale (*e.g.*, nitrogen, oxygen, argon, xenon, hydrogen, carbon dioxide, acetylene, ethylene, ammonia, etc.) which are manufactured for a broad use in industry. On the basis of their application, the industrial gases market is highly segmented, where the main sectors covered are: chemical, petrochemical, automotive, metallurgy, energy and oil & gas, transportation, food, medical, pharmaceutical, among others. Metallurgy industry is currently the segment dominating this market and it is expected that it will maintain its dominance over the next years. Industries use these gases in a great range of applications: medical gases, cutting and welding, refrigeration or food processing and packaging, etc. For instance, oxygen is used in many oxidation reactions in the chemical industry, in sewage treatment plants, in chemical synthesis, in burners to supplement or replace air, in the transportation of live fish, in hospitals for assisted breathing, etc.; nitrogen is used in the chemical industry for blanketing, in purging and pressure transfer of flammable chemicals, as a purge gas, in freeze and protect food, in cryogenic grinding of plastics, in cryosurgery, etc.; and argon is used as a shielding gas for arc welding, as carrier gas in gas chromatography, in filling incandescent lamps, etc.

The industrial gas industry is relatively stable in economic terms (as shown in Figure 1.3), since this market has a diversified end-customer industries and most industrial gases are not easily replaceable in production processes as they offer quality and productivity gains (Research and markets, 2017).

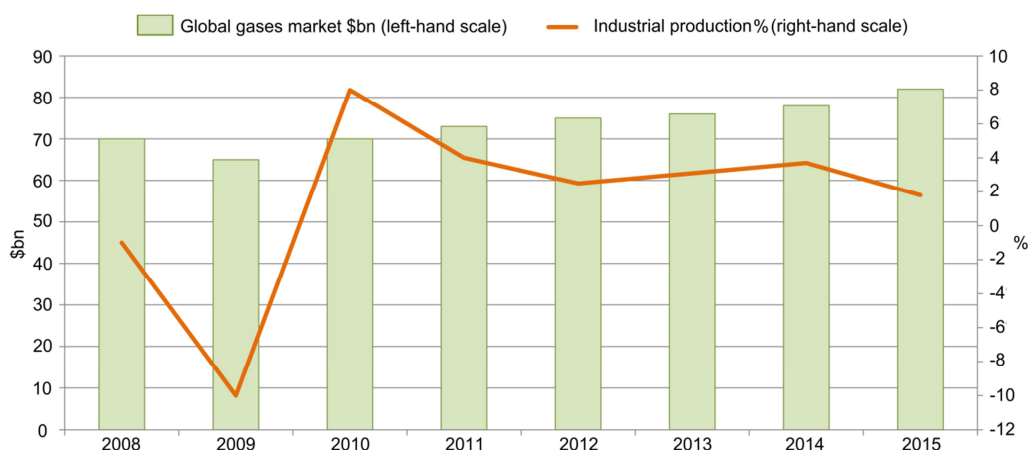


Figure 1.3. Global industrial gases market. Adapted from Eurostat.

The global market for industrial gases is expected to grow over the next few years as a result of the strong demand from various end-use industries (especially in energy and oil & gas sectors). A Compound Annual Growth Rate (CAGR) of 7.7% is estimated for the period between 2017 and 2025, reaching 114.5\$bn in revenue in 2025 (Persistence Market Research, 2018).

By product type, industrial gases market includes oxygen, nitrogen, helium, acetylene, argon, hydrogen, carbon dioxide and others (krypton, xenon, methane, carbon monoxide, etc.). In 2017, the hydrogen gas segment market was the dominant in terms of revenue contribution, and it is expected to further remain dominant during the period from 2017 to 2025.

Regarding regions, Europe and Asia Pacific showed the largest market for industrial gases in 2016, while Asia Pacific, China and India are the regions expected to show a higher market potential for industrial gases in the next ten years (Persistence Market Research, 2018).

By companies, Air Liquide S.A., Linde Group and Praxair Inc. are the three major players in the industrial gases market, with a collective market share of more than 50%. In this field, Messer is the largest privately managed industrial gases specialist, achieving consolidated sales of 1146 billion euros and an operating profit (EBITDA) of 249 million euros in the 2016 financial year (Messer Group, 2018). The company is a family-owned gas producer with a product portfolio concentrating on European and

Asian customers, and is active in over 36 countries with more than 90 operating companies. The current leader in Iberian industrial gases market is Air Liquide (38% market share), commanding the largest share of revenues in both Spain and Portugal. Conversely, the Iberia market share of Messer is around 3% (Gasworld, 2017).

This thesis focuses on Air Separation Units, whose history and technology are briefly described in the following sections.

1.3.1. Brief history

The history of industrial gases is linked to the industrialization of the nineteenth century. The liquefaction of air proposed by Carl von Linde (Figure 1.4) found the birth of a whole new industry, and the generation of gases at large-scale drove to new types of technologies and production processes.

Linde used the Joule–Thomson effect, which consists in decreasing the temperature of a gas by means of an adiabatic expansion. The experiments performed by Linde were based in James Prescott Joule and William Thomson findings (1853). They discovered that when compressed gases are expanded in a valve, their temperature decreases. Johannes van der Waals gave an explanation for this effect (1873), saying that the molecules in compressed gases are no longer freely movable and the interaction among them leads to a temperature decrease after decompression.

In 1895, Linde could generate in a continuous mode 3 L/h of liquid air in his laboratory in Munich (Dienel, 2004). For this invention, air was compressed from 20 bar to 60 bar in a compressor, and cooled down in a water cooler to ambient temperature. The pre-cooled air was fed into a countercurrent heat exchanger and expanded in a Joule-Thomson valve until liquefaction temperature. The gaseous content of the air was then warmed up again in the heat exchanger and fed into the suction side of the compressor. During the following years, the first small commercial air liquefaction plants were constructed and delivered.

In 1902, Linde applied a rectification process to separate liquid air for continuous oxygen production with purity above 99%, and in 1905 the first high-purity nitrogen was recovered. In 1910, the double column rectifier allowed the simultaneous production of oxygen and nitrogen. Figure 1.5 shows one of these plants. Georges

Claude also had an important role in further developing the air separation technology and obtaining important improvements. A deeper analysis about historical steps and developments in industrial gases industry can be found in Almqvist *et al.* (2003), Winnacker-Küchler (1983), Linde (1997) and Häring (2008).

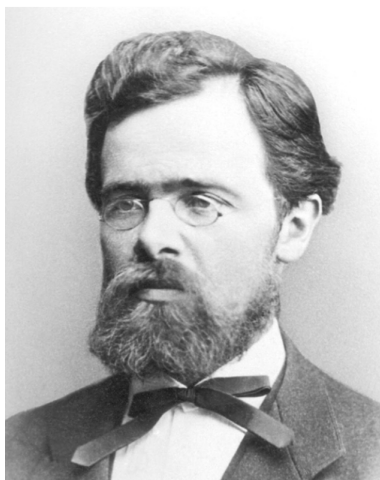


Figure 1.4. Carl Paul Gottfried Linde: 11 June 1842 (Berndorf, Germany) – 16 November 1934 (Potsdam, Germany).

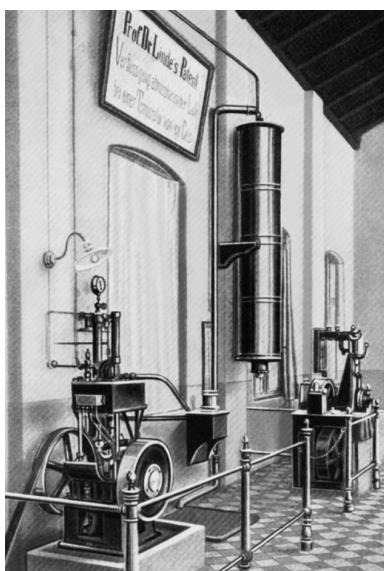


Figure 1.5. Small air liquefaction plant shown by Linde in the Bavarian Industrial and Commercial Exhibition in Nuremberg, Germany (1896).

1.3.2. Air Separation Process

Nitrogen, oxygen and argon are the three main components of the atmospheric air as shown in Table 1.1. Three main methods have been used historically to separate the air components: membrane separation, pressure swing adsorption (PSA) and cryogenic distillation. These techniques have different process properties, investment and operating costs. Figure 1.6 compares these techniques by their production and consumption capacities and gas purity, and identifies two main industrial gases consumption methods (*i.e.*, bottles and tankers).

Table 1.1. Composition of dry air

		Volume fraction in the air	Boiling point [°C]
N ₂	Nitrogen	78.08%	-195.8
O ₂	Oxygen	20.95%	-183.0
Ar	Argon	0.93%	-185.9
CO ₂	Carbon dioxide	400 ppm	-78.5
Ne	Neon	18 ppm	-246.1
He	Helium	5.2 ppm	-268.9
Kr	Krypton	1.14 ppm	-153.2
H ₂	Hydrogen	0.5 ppm	-252.7
Xe	Xenon	0.086 ppm	-108.0

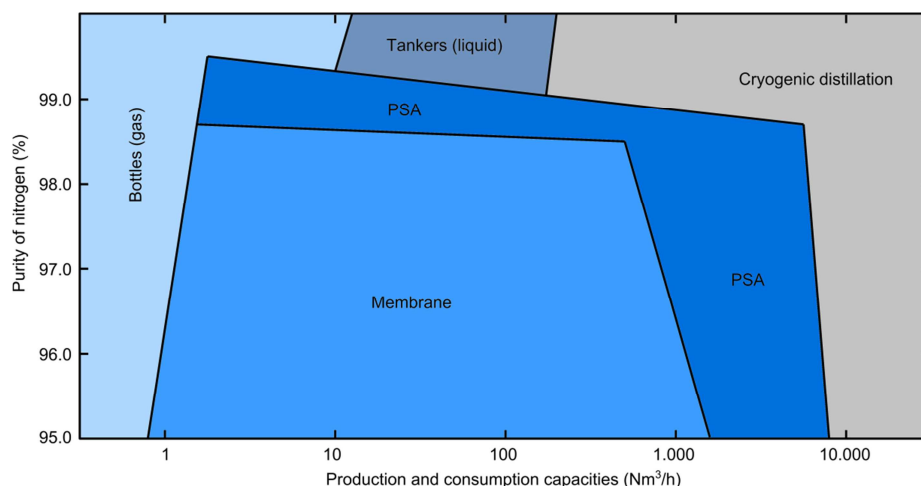


Figure 1.6. Capacities and purities of the main production (cryogenic distillation, PSA and membrane) and consumption methods (bottles and tankers) of industrial gases.

Cryogenic distillation is the state of the art technology for air separation units, used more than 90% on the worldwide production. In addition, the Messer plant located in El Morell (Tarragona), in which this thesis is based on, uses this technology. It will be presented in more detail in the following sections.

The separation of the air into its constituents using cryogenic distillation requires a large part of the air volume to be liquefied. The air, as well as any other gas, can only be transformed into liquid state at temperature and pressure conditions below those of its critical point. The critical temperature of air is -140.7°C (132.5 K) and its critical pressure 37.7 bar. The vapor pressure curve of Figure 1.7 illustrates the allocation of temperatures and pressures at which the air and its components condense or evaporate. We can see that air below atmospheric pressure (1 bar) must be chilled to -192°C (81 K) before it condensates, and at pressures below 6 bar, air must be chilled to -172°C (101 K) before condensation begins.

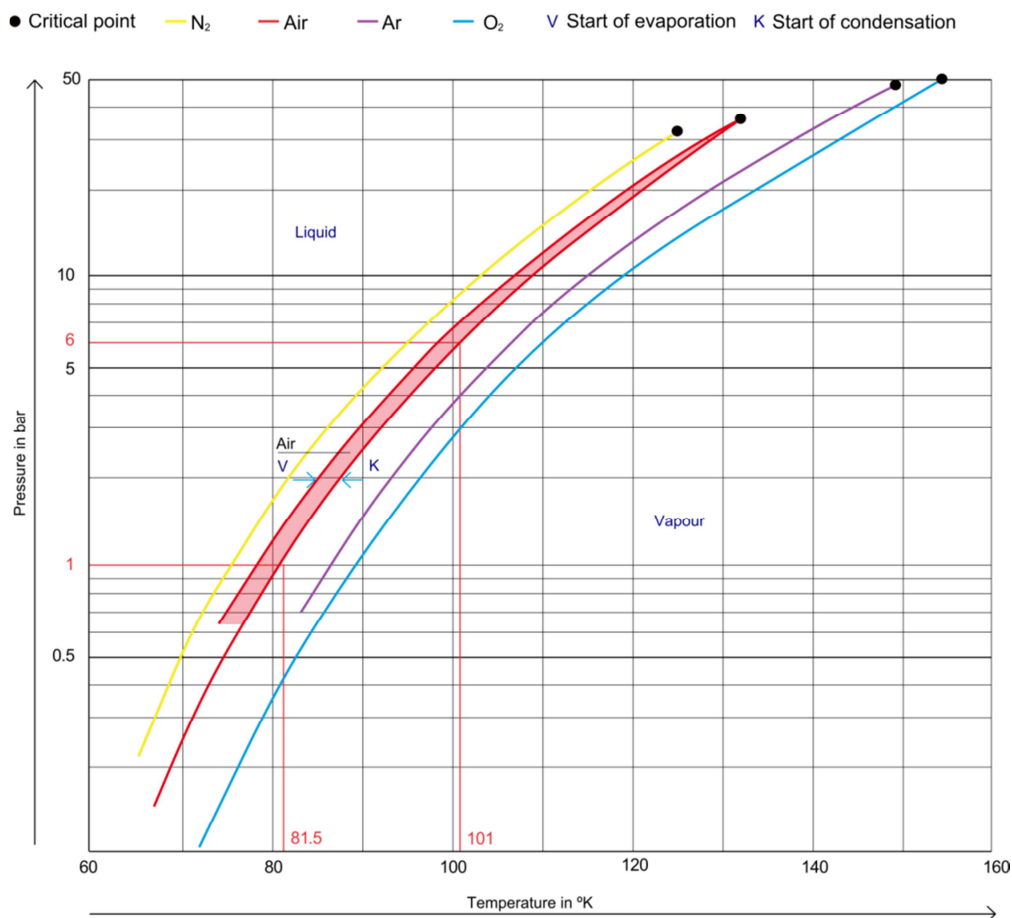


Figure 1.7. Vapour pressure curves of atmospheric gases. Adapted from The Linde Group (2018).

The cryogenic distillation process enables separating with a high purity and yield the individual components of the air mixture, despite their boiling points are relatively close. Due to the different vapor pressures of the individual components ($p_{N_2} > p_{O_2}$) the composition of the vapor mixture differs from the composition of the liquid mixture. Therefore, a higher percentage of the component with the greater pressure vaporizes during the evaporation process. In the oxygen/nitrogen mixture, the vapor produced from the boiling liquid of the mixture has a higher nitrogen concentration than the liquid mixture from which it originates. Accordingly, the condensate produced when the oxygen/nitrogen vapor mixture is liquefied displays a higher oxygen concentration because the component with the lower partial pressure tends to transform into liquid. See Figure 1.8 and Figure 1.9 for a graphical explanation.

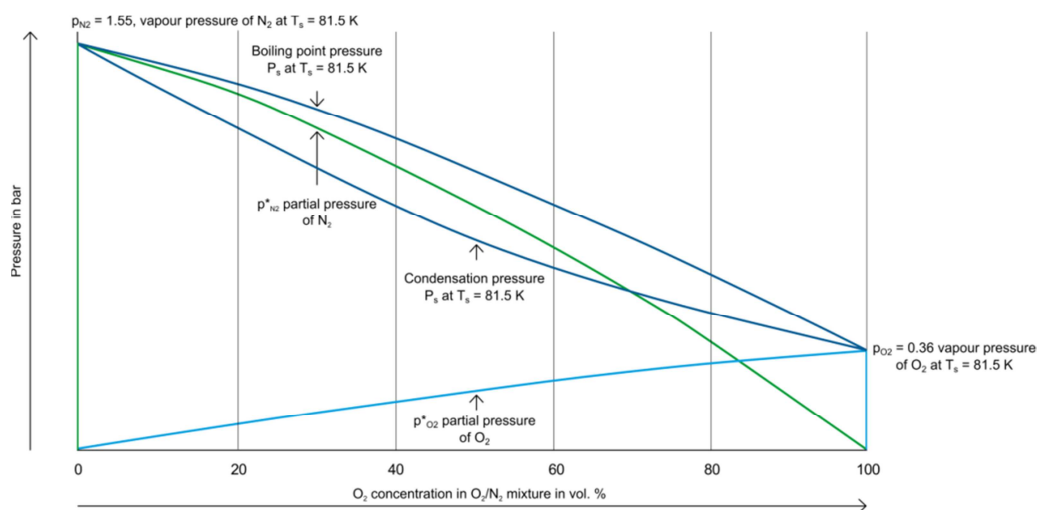


Figure 1.8. Pressure/composition diagram in a O_2/N_2 mixture. Adapted from The Linde Group (2018).

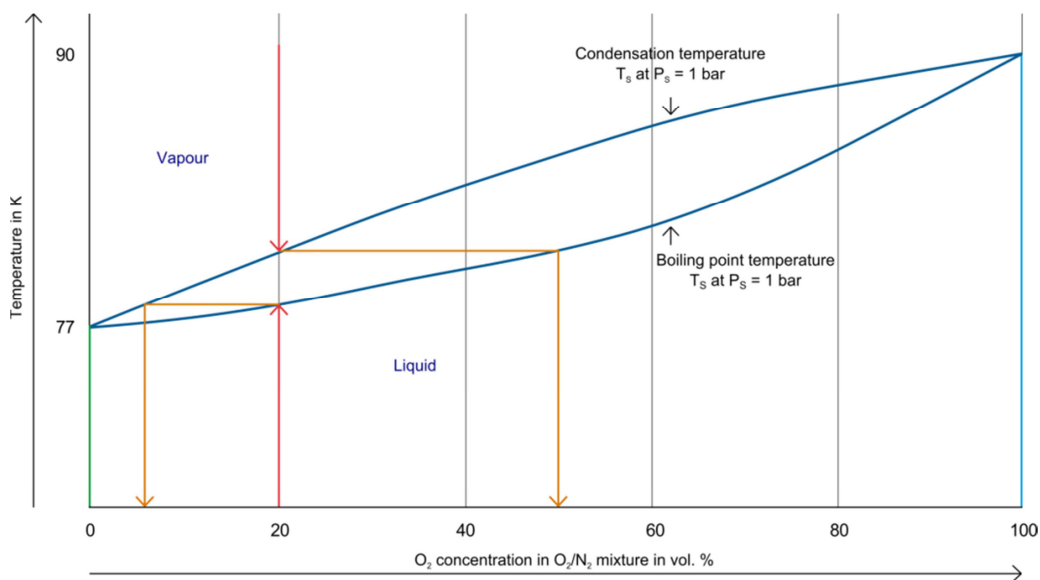


Figure 1.9. Temperature/composition diagram in a O_2/N_2 mixture. Adapted from The Linde Group (2018).

A typical Air Separation Unit (as depicted in Figure 1.11) consists of four main sections: (1) Air compression and precooling system; (2) Molecular sieve station; (3) Heat exchanger network; and (4) Tanks and pumping systems.

In the first section, the air (represented by red lines in Figure 1.11) is compressed and precooled. The atmospheric feed air is absorbed and an air filter is used to remove

dust and other particles. Then, air is compressed to around 6 bar(a) in a multistage turbo-type air compressor. The compressed air leaves the compressor at about 70°C and enters at the bottom of an air cooler equipment named Direct Contact After Cooler (DCAC). In the DCAC, the air passes through a set of packed beds while it is washed by trickling water (water streams are represented by green lines in Figure 1.11). The air is cooled down to around 9°C before leaving the DCAC by the top. The DCAC has two cooling water feeding points: one is placed in the intermediate part of the equipment and uses water from the cooling water system (~25°C), while the second is located in the upper part and uses chilled water (~8°C), obtained from the refrigeration unit called Chill Tower and/or other mechanical coolers. In the Chill Tower, water is cooled in counter-current flow with the nitrogen-rich residual gas from the separation which is saturated with moisture. The required evaporation heat is withdrawn from the water, what causes its cooling. The cooling water and condensed water resulting of this process is collected by the bottom of DCAC and recycled to the cooling water system.

The air leaving the DCAC still has contaminants (at molecular level) such as H₂O, CO₂, and potentially hazardous hydrocarbons, which are removed in the molecular sieve station. They pass through one of the two *Molsieve* adsorbers to guarantee that these molecules would not gradually block the heat exchanger located downstream. In the case of hydrocarbons, they would accumulate in the liquid oxygen bath formed in the evaporator and they could cause an explosion if their concentration surpasses the solubility and explosion limit. The *Molsieve* operates in semi-batch (one adsorber is working while the other is regenerated); with one unit typically operating during roughly seven hours before its capacity is exhausted. The regeneration gas coming from the distillation heats up in the regeneration gas heater during the heating period and then, during the cooling period, the electric heater is switched off and the cooling gas pushes the heat out of the adsorber. The adsorbent material can operate up to ten years until it must be replaced.

The air which leaves the *Molsieve* is divided in two streams that go through the heat exchanger network. The main fraction (around 90%) is sent to the heat exchanger where it is cooled in counter-flow using gaseous nitrogen, gaseous residual nitrogen and gaseous oxygen from the low-pressure column. The second fraction is further

compressed in a booster, cooled in a water heat exchanger and expanded via a turbine. The turbine controls the plant refrigeration balance and it is coupled with a work unit used by the associated booster compressor. The expanded air fraction enters the low pressure column partially liquefied.

In air separation plants, the main column system employed is typically a double column system. The double column consists of a low pressure (LP) column and a medium pressure (MP) column where the feed air enters at the bottom at approximately 5.5 bar(a). Both columns are thermally linked by a condenser/reboiler. The enriching section of the MP column is determined by the volatilities of its components (see Table 1.1). The vapor becomes enriched in nitrogen, thus at the top of the MP column the vapor stream is highly pure nitrogen (~ 1 ppm O_2). This vapor nitrogen stream (nitrogen streams are represented by orange lines in Figure 1.11) is sent to the main condenser where it is totally condensed against boiling liquid oxygen in the sump of the LP column (oxygen streams are represented by blue lines in Figure 1.11). This liquid nitrogen stream is used as a reflux in two different places: one portion is sent to the top of the MP column and the other one is sent to the top of the LP column. The liquid nitrogen stream going down through the MP column serves to condense the oxygen, and at the bottom of the MP column a liquid stream enriched in oxygen ($\sim 35\%$ oxygen) is obtained. This liquid stream is sent to an intermediate feed stage within the LP column. The LP column works with the same principle as the MP column, but it operates a lower pressure (~ 1.3 bar(a)). The turbine air stream is fed to the LP column, since this location is designed to be at a point within the LP column where the composition is very close to that of air. The turbine provides the low level (cold temperature) refrigeration required by the process. Some stages below the location of the turbine air feed, the enriched oxygen liquid stream from MP column is fed to the LP column, serving as an intermediate source of reflux to enhance the separation within the LP column. The final separation takes place in the LP column, obtaining pure oxygen at the bottom and pure nitrogen (GAN) at the top ($\sim 99.5\%$ and 99.9% purity, respectively). An additional stream is recovered at an intermediate stage of the LP column, called waste nitrogen stream since it is nitrogen with a small oxygen

content. This stream is used to be heated in the regeneration heater of *Molsieves* and is also used in the heat exchangers in order to cool the air.

In the LP column some of the liquid oxygen in the sump is boiled by the main condenser (also reboiler). This vaporized oxygen provides the necessary vapor flow for the distillation, since the heat required to vaporize this oxygen is provided by the condensing of the nitrogen at the top of the MP column (both columns are thermally linked). The reason why the MP column is operated at a higher pressure than the LP column is that the temperature at which the nitrogen condenses (boiling point) must be raised so that the vaporizing liquid oxygen can condense it.

Oxygen product can be withdrawn as gaseous (GOX) or liquid (LOX) product from the lower part and the bottom of the LP column, respectively. In order to withdraw more liquid product from the distillation column, more refrigeration is required. This is achieved by adding liquid nitrogen (LIN) from an external source (*e.g.*, tank or a nitrogen liquefier) to the top of the LP column.

Finally, in an intermediate stage of the LP column, the concentration of argon (argon streams are represented by purple lines in Figure 1.11) reaches a peak of 10-15% and the composition of nitrogen is very low (a few ppm). At this point, a portion of the vapor stream (~3%) is sent to the bottom of the crude argon column, where it is concentrated into crude argon as top product (~97.5% argon, 1ppm O₂ and 0.5% N₂). The bottom liquid product from this crude argon column is returned to the LP column at the same stage where the crude feed is withdrawn. In the pure argon column, the residual nitrogen is rectified towards the top and ejected into the atmosphere by blowing off a small amount of waste gas with a typical nitrogen content of 40%. Then, the liquid argon product (LAR) is sent to the tank from the bottom of the pure argon column.

Figure 1.10 shows a typical purity profile of a low pressure distillation column.

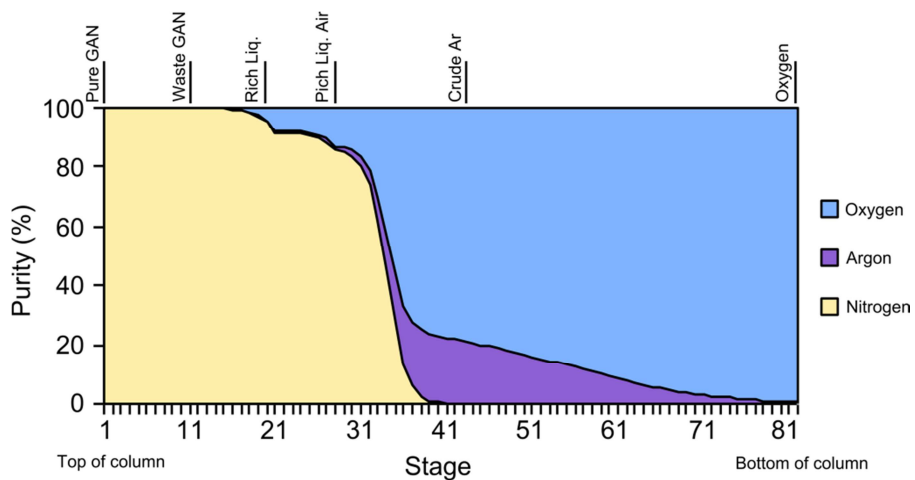


Figure 1.10. Low pressure column composition profile.

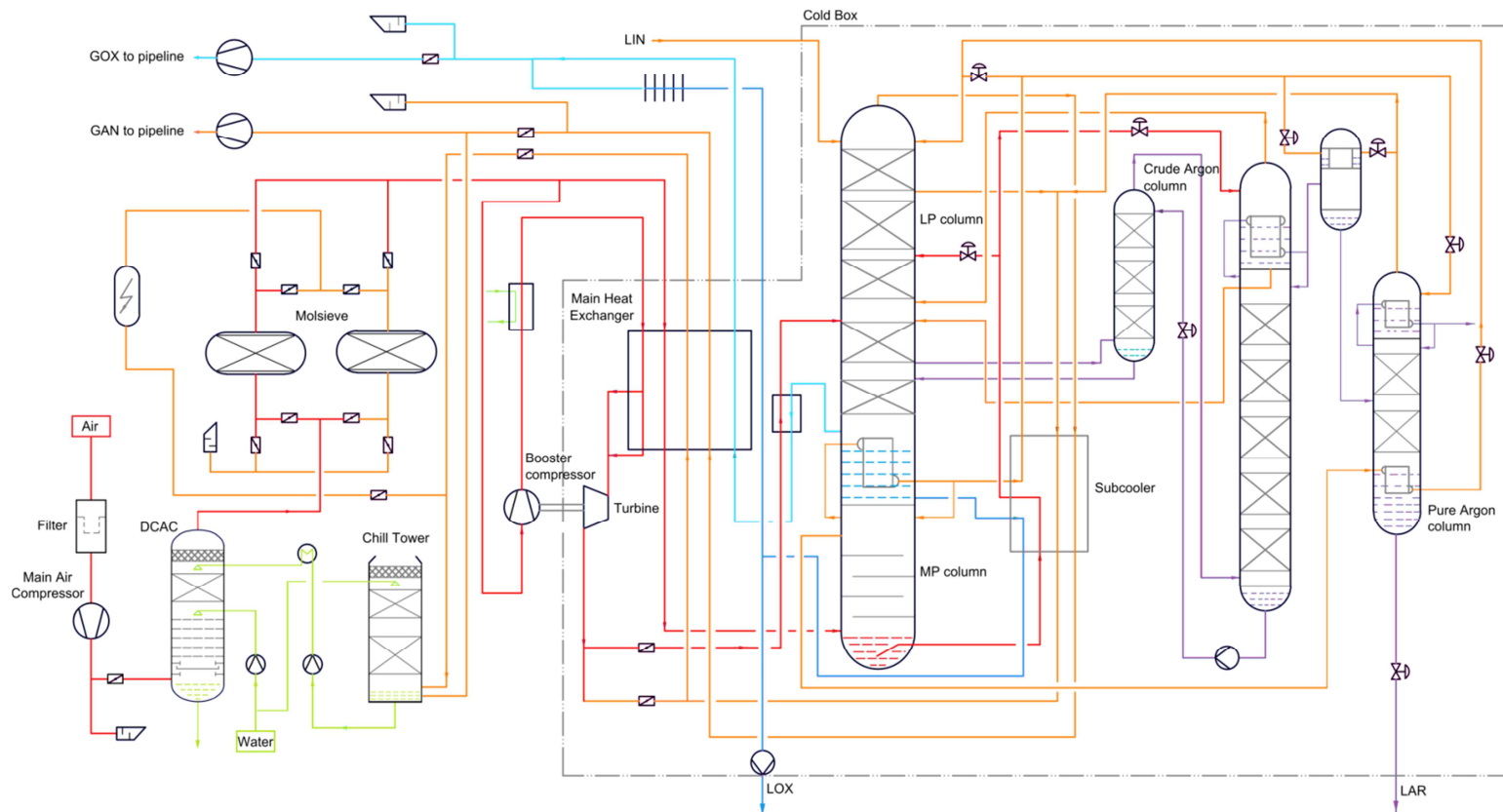


Figure 1.11. Process flow diagram of an Air Separation Unit. (GOX: Gaseous Oxygen, GAN: Gaseous Nitrogen, LIN: Liquid Nitrogen; LOX: Liquid Oxygen, LAR: Liquid Argon)

Once the separation of the air in its different components has been done, these products are sent to the final customers in different ways. For large consumer customers located in large industrial areas (around the air separation unit), products are supplied through a network of gas pipelines to ensure flexibility and reliability of supply; for medium consumer customers (located at larger distances), oxygen, nitrogen and argon are stored in liquid phase in tanks and, then, they are transported to customers by means of road tankers; and for small consumer consumers, product is sent to bottling units where cylinders are filled and, then, they are distributed in delivery trucks to end customers. Figure 1.12 shows a graphical representation of the different delivery methods.

In the case of pipeline distribution, before fed the pipeline, gas products are sent to the plant compressors, which are operated accordingly to guarantee a constant pipeline pressure and to manage peak volume demands in a prompt and cost-effective way. On the other hand, products obtained in liquid phase are stored in cryogenics tanks before being sent to customers in road tankers. To this end the liquefaction units are normally used, in which part of the gas product (obtained from the air separation unit at a temperature between 20°C and 30°C and approximately at 1.1 bar(a)) is fed. This gas stream is compressed into two turbo compressors (the first compressor is known as "feed compressor" and the second one as "recycling compressor") until reaching a pressure between 26 and 28 bar(g). The refrigeration is generated in two stages, expanding the high pressure nitrogen to the suction pressure of the recycle compressor and, consequently, performing a work on the booster compressors associated with the turbines. There are two booster compressors associated with their corresponding turbines. The resulting stream of the series compressors, is the point where the highest pressure is reached in the plant, about 56 bar(a). The hot turbine provides cold for the cold turbine feed that generates the decompression and the consequent nitrogen cooling. The liquid nitrogen is subcooled to a temperature of -192°C to be able to store it in the tank with minimum losses due to the flash effect.

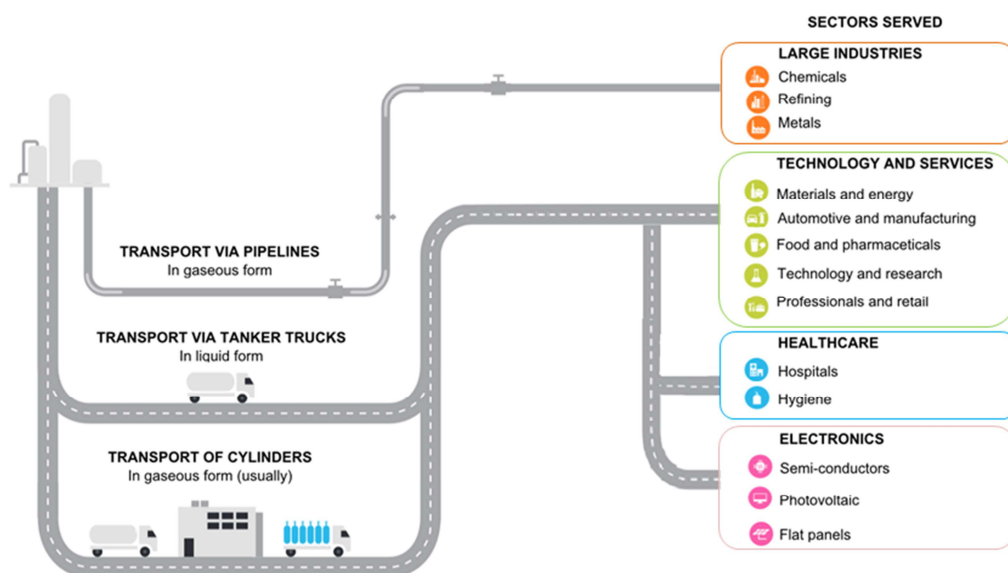


Figure 1.12. Industrial gases distribution to final customers

In section 2.3., we present a mathematical formulation to optimize the process shown in Figure 1.11, which is complemented with the compression and liquefaction units and the possibility to purchase product from an external supplier to cover the entire demand. Furthermore, the model also incorporates the possibility of sending products in liquid phase to external tanks, which are used as an additional storage station. This allows avoiding interruptions in the production stemming from shortages in storage capacity, and therefore, taking full advantage of the time periods with cheaper tariffs.

The complexity to optimally manage this kind of facilities is very high due to the large number of interactions between variables, changing product prices, fluctuations in customers' product demand, utilities price, etc. Furthermore, this process is a high electricity consumer, and in the last few years, the electricity prices and the instability of the Spanish electrical market (in which the process studied in section 2 is located) have increased. The electricity price can change every hour since it is daily set for the following 24 hours based on the electricity supply and demand balance of the market. Electricity supply and demand do not match in the same way throughout the hours of the day depending on the weather conditions, nuclear plants shutdowns, working days,

and consumers' energy use. In order to hedge against the instability of daily market, companies with large energy consumption have the possibility to purchase certain power blocks that will be consumed in the future at a price fixed in the present (this is known as future market). In this scenario, the need of planning and scheduling tools that can improve the process behavior in each time period is crucial, and the computer-aided tools presented in this thesis constitute a promising strategy to deal with the fluctuations in process variables, increasing the business competitiveness and reducing the energy usage.

1.4. Decision making tools

Decision making tools attempt to apply mathematical methods to solve the difficult problems confronting modern managers (Winston and Albright, 1997). Their application cover a wide variety of business, industrial, military, and public-sector problems. In fact, management science tailored for efficiency and profitability constitutes the main goal of this thesis where mathematical programming is employed to increase the managerial effectiveness. Mathematical programming, and especially linear programming, is one of the best developed and most used branches of management science (Charnes and Cooper, 1957). In our case, the aim is to develop mathematical programming tools to provide guidelines to managers for making effective decisions within the state of the current information, and to seek further information if current knowledge is not enough to reach a proper decision.

The essence of management science is the model-building approach, which is an attempt to capture the most significant features of the decision under consideration by means of a mathematical abstraction. Models are simplified representations of the real world and, in order to be useful in supporting management decisions, they have to be simple to understand and easy to use. At the same time, they have to provide a complete and realistic representation of the decision environment by incorporating all the elements required to characterize the essence of the problem under study. This is not an easy task but, if done properly, it will supply managers with a formidable tool to be used in complex decision situations. Second, through this model-design effort,

management science tries to provide guidelines to managers or, in other words, to increase managers' understanding of the consequences of their actions.

The process of solving a decision-making problem is shown schematically in Figure 1.13.

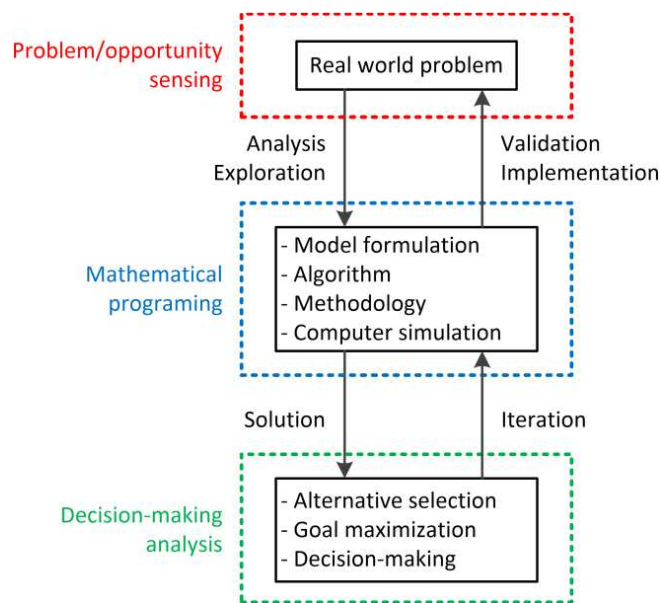


Figure 1.13. Steps to solve decision-making problems programming

The first step of such process is to identify a real problem or opportunity, and then, it is necessary to collect and analyze the required information to define and understand such problem/opportunity. The next step consists in building the model to solve the stated problem, which requires a set of mathematical functions containing the decision variables and parameters used to represent the problem under study. Sometimes, problems are extremely difficult to handle with mathematical techniques and simplifications, approximations or assumptions are required.

In order to solve the mathematical models and obtain solutions, different strategies can be used, each with advantageous features for a particular subset of problems (further information on this is provided in the next section). Furthermore, several modelling software systems as well as *ad hoc* and commercial solvers are available to assist the computer implementation of the optimization-based model. In this thesis GAMS (Brooke *et al.*, 1998) has been used as modelling system.

Finally, the optimal solution(s) representing the best solution(s) of the stated problem, is(are) obtained as a result of the mathematical programming simulation. Then, it is convenient to check the feasibility of the proposed solution by coming back to the real problem and assessing its robustness in light of uncertainties. Once mathematical programming provides an optimal solution to the decision-makers, these are capable of combining it with their knowledge in order to implement the solution. This solution is often not feasible in the real world and it is necessary to slightly adjust the model until it is able to reproduce reality more accurately. In this step, decision-makers play a fundamental role by introducing their preferences in an iterative process until a satisfactory solution is obtained (Jaimes *et al.*, 2009). At the end, the framework obtained after the iterative process stated in Figure 1.13, constitutes a powerful tool to make decisions achieving efficient solutions.

This model-design effort, tries to provide guidelines to managers and support management actions. It is critical, then, to recognize the strong interaction required between managers and models. Models can expediently and effectively account for the many interrelationships that might be present among the alternatives being considered, and can explicitly evaluate the economic consequences of the actions available to managers within the constraints imposed by the existing resources and the demands placed upon the use of those resources. Managers, on the other hand, should formulate the basic questions to be addressed by the model, and then interpret the model's results in light of their own experience and intuition, recognizing the model's limitations. The complementarity between the superior computational capabilities provided by the model and the higher judgmental capabilities of the human decision-maker is the key to a successful management-science approach. In this regard, the "Industrial Doctorates Plan" offers an ideal environment to test and validate such modelling efforts.

1.5. Mathematical programming

Mathematical programming or optimization devotes to the formulation of models aiming at finding the best element (under some conditions) from a set of alternatives. In other words, an optimization problem consists of maximizing or minimizing a

system by systematically choosing the best values for the continuous or integer decision variables.

Mathematical models are formed by one (or several) objective function and constraints (*i.e.*, expressions which impose bounds in the variables) in form of either equalities or inequalities. Each of these functions can be formulated by means of either linear or nonlinear algebraic equations. All the feasible solutions of the stated problem satisfy the set of constraints, but the optimal solution is the one with the best performance as ranked by the objective function. Therefore, the objective function is the mathematical representation of a goal for use in decision analysis, operations research or optimization studies. The objective function can be an economic (*e.g.*, maximize the profit of a firm), an environmental (*e.g.*, minimize the environmental impact) or a social (*e.g.*, minimize the obesity) goal, among others.

The mathematical programming techniques used as a methodological basis of this thesis (single-objective optimization (SOO), multi-period optimization, data envelopment analysis (DEA) and Malmquist productivity index (MPI)) are next explained in more detail. Then, section 1.6 and sections 2 and 3 describe how these methods can be used to address the complexity in operating air separation networks attaining economic and energy savings as well as guidelines to improve the efficiency of existing plants and reference facilities that could be used for benchmarking.

1.5.1. Objective optimization problems

Standard single-objective optimization (SOO) models are canonically stated (Grossmann *et al.*, 2000) as in Eq. 1-1:

$$\begin{array}{ll} \text{SOO} & \min \quad f(x,y) \\ & \text{s.t.} \quad h(x,y) = 0 \\ & \quad \quad g(x,y) \leq 0 \\ & \quad \quad x \in \mathbf{R}, y \in \mathbf{Z} \end{array} \quad \text{Eq. 1-1}$$

where $f(x,y)$ represents the objective function (unique) to be minimized. If the objective function has to be maximized, then $-f(x,y)$ is used. x and y are the vectors of

continuous and integer decision variables, respectively. Continuous variables can represent physical quantities such as operating conditions, equipment sizes and capacities while integers variables can denote switches between process units or equipment startups and shutdowns, among others. A particular case of integer variables are binary variables ($y \in \{0, 1\}$), which allow modeling logical decisions. The set of feasible solutions is defined by the set of constraints which impose boundaries on variables. In Eq. 1-1, $h(x,y)$ represents equality constraints whereas $g(x,y)$ denotes inequality constraints. The (x,y) point which satisfies all the imposed constraints is a feasible point and this means a feasible solution to the problem. Feasible points create the feasible region of the problem and, finally, the optimization selects the optimal point from the feasible solutions set. A point from the feasible region is a local minimum (maximum) if it is the lower (higher) function value in some feasible proximities. In an optimization problem there can be many local minimums (maximums) but in most cases only one of them is the global minimum (maximum). Figure 1.14 illustrates these concepts.

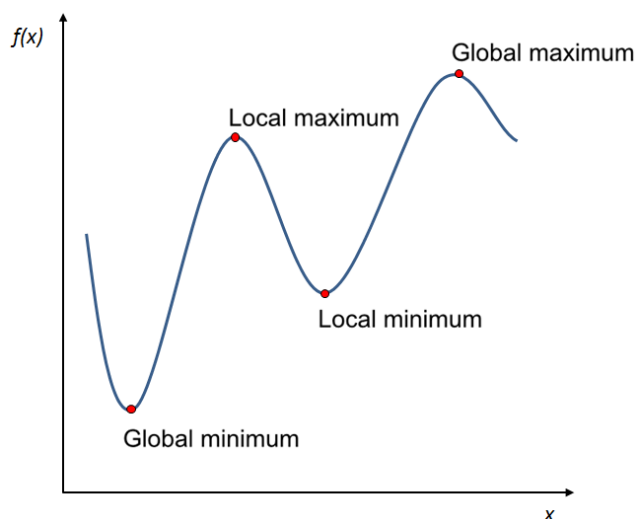


Figure 1.14. Graphical representation of optimality concept

There are properties affecting the feasible region and objective function which imply that any local optimum is indeed a global optimum. One of these properties is the convexity. A feasible region ω is convex if, and only if, for any two points x_1 and

x_2 , their linear combination lies in the feasible region ω ($x = \alpha x_1 + (1 - \alpha)x_2 \in \omega$ $\forall \alpha \in [0,1]$). If $h(x,y)$ is linear and $g(x,y)$ is convex, then the feasible region ω is a convex region. A function f is convex if, and only if, for any two points x_1 and x_2 the following is satisfied: $f(\alpha x_1 + (1-\alpha)x_2) \leq \alpha f(x_1) + (1-\alpha)f(x_2) \forall \alpha \in [0,1]$. If the function f is convex and the feasible region ω defined by the equality and inequality constraint is convex, then any local optimum will be a global optimum. Figure 1.15 illustrates convexity concepts.

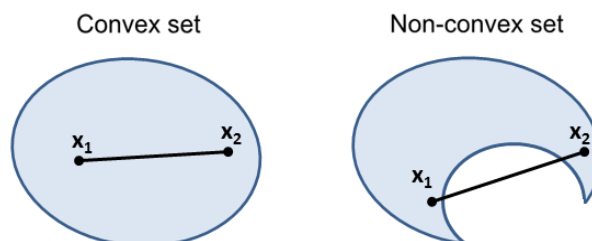


Figure 1.15. Graphical representation of convexity concept

Mathematical models can be classified depending on the nature of their objective function and constraints in either linear or nonlinear models, and depending on the typology of their decision variables in continuous or binary (or integers in the more general case) models. The combination of these two features gives rise to four main groups where mathematical models can be classified in: linear programming (LP), nonlinear programming (NLP), mixed-integer linear programming (MILP) and mixed integer nonlinear programming (MINLP). These types of model are depicted in Figure 1.16 and described later.

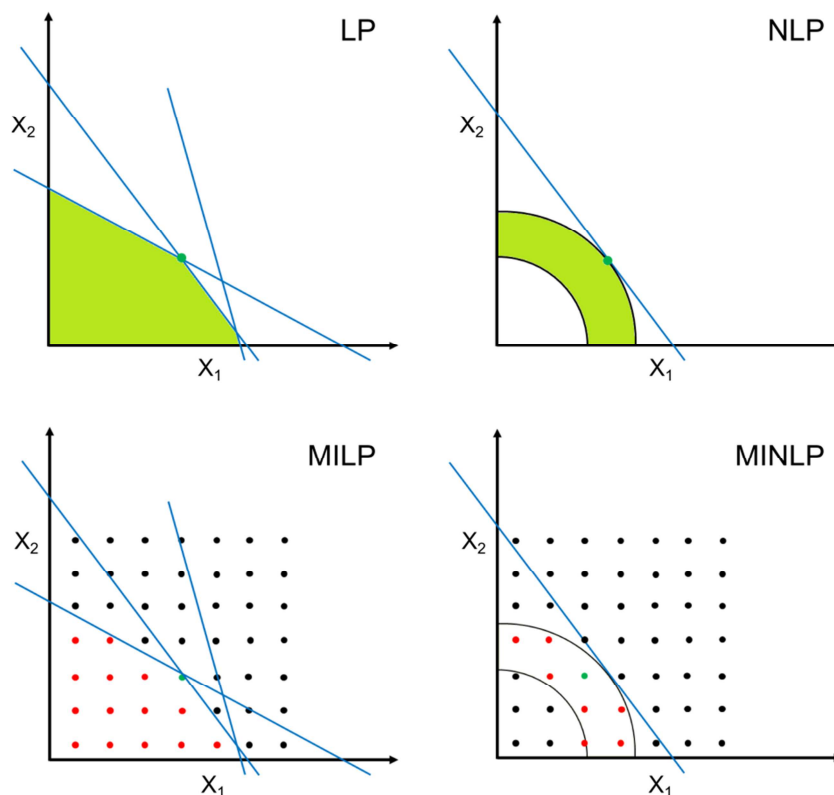


Figure 1.16. Illustration representing the four main types of mathematical optimization problems. Blue lines represent the linear equations, green regions represent the feasible region, red points represent the feasible region of integer solutions, and green points represent the hypothetical optimal solution.

A linear program (LP) is an optimization problem where the variables are continuous, the objective function is linear and the constraints consist of linear equalities and linear inequalities. In Figure 1.16 blue lines represent the linear equations (equalities and inequalities) and the region formed within them (depicted in green color) is the corresponding feasible region. The optimal solution of an LP is represented by a green dot and is always a vertex of the feasible region that is optimal. Usually, the simplex method (Dantzig *et al.*, 1995) is used to solve LP problems, in which successive checking is performed along the vertexes of the feasible region until the optimal solution is identified. There are several commercial solvers optimizers suitable to solve LP problems such as CPLEX (IBM, 2009), LINDO (Schrage, 1995) or GUROBI (Optimisation, 2012), among others.

NLP arise when at least one of the model equations is non-linear (either objective function or constraints) and all variables are continuous. NLPs can be convex or non-convex. In convex NLPs, a local optimum is as well a global optimum. In the case of non-convex NLPs, multiple local optima may appear, causing standard gradient methods to get trapped thereby offering no guarantee of reaching the global optimum. The optimizer BARON (Sahinidis, 1996) is a general non-linear optimizer capable of solving nonconvex optimization problems to global optimality.

MILP models contain only linear equations (as LPs), but include both continuous and integer variables. Note that in the special case that all variables are restricted to be integer, these models are known as integer linear programming (ILP or simply IP). The standard procedures to solve MILP problems are cutting plane methods, and the most common is the branch-and-bound algorithm (Land and Doig, 2010), which consist in relaxing the original integer variables imposing restrictions over them. Specifically, in the branch-and-bound, the original MILP is divided into several LP sub problems that are solved until all integrality restrictions are satisfied, since this implies that the solution found for the relaxed problem is an optimal solution to the original MILP. Common commercial solvers that combine those strategies are CPLEX (IBM, 2009), GUROBI (Optimization, 2012) or XPRESS (Optimization, 2007), among others.

Finally, MINLPs are problems that contain at least one non-linear equation and both continuous and integer variables. MINLP problems are hard to solve, however several algorithms and commercial solvers have been developed to tackle them: BARON (Sahinidis, 1996), DICOPT (Grossmann *et al.*, 2002) or SBB (Bussieck and Drud, 2001) are examples of such methods.

As will be shown next, the problems addressed in this thesis are LPs and MILPs, and have been solved by means of the commercial solver CPLEX (IBM, 2009).

1.5.1. Multiperiod optimization problems

Plant production scheduling decisions must be made weekly or in a certain future time period. These decisions are affected by changing conditions (*e.g.*, demand, inventories, power boundaries, electricity prices, etc.), which complicate the identification of effective solutions just by problems inspection. To overcome these

issues, in this thesis has been developed a tailored multiperiod formulation for the optimal scheduling of the ASU operated by Messer Ibérica de Gases S.A.U. in El Morell (Tarragona).

Multiperiod planning/scheduling is one of the most important uses of optimization. Multiperiod optimization does not mean solving multiple optimization problems for different periods, either simultaneously or sequentially. In multiperiod optimization the problem is viewed as a single optimization problem, and it involves input data for multiple time periods to produce optimal solutions for the whole time span. The objective function of the multiperiod optimization is a weighted sum of the objective functions of its component periods. The objective function for each period is a single-period objective function. The constraints of the multiperiod optimization can be *per-period constraints* and *cross-period constraints*. Per-period constraints are specific and apply for each respective period (some periods may have the same or similar constraints). Cross-period constraints apply to at least two periods, and control certain interactions among periods (*e.g.*, tank inventories). Multiperiod optimization requires users to provide input data for all periods beforehand to obtain the optimal solution for the whole time span. Most large linear programs encountered in practice are multiperiod models, and are widely used in batch processes. See for instance (Birewar and Grossmann, 1990) that presented a multiperiod linear programming model for production planning of batch plants that considers benefits and product inventory cost, and (Susana and Marcelo, 2009) which proposed a multiperiod model to optimize simultaneously production planning and design decisions applied to multiproduct batch plants. Despite this, multiperiod models are also applied in the continuous industry. In the case of the present thesis, the multiperiod model proposed takes the form of a MILP problem with variable size depending on the amount of time periods addressed. Further details on the problem formulation can be found in section 2.3.

1.5.2. Data Envelopment Analysis

Multiperiod models can identify and optimize operation problems of a given facility, yet it cannot identify design problems. Therefore, to identify design problems as well as further inefficiency sources, comparison between different facilities is

necessary. To this end, a standard mathematical programming method named Data Envelopment Analysis (DEA) is used. DEA is a non-parametric mathematical technique used to evaluate observations representing the performances of a set of entities. DEA has been used to assess a wide range of different kinds of entities (from business firms to government and non-profit agencies such as schools, hospitals, police, countries, regions, etc.).

In DEA context, the term "Decision Making Unit" (DMU) refers to any entity to be evaluated as part of a set of entities that utilize similar inputs to produce similar outputs. In our case, the DMUs correspond to the existing ASUs around the world (see section 3.3 for further details). The evaluation of each DMU results in a performance score that ranges between zero and one, which represents the degree of efficiency obtained by the entity. DEA identifies the DMUs which form the "efficient frontier" (those with efficiencies equal to one), and also shows the sources and amounts of inefficiency in each input and output for every inefficient DMU. DEA provides useful findings to guide the changes required to turn the inefficient units into efficient ones, for instance by identifying the so-called peer (comparison) group: a set of efficient units that could be used as reference to obtain these improvements. Furthermore, DEA allows to combine many metrics into a single score without the need of defining subjective weights since, in DEA, weights are optimized so as to favor the assessed DMU (and therefore, optimal weights generally change from one DMU to another).

The first DEA model, proposed by Charnes Cooper and Rhodes in 1978 (Charnes *et al.*, 1978), is based on Farrell's work (Farrell, 1957) and named the CCR model. It measures, using a nonlinear (*i.e.*, fractional) model, the efficiency of each DMU as the ratio between the weighted sum of its outputs to the weighted sum of its inputs.

In DEA models, inefficient DMUs are projected onto the efficient frontier in order to obtain improvement targets for them (see Figure 1.17). These projections can be done using different orientations, where two main variants exist. One approach aims to minimize inputs while satisfying at least the given output levels (input-oriented model), while the output-oriented model attempts to maximize outputs without requiring more of any of the input values. The orientation (input or output oriented) of DEA models depends on the application (Lozano *et al.*, 2009). Usually, input oriented models are

used when the defined inputs are more easily manipulated than outputs. For instance, the DEA model applied in this thesis (section 3.3) is input orientated since the outputs considered (*i.e.*, amount of products) are connected to the customer's demand, thus offering little opportunity for influence (if any). In the case of output oriented models, they are normally used when inputs are very hard to control and manage, while outputs allow a greater margin of incidence.

We next present the formulation of the original DEA CCR model (Eq. 1-2), defined for each of the $|J|$ DMUs j ($j=1, \dots, |J|$), each using $|I|$ inputs x_{ij} ($i=1, \dots, |I|$) to produce $|R|$ outputs y_{rj} ($r=1, \dots, |R|$):

$$\begin{aligned} \max \theta_o &= \frac{\sum_{r \in R} u_r y_{ro}}{\sum_{i \in I} v_i x_{io}} \\ \text{s. t. } \sum_{r \in R} u_r y_{rj} - \sum_{i \in I} v_i x_{ij} &\leq 0 \quad \forall j \in J \\ u_r, v_i &\geq 0 \quad \forall r \in R, i \in I \end{aligned} \quad \text{Eq. 1-2}$$

Here, θ_o is the technical efficiency of the DMU being assessed (DMU_o); u_r and v_i are variables representing the weights given to each output r and input i , respectively; x_{ij} , is the amount of input i consumed by DMU_j and y_{rj} is the amount of output r produced by DMU_j . When $\theta_o = 1$, DMU_o is efficient, while $\theta_o < 1$ means that DMU_o is inefficient. CCR model assumes that DMU's outputs and inputs change in the same scale, which means that the CCR model considers constant returns to scale (CRS).

The original input-oriented CCR DEA model (Charnes et al., 1978) stated in Eq. 1-2 is nonlinear and nonconvex. However, it can be reformulated (from fractional to linear) into the LP model stated below (Cooper *et al.*, 2004):

$$\begin{aligned}
\max \quad & \theta_o = \sum_{r \in R} u_r y_{ro} \\
\text{s. t.} \quad & \sum_{i \in I} v_i x_{io} = 1 \\
& \sum_{r \in R} u_r y_{rj} - \sum_{i \in I} v_i x_{ij} \leq 0 \quad \forall j \in J \\
& u_r, v_i \geq 0 \quad \forall r \in R, i \in I
\end{aligned} \tag{Eq. 1-3}$$

where the subscript o denotes the specific DMU being assessed.

The fractional program (Eq. 1-2) is equivalent to the linear program (Eq. 1-3). The previous LP problem in (Eq. 1-3) can be formulated as a dual partner problem (duality), providing the same information (*i.e.*, efficiency scores) but calculating in turn targets for the inefficient DMUs so as to become efficient. The LP DEA dual model is formulated by assigning one dual variable to each constraint in the primal model as follows (Cooper *et al.*, 2011). Note that slack variables have been appropriately added to transform inequalities into equality constraints. As will be discussed next, these slacks have a clear physical interpretation in DEA, reason why their incorporation to the objective function is convenient.

$$\begin{aligned}
\min \quad & \theta_o - \varepsilon \left(\sum_{r \in R} S_r^+ + \sum_{i \in I} S_i^- \right) \\
\text{s. t.} \quad & \sum_{j \in J} \lambda_j x_{ij} + S_i^- = \theta_o x_{io} \quad \forall i \in I \\
& \sum_{j \in J} \lambda_j y_{rj} - S_r^+ = y_{ro} \quad \forall r \in R \\
& \lambda_j, S_i^-, S_r^+ \geq 0 \quad \forall j \in J, i \in I, r \in R
\end{aligned} \tag{Eq. 1-4}$$

Here, o is the DMU being assessed; ε , non-Archimedean infinitesimal value to enforce the variables to be positive; S_i^- and S_r^+ , vector of slack variables representing the amount of input i and output r , respectively, that, if reduced/increased, shifts the

projection of DMU_o from the *weakly efficient* frontier to the *strongly efficient* frontier (later explained); λ_j , linear weights assigned to every single DMU_j to form a linear combination.

In the efficient units ($\theta_o = 1$), when the values of the slacks are all zero ($S_r^+ + S_i^- = 0$ over all r and i respectively), the DMU_o is considered *strongly efficient*, whereas when any slack is different from zero ($S_r^+ + S_i^- \neq 0$ for some r or i), the corresponding DMU_o is considered *weakly efficient*. For any inefficient DMU ($\theta_o < 1$), it is possible to find a composite DMU (linear combination of existing units) that can reduce its input level maintaining the same output level. Any inefficient DMU can become efficient by its projecting onto the “efficient frontier”, which is formed by the efficient DMUs.

The model formulated in Eq. 1-4 is input-oriented, that is, inefficient units are turned efficient through a proportional reduction of inputs while keeping the output constant. It is possible to reformulate its equivalent output-oriented model, where an inefficient unit would be turned efficient by increasing its outputs while keeping its inputs constant.

As explained before, the CCR model considers CRS. If the variable returns to scale (VRS) property is desired (*i.e.*, if it is suspected that an increase in inputs does not result in a proportional change in the outputs) a different DEA model called BCC must be used (Banker *et al.*, 1984). The dual version of such model, which is a variant of the CCR one, can be formulated by simply adding the following convexity constraint to Eq. 1-4: $\sum_{j \in J} \lambda_j = 1$.

Figure 1.17 and Figure 1.18 shows an illustrative example to further clarify the previous DEA concepts. Figure 1.17 shows the case of one single input and one single output, while Figure 1.18 illustrates the case of two inputs and one output.

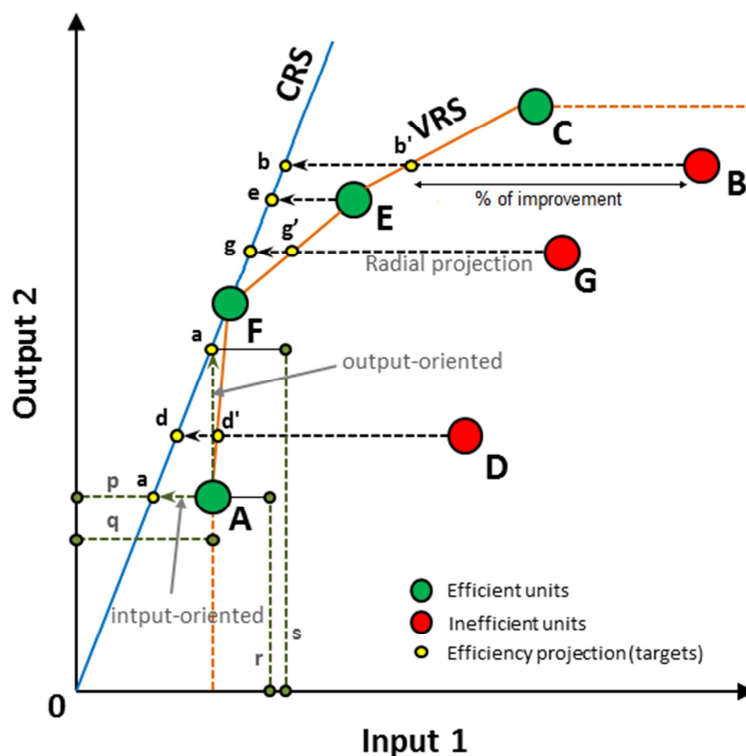


Figure 1.17. Illustration of DEA results: case with one input and one output.

Figure 1.17 illustrates DEA results when the model is formulated assuming CRS (*i.e.*, CCR model, Eq. 1-4) or VRS (*i.e.*, BBC model, that is, Eq. 1-4 plus the convexity constraint for λ). Under CRS assumption, the best efficiency (equal to one) is obtained by DMU F, which is the referent set for the remaining DMUs. The CRS efficiency frontier is represented by the blue ray starting at the origin, passing through F and from F onwards. The efficiency scores of inefficient units (scores lower than one) are measured by the radial projection of the inefficient units onto the blue line. The relative efficiency of an inefficient DMU depends on the model orientation: input-oriented or output-oriented. Taking A as an example of inefficient DMU, its relative efficiency under input-oriented assumption (*i.e.*, horizontal projection) is the ratio between segments p and q , while its relative efficiency under output-oriented assumption (*i.e.*, vertical projection) is the ratio between segments r and s . The projection of inefficient units onto the efficient frontier determine the improvement targets that, if achieved, would make efficient the inefficient units. For instance, DMU A should reduce its

input by 8% to become efficient under an input oriented CRS DEA, and increase its output by 21% to become efficient under an output oriented CRS DEA.

Under VRS assumption, the strong efficient frontier is formed by the orange line connecting \overline{AFEC} . The extremes of this frontier (*i.e.*, A and F) are extended with parallel lines to the axes to build the weakly efficient frontier. \overline{AF} is the portion of the frontier with increasing returns to scale, while in \overline{FE} and \overline{EC} the returns to scale decreases. As expected, we can observe notorious differences depending on whether a CRS or VRS assumption is considered. For instance, unit E is inefficient under CRS formulation but efficient under VRS. The efficiency values (as well as targets) are also different in both cases, since the projection for unit G under CRS is g while it is g' under the VRS formulation.

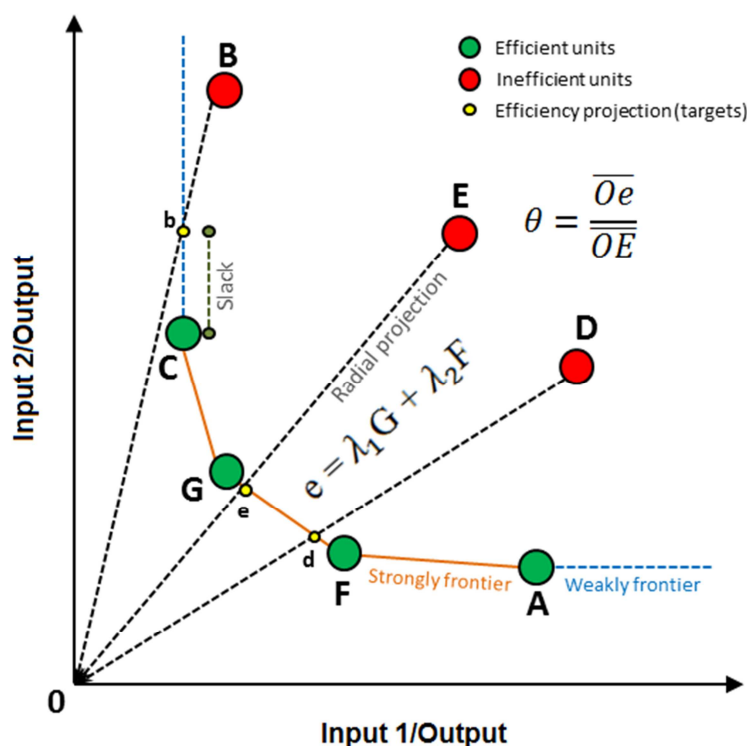


Figure 1.18. Illustration of DEA results: case with two inputs and one output.

Figure 1.18 illustrates a case of DEA considering two inputs and one output. The convex line (depicted in orange) which connects the efficient units (\overline{AFEC}) forms the

efficient frontier. It means that units A, F, G and C need lower input values than B, E and D to obtain the same output level. Inefficient units (B, E, D) are radially projected onto the efficient frontier (b, e, d) to determine the targets that, if achieved, would make them efficient. The composite efficient unit for E is given by point e, where the efficient frontier is crossed by segment OE , connecting the inefficient DMU (E) with the origin (radial projection). Thus, the efficiency of E is given by the ratio $\frac{Oe}{OE}$. The efficiency score represents the extent to which all the inputs should be proportionally reduced to reach the efficient frontier. Furthermore, the inefficient units projection allows to identify benchmarks. For instance, units G and F are the reference set (peer group) for E because b is placed in the segment (*i.e.*, facet) connecting them. It means that the efficiency of E is evaluated using a linear combination of G and F (using linear weights from the DEA model: $e = \lambda_1 G + \lambda_2 F$). Thus, E should operate in a similar way to these units so as to improve its performance. The inefficient unit B is not projected on the strongly frontier but in the weakly frontier, which is obtained by extending the efficient frontier (\overline{AFGC}) parallel to the axes. This occurs because B shows a slack measured by \overline{bC} distance, which means that B presents an excess in input 2 which implies an extra reduction in inputs (equals to bC) to become strongly efficient.

For further information about DEA models and extensions the reader is referred to Cook and Seiford (2009), Cooper *et al.* (2004), Hosseinzadeh Lotfi *et al.* (2013) and section 3.2.1. of this work. Other methodological developments in DEA such as the distinction between *discretionary* variables (D) (*i.e.*, input variables which can be proportionally reduced) and *non-discretionary* variables (ND) (*i.e.*, those input variables not subject to management control), or the super-efficiency methodology in DEA (*i.e.*, those models that allow to further discriminate among efficient units) are also discussed in section 3.2.1.2 and 3.2.1.3, respectively.

1.5.3. Malmquist Productivity Index

The previous explained DEA methodology uses snapshot information and applies to a certain time period (*e.g.*, a single year, month, etc.). In order to evaluate temporal data and identify productivity changes over time the Malmquist Productivity Index (MPI) is used. MPI is defined as the ratio of the efficiency measures for the same

production unit in two different time periods. MPI was first suggested by Malmquist (1953) as a quantitative index in the analysis of consumption of inputs (Färe and Grosskopf, 1992), combining ideas on the measurement of efficiency from Farrell (1957) and the measurement of productivity from Caves *et al.* (1982). MPI has been used in a wide range of applications, such as hospitals (Färe *et al.*, 1994), banks (Grifell-Tatje and Lovell, 1996), agricultural productivity (Fulginiti and Perrin, 1997), countries (Taskin and Zaim, 1997), etc.

The Malmquist input-based productivity index for any unit between periods t and $t+1$ ($t < t + 1$) with frontier technology of period o as a reference, can be formulated as:

$$M_o = \left[\frac{D_o^t(x_o^t, y_o^t)}{D_o^t(x_o^{t+1}, y_o^{t+1})} \frac{D_o^{t+1}(x_o^t, y_o^t)}{D_o^{t+1}(x_o^{t+1}, y_o^{t+1})} \right]^{1/2} \quad \text{Eq. 1-5}$$

Under this definition, $M_o > 1$ means efficiency decrease from t to $t + 1$; $M_o = 1$, denotes that efficiency is unchanged from t to $t + 1$, while $M_o < 1$ indicates an efficiency increase from t to $t + 1$.

MPI can be decomposed into two components: one measuring the technical change (TEC_o) and the other measuring the frontier shift (FS_o). These components allow identifying the strategy shifts of individual DMUs based upon isoquant changes, revealing sources and patterns of productivity change and making judgments on whether or not such strategy shifts are promising. The decomposition is as follows:

$$M_o = TEC_o FS_o \quad \text{Eq. 1-6}$$

$$\text{with } TEC_o = \frac{D_o^t(x_o^t, y_o^t)}{D_o^{t+1}(x_o^{t+1}, y_o^{t+1})}, FS_o = \left[\frac{D_o^{t+1}(x_o^{t+1}, y_o^{t+1})}{D_o^t(x_o^{t+1}, y_o^{t+1})} \frac{D_o^{t+1}(x_o^t, y_o^t)}{D_o^t(x_o^t, y_o^t)} \right]^{1/2} \quad \text{Eq. 1-7}$$

The term TEC_o measures the change in the technical efficiency relative to the rest of DMUs. $TEC_o > 1$ indicates a decline in technical efficiency (*i.e.*, $\theta_o^t > \theta_o^{t+1}$), $TEC_o = 1$ no improvement or decline, and $TEC_o < 1$ an improvement (*i.e.*, $\theta_o^t < \theta_o^{t+1}$). On the other hand, the term FS_o measures the frontier shift between time periods t and $t + 1$. In

this case, $FS_o > 1$ indicates a regress of the frontier, $FS_o = 1$ no frontier shift, and $FS_o < 1$ a progress of the frontier.

The calculation of the MPI requires two single periods and two mixed (cross) period measures. The technical efficiency for the first mixed period model ($D_o^t(x_o^{t+1}, y_o^{t+1})$) is obtained as follows:

$$\begin{aligned}
 D_o^t(x_o^{t+1}, y_o^{t+1}) &= \min \theta \\
 \text{s. t. } \sum_{j=1} \lambda_j x_{ij}^t &\leq \theta x_{io}^{t+1} \quad \forall i \in I \\
 \sum_{j=1} \lambda_j y_{rj}^t &\geq y_{ro}^{t+1} \quad \forall r \in R \\
 \sum_{j=1} \lambda_j &= 1 \\
 \lambda_j &\geq 0 \quad \forall j \in J, i \in I, r \in R \quad \theta \text{ unconstrained}
 \end{aligned} \tag{Eq. 1-8}$$

where x_{io}^{t+1} and y_{ro}^{t+1} are the i^{th} input and the r^{th} output for DMU_o in time period $t + 1$, and θ is the technical efficiency score determining the inputs reduction to produce the given output level. In essence, in this model, the technical efficiency of DMU_o in time period $t+1$ is assessed against the efficient frontier of time period t .

The model for the second mixed period ($D_o^{t+1}(x_o^t, y_o^t) = \min \theta$) is calculated by reversing the period of the frontier and the DMU_o analyzed (*i.e.*, inputs and outputs of period t instead of $t + 1$ are used for DMU_o, while inputs and outputs of period $t+1$ instead of t are used for the efficient frontier).

Finally, the calculations of the two single periods are obtained by applying Eq. 1-3 (or any other relevant DEA model) in time periods t and $t + 1$, respectively.

Note that this formulation corresponds to a VRS input-oriented MPI, consistent with the rest of the contribution, but MPI is general enough to accommodate other DEA models if required.

Figure 1.19 further clarifies the previous MPI concepts. The inputs of each unit in time period t are represented using orange dots, whereas the efficient frontier in t is represented by the orange line. Blue dots represent the inputs of the units in time period $t + 1$, and the efficient line in this time period is represented by the blue line. In order to illustrate changes in technical efficiencies, if a unit (*e.g.*, unit D) shows technical efficiencies of 0.5 and 0.8 in t and $t+1$ respectively, then TEC_o will be lower than one, which means improvement in TEC_o . Despite this, changes in frontier FS_o between t and $t+1$ can also vary over time and modify the MPI scores. For example, even if the technical efficiency of unit D could be improved between t and $t+1$, the MPI can indicate a regression of the DMU as a result of the regression of the frontier, as reflected by a $FS_o > 1$. Therefore, the relative movement of any given unit over time depends on both its position relative to the corresponding frontier (technical efficiency) and the position of the frontier itself (technology change). If inefficiency is not noticed, then productivity growth over time will be unable to distinguish between improvements that derive from the unit ‘catching up’ to its own frontier, or those resulting from the frontier itself ‘shifting up’ over time.

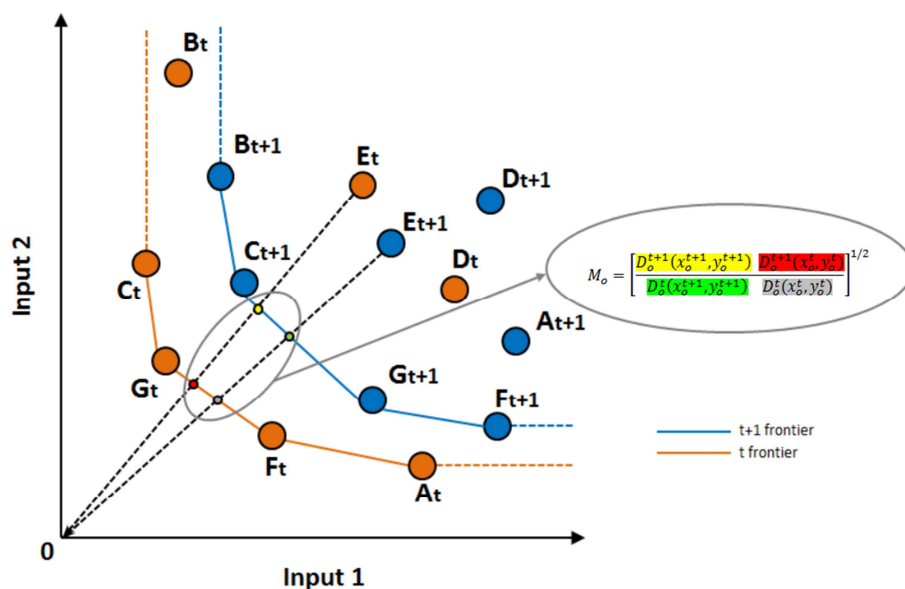


Figure 1.19. Malmquist productivity index illustrative example for period t and $t + 1$.

We would like to remark that problems in Eq. 1-8 can be infeasible. The reason for this is analogous to that causing infeasibilities in super-efficiency models (see section 3.2.1.3): the efficient frontier of these problems is built without the DMU analyzed (note the difference in time periods between the left-hand side and the right-hand side of the constraints). Despite the possible infeasibilities from Eq. 1-8, a numerical value is needed as a result of these models, otherwise the MPI assessment cannot be determined. To overcome this limitation, we use the algorithm proposed by Seiford *et al.* (1999) and described in Figure 3.3 (see in more detail in section 3.2.3.) to obtain such numerical value.

1.6. Outline: problems addressed

Real industrial problems aiming at obtaining more efficient and sustainable processes can be addressed by using the mathematical programming tools previously described. A brief summary of the problems addressed in this thesis follows, while these problems are detailed and developed in Chapters 2 and 3.

1.6.1. Multiperiod optimization (Article 1, Chapter 2)

Cryogenic air separation to produce nitrogen, oxygen and argon with high quality requirements is an energy-intensive industrial process that requires large quantities of electricity. The complexity in operating these networks systems, namely electricity prices and products demands, which vary every hour, creating a clear need for computer-aided tools to attain economic and energy savings. In this article, we present a multiperiod mixed-integer linear programming (MILP) model to determine the optimal production schedule of an industrial cryogenic air separation process so as to maximize the net profit by minimizing energy consumption (which is the main contributor to the operating costs). The capabilities of the model are demonstrated by means of its application to an existing industrial process, where significant improvements are attained through the implementation of the MILP (Figure 1.20).

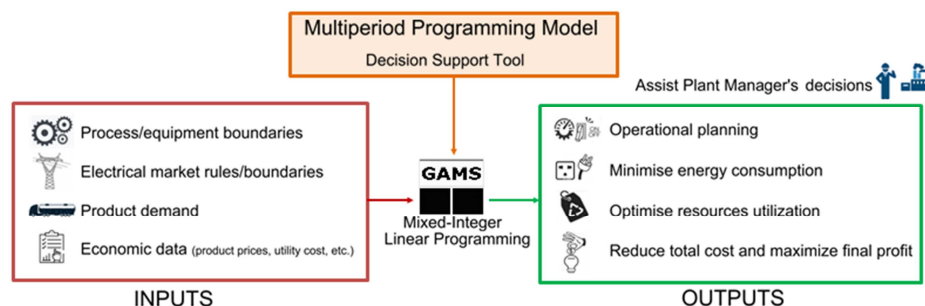


Figure 1.20. Graphical abstract of article 1: Multiperiod model for the optimal production planning in the industrial gases sector.

1.6.2. Data Envelopment Analysis and Malmquist Productivity for efficiency assessment (Article 2, Chapter 3)

The current trend towards improving energy efficiency in industry calls for advanced decision-support tools for quantifying the level of efficiency of industrial facilities. This work applies Data Envelopment Analysis (DEA) to assess the performance of a set of 34 Air Separation Units (ASUs) producing industrial gases via air distillation. We identify the best ASUs according to energy efficiency and productivity criteria and define improvement targets for the units found inefficient. Furthermore, we analyze the temporal evolution of the efficiency scores using the Malmquist Productivity Index (MPI), which is calculated from real data gas companies operating plants around the world for years 2013-2016. Our results provide insight on how to improve the efficiency of existing plants by identifying sources of inefficiency and reference facilities that could be used for benchmarking (Figure 1.21).

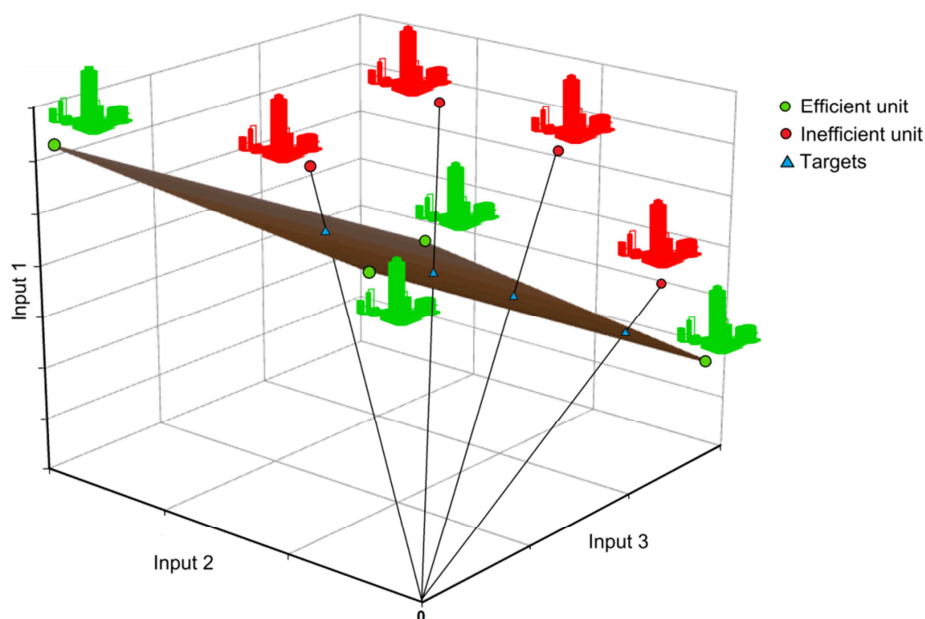


Figure 1.21. Graphical abstract of article 2: Productivity and energy efficiency assessment of existing industrial gases facilities via Data Envelopment Analysis and the Malmquist Index.

1.7. Conclusions

The works of this thesis have been focused on creating mathematical programming models to assist the decision making of plant managers and engineers from air separation units. Several models based on mathematical programming have been developed in order to increase the profitability of these plants while reducing their energy consumption and improving their energy efficiency. These contributions aims to promote the move towards more sustainable energy processes in the industrial gases sector without compromising their economic growth. The general conclusions and knowledge derived from this thesis are stated below. Note that further discussions and conclusions can be found in each corresponding chapter (sections 2.5. and 3.4).

- A multiperiod model tool for the optimal scheduling of an industrial air separation unit has been developed. The tool relies on maximizing profit by minimizing energy consumption, and identifies the most profitable way to operate the plant. This tool assists engineers in their daily activities by effectively optimizing production planning, energy rules, sales and product

stocks, while considering external constraints and dynamic market conditions.

- Data Envelopment Analysis has been applied to assess the energy efficiency of existing industrial facilities. This method allows ranking a set of air separation units according to energetic and efficiency aspects. Furthermore, the tool identifies sources of inefficiency in each air separation unit and establishes quantitative targets for them to become efficient.
- MPI has been used to study the productivity of the air separation units over time.
- The capabilities of the mathematical programming tools developed in this thesis have been tested by applying them to real world cases studies and using real data from air separation units. Actually, some tools are currently used in an air separation plant facilitating the decision making of the plant manager and obtaining important economic improvements in the process operation.
- The tools developed in this thesis can be extended to other plants that the company has in the rest of the world and apply them as good practices to improve the management and efficiency of their processes.
- The two previous methods can be applied in a wide range of energy intensive industrial processes (*i.e.*, chemical, automotive, metallurgy, etc.) to minimize energy losses in their process moving towards a more sustainable world. Especially, the method developed to optimize the scheduling in an industrial air separation unit constitutes a promising alternative for any other energy-intensive industrial process (*e.g.*, iron, cement, steel, petroleum refinery, bulk chemical processes) where energy savings play an important role.

1.8. Future work

There are many possibilities to improve and expand the work started in this thesis. We state below some ideas for potential research that could be developed in the future:

- In a competitive environment, obtaining the maximum profit plays a key role in the company success. Logistics costs include a portion of the total costs of industrial gases producers but can be reduced through supply chain optimization. Therefore, optimization of transportation costs in both, the bulk industrial gases delivery and the fleet size used to serve the customers could be attained by means of a mathematical model devoted to this aim.
- Investigate and evaluate the benefits of introducing cryogenic energy storage (CES) in an air separation unit to store energy during off-peaks electrical periods and releasing it during on-peak hours. With CES, instead of venting overproduced products, it is possible store them and recover energy from them to increase the plant flexibility for load shifting. Power generated from CES system can be sold to the electricity market. Furthermore, the plant can also participate in the ancillary services market by providing operating reserve capacities which can be dispatched upon request. These reserves are demanded when real-time electricity demand in the grid is higher than the supply.
- Introduce life-cycle assessment (LCA) to evaluate environmental impacts associated with the stages of a product's life from raw material extraction through materials processing, manufacture, distribution, use, repair and maintenance, and disposal or recycling. Compiling an inventory of relevant energy and material inputs and environmental releases can help designers to develop more environmentally-friendly products. Evaluating the potential impacts associated with identified inputs and releases can help to prioritize actions.
- Introduction stochastic formulations considering data uncertainty in order to provide more robust solutions. For instance, one alternative is to develop mathematical algorithms that would allow accurate prediction of the electricity prices in the future, which would facilitate the management of electricity purchases. This could be linked with the current mathematical

model developed in this thesis and it could represent important savings to the company.

1.9. Nomenclature

Abbreviations

ASU	air separation unit
BCC	banker, charnes and cooper
CAGR	compound annual growth rate
CCR	charnes cooper and rhodes
CES	cryogenic energy storage
CRS	constant returns to scale
DCAC	direct contact after cooler
DEA	data envelopment analysis
DMU	decision making unit
GAN	gas nitrogen
GOX	gas oxygen
LAR	liquid argon
LCA	life-cycle assessment
LIN	liquid nitrogen
LOX	liquid oxygen
LP	linear programming
LP column	low pressure column
MINLP	mixed integer nonlinear programming
MILP	mixed-integer lineal programming
MOO	multi-objective optimization
MP column	medium pressure column
MPI	malmquist productivity index
NLP	nonlinear programming
PSA	pressure swing adsorption
SOO	single-objective optimization
VRS	variable returns to scale

Sets

i	set of inputs indexed by i
j	set of decision making units indexed by j
r	set of outputs indexed by r
t	set of time intervals indexed by t

Subsets

D	set of inputs which are discretionary
ND	set of inputs which are non discretionary

Variables

F	objective function
FS_o	frontier technology shift in DMU_o
G	inequality constraints
h	equality constraints
λ_j	linear weight for every single DMU_j to form a linear combination
M_o	Malmquist index to measure efficiency changes in DMU_o
θ	relative efficiency score in input oriented model
o	assessed DMU
S_i^-	amount of input i that, if reduced, shifts the DMU_o projection until the strongly efficient frontier
S_r^+	amount of output r that, if increased, shifts the DMU_o projection until the strongly efficient frontier
TEC_o	technical efficiency change in DMU_o
W	feasible region
x	vector of continuous variables
y	vector of integer variables

Parameters

ε	non-archimedean value designed to enforce strict positivity on the variables
---------------	--

m	number of inputs consumed by a DMU
n	number of decision making units
p	vapour pressure
s	number of outputs produced by a DMU
x_{ij}	amount of input i consumed by DMU $_j$
y_{rj}	amount of output r produced by DMU $_j$

1.10. References

Almqvist E. History of Industrial Gases. Kluwer Academic/Plenum Publishers 2003.

Banker RD, Charnes A, Cooper WW. Some models for estimating technical and scale inefficiencies in data envelopment analysis. Manage. Sci 1984.

Birewar DB, Grossmann IE. Simultaneous production planning and scheduling in multiproduct batch plants. Industrial and Engineering Chemistry Research 1990;29:570-580.

Brooke A, Kendrick D, Meeraus A, Raman R, America U. The general algebraic modeling system. GAMS Dev. Corp 1998.

Bussieck MR, Drud A. SBB: A new solver for mixed integer nonlinear programming. GAMS Dev. Corp. 2001.

Caves W, Christensen LR, Diewert WE. The economic theory of index numbers and the measurement of input, output and productivity. Econometrica 1982;50:1393-1414.

Charnes A, Cooper WW. Management Models and Industrial Applications of Linear Programming. Management Science 1957;4(1):1:113.

Charnes A, Cooper WW, Rhodes E. Measuring the efficiency of decision making units. *Eur. J. Oper. Res.* 1978;2:429–444.

Cooper WW, Seiford LM, Zhu J. *Data Envelopment Analysis: History, models and interpretations.* Kluwer Academic Publishers 2004.

Cooper WW, Seiford LM, Zhu J. *Handbook on data envelopment analysis* 2nd ed. New York: Springer; 2011.

Cook WD, Seiford LM. Data envelopment analysis (DEA) – Thirty years on. *Eur. J. Oper. Res.* 2009;192:1–17.

Dantzig GB, Orden A, Wolfe P. The generalized simplex method for minimizing a linear form under linear inequality restraints. *Pacific J. Math.* 1955;5:183–195.

Dienel H. *Linde: History of a technology corporation 1879-2004.* Palgrave MacMillan 2004.

European Environment Agency. *Energy and climate change (Article).* Aug. 2017.

Enerdata. *Global energy trends, 2017 edition. (Report).* 2017.

(EIA) U.S. Energy Information Administration. *World petroleum and other liquid fuels. International Energy Outlook 2014.*

(EIA) U.S. Energy Information Administration, 2017. *International Energy Outlook 2017.*

Fare R, Grosskopf S, Lindgren B, Ross P. Productivity changes in Swedish pharmacies 1980-1989: A non-parametric Malmquist approach. *The Journal of Productivity Analysis* 1992;3:85-101.

Fare R, Grosskopf S, Norris M, Zhang Z. Productivity growth, technical progress, and efficiency change in industrialized countries. *The American Economic Review* 1994;84(1):66-83.

Farrell MJ. The measurement of productive efficiency. *J. R. Stat. Soc. Series A*, 1957;253–281.

Fulginiti EL, Perrin RK. LDC agriculture: Nonparametric Malmquist productivity indexes. *Journal of Development Economics* 1997;53(2):373-390.

Gasworld. Regional Focus-Iberia. (Report). 2017.

Grifell-Tatje E, Lovell C. Profits and productivity. *Manage. Sci.* 1999;45(9):1177-1193.

Grossmann IE, Caballero JA, Yeomans H. Advances in mathematical programming for the synthesis of process systems. *Lat. Am. Appl. Res.* 2000;30:263–284.

Grossmann IE, Viswanathan J, Vecchietti A, Raman R, Kalvelagen E. GAMS/DICOPT: A discrete continuous optimization package. GAMS Corp. Inc 2002.

Ghulam A, Khalid Z, Tan S, Faiza S. Does energy consumption contribute to climate change? Evidence from major regions of the world. *Renewable and Sustainable Energy Reviews* 2014;36:123-134.

Häring HW. Industrial gases processing. Wiley-VCH 2008.

Hosseinzadeh F, Jahanshahloo GR, Khodabakhshi M, Rostamy-Malkhlifeh M, Moghaddas Z, Vaez-Ghasemi M. A review of ranking models in Data Envelopment Analysis. *J. Appl. Math.* 2013;1–20.

IBM ILOG CPLEX V12. 1. User's Manual for CPLEX. Int. Bus. Mach. Corp. 2009.

Ierapetritou MG, Wu D, Vin J, Sweeney PG, Chigirinsky M. Cost minimization in an energy-intensive plant using mathematical programming approaches. *Industrial and Engineering Chemistry Research* 2002;41:5262-5277.

(IEA) International Energy Agency. Energy efficiency. (Report) France, 2017.

Jaimes AL, Martinez SZ, Coello CAC. An introduction to multiobjective optimization techniques. *Optim. Polym. Process* 2009;29-57.

Land AH, Doig AG. An automatic method for solving discrete programming problems. *50 Years Integer Program. 1958-2008* 2010;105-132.

Linde W. *The Invisible Industries/The Story of the Industrial Gas Industry*. International Oxygen Manufacturers Association (IOMA), 1997.

Lozano S, Iribarren D, Moreira MT, Feijoo G. The link between operational efficiency and environmental impacts. A joint application of Life Cycle Assessment and Data Envelopment Analysis. *Sci. Total Environ.* 2009;407:1744-54.

Malmquist, S. Index numbers and indifference curves. *Trabajos de Estadística* 1953;4:209-242.

Messer Group. www.messergroup.com (accessed 17.05.2018)

Optimization D. Xpress-optimizer reference manual. Dash Optim. Ltd., Englewood Cliffs 2007.

Optimization G. Gurobi optimizer reference manual. 2012. URL <http://www.gurobi.com> 2, 1–3.

Persistence Market Research. Global Market Study on Industrial Gases: Oxygen to Witness Substantial Growth During 2017 – 2025. (Report). New York, March 2018.

Research And Markets. Global Industrial Gases Market Size, Market Share, Application Analysis, Regional Outlook, Growth Trends, Key Players, Competitive Strategies and Forecasts, 2017 to 2025. (Report) September 2017.

Riahi K, Dentener F, Gielen D, Grubler A, Jewell J, Klimont Z, Krey V, McCollum DL, Pachauri S, Rao S. Energy pathways for sustainable development. 2012.

Rockström J, Steffen W, Noone K, Persson Å, Chapin FS, Lambin E, Lenton TM, Scheffer M, Folke C, Schellnhuber HJ, Nykvist B, de Wit CA, Hughes T, van der Leeuw S, Rodhe H, Sörlin S, Snyder PK, Costanza R, Svedin U, Falkenmark M, Karlberg L, Corell RW, Fabry VJ, Hansen J, Walker B, Liverman D, Richardson K, Crutzen P, Foley J. Planetary boundaries: Exploring the safe operating space for humanity. *Ecol. Soc.* 2009;14.

Rockström J, Sachs JD, Öhman MC, Schmidt-Traub G. Sustainable Development and Planetary Boundaries. Backgr. Res. Pap. Submitt. to High Lev. Panel Post-2015 Dev. Agenda. Paris, New York Sustain. Dev. Solut. Netw. 2013.

Sahinidis NV. BARON: A general purpose global optimization software package. *J. Glob. Optim.* 1996;8:201–205.

Savitz AW, Weber K. The triple bottom line. San Fr. Jossey-Bass. 2006.

Schrage L. LINDO: Optimization software for linear programming. Lindo Syst. Inc. 1995.

Seiford LM, Zhu J. Infeasibility of super-efficiency data envelopment analysis models. *INFOR* 1999;37:174–187.

Smith AR, Klosek JA. Review of air separation technologies and their integration with energy conversion processes. *Fuel Processing Technology* 2001;70(2):115-134.

Steffen W, Richardson K, Rockstrom J, Cornell SE, Fetzer I, Bennett EM, Biggs R, Carpenter SR, de Vries W, de Wit CA, Folke C, Gerten D, Heinke J, Mace GM, Persson LM, Ramanathan V, Reyers B, Sorlin S. Planetary boundaries: Guiding human development on a changing planet. *Science* 2015;347.

Susana M, Marcelo J. A multiperiod model for production planning and design in a multiproduct batch environment. *Mathematical and Computer Modelling* 2009;49:1372-1385.

Taskin F, Zaim O. Catching-up and innovation in high- and low-income countries. *Economics Letters* 1997;54(1):93-100.

Tester JW, Drake EM, Driscoll MJ, Golay M, Driscoll, Peters WA. *Sustainable Energy: choosing among options*. MA: MIT Press 2005;870.

The Linde Group. *Air separation plants. History and technological progress in the course of time (Report)*. 2018.

Van Vuuren D, Nakicenovic N, Riahi K, Brew-Hammond A, Kammen D, Modi V, Nilsson M, Smith K. An energy vision: the transformation towards sustainability—interconnected challenges and solutions. *Curr. Opin. Environ. Sustain.* 2012;4:18–34.

Winnacker-Küchler. *Chemische Technik*. Wiley-VHC 1983;3:566-650.

Winston WL, Albright SC. Practical Management Science: Spreadsheet Modeling and Applications. Duxbury Press 1997.

Zhu Y, Legg S, Laird CD. A multiperiod nonlinear programming approach for operation of air separation plants with variable power pricing. American Institute of Chemical Engineers 2011;57:9

Chapter 2.

Optimal operation planning in industrial gases production

UNIVERSITAT ROVIRA I VIRGILI
MULTIPERIOD MODELLING PLANNING AND PRODUCTIVITY AND ENERGY EFFICIENT ASSESSMENT OF AN INDUSTRIAL GASES
FACILITY

David Fernández Linares

2. Optimal operation planning in industrial gases production

Multiperiod model for the optimal production planning in the industrial gases sector

David Fernández^{a,b}, Carlos Pozo^c, Rubén Folgado^a, Gonzalo Guillén-Gosálbez^{b,c},
Laureano Jiménez^b

^a *Messer Ibérica de Gases S.A.U, Autovía Tarragona-Salou, km. 3.8, 43480, Vilaseca, Tarragona, Spain*

^b *Departament d'Enginyeria Química, Universitat Rovira i Virgili, Av. Països Catalans, 26, 43007, Tarragona, Spain*

^c *Department of Chemical Engineering, Centre for Process Systems Engineering, Imperial College London, South Kensington Campus, London SW7 2AZ, United Kingdom*

Keywords: Energy-intensive process; Multiperiod model; Optimization; Production scheduling; Cryogenic air separation.

2.1. Introduction

At present, cryogenic air distillation is the most efficient technology (Smith *et al.*, 2001) to obtain technical gases (*i.e.*, nitrogen, oxygen and argon) in large quantities with high standard requirements. Compression and liquefaction in the cryogenic separation require large amounts of electricity which leads to large operating costs. Therefore, it is not surprising that energy saving opportunities in the air separation technology have been object of study since long ago (Yan *et al.*, 2010). Xenos *et al.* (2015) attempted to reduce power consumption and therefore operational costs in a network of compressors by introducing models to estimate the best distribution of the load. Similarly, Kopanos *et al.* (2015) developed a mathematical framework for compressors operations in the context of air separation plants to simultaneously

optimize maintenance and operational tasks. Üster and Dilaveroglu extended the scope of the analysis beyond compression stages to address the optimization of a natural gas network while satisfying customers' demand (Üster *et al.*, 2014).

We note that in the present contribution we address a more complex problem, as we consider the volatility of the electricity market price. Electricity is purchased in an organized wholesale market, also called “spot market”, which works similarly in all European Union regions. OMIE is the electricity market operator who manages the “spot market” in the Iberian Peninsula (OMI-Polo Español S.A., 2016), similarly as Nord Pool Spot does in the Nordic countries (Nord Pool Spot, 2016), EPEX Spot in France (EPEX, 2016), Germany and other Central European countries, or GME (GME, 2016) in Italy. The electricity market allows the purchase and sale of electricity between agents (producers, consumers, traders, etc.) at a price subject to market fluctuations (Madlener *et al.*, 2012). Furthermore, the steeping up of renewable energy sources in electricity generation promoted since the European directive on renewable energies (European Commission, 2001), has increased the difficulty of balancing supply and demand. In this context, dynamic electricity tariffs (*i.e.*, dynamic pricing) encourage customers to shift demand away from peak times, thus facilitating demand-side response to reduce peak load. See (Klaassen *et al.*, 2016) and (Granell *et al.*, 2016).

The electricity price in this market is daily set for the next 24 hours, and it is fixed based on the balance between the electricity supply and demand in the electrical system. Unavailability of power plants, fuel costs, demand profiles or weather conditions affect the “spot market” price schedules, which vary from day to day or, even, from hour to hour, with an eventual risk of uncontrolled prices. This fact forces companies to plan ahead the operation (*e.g.*, switches in equipment loads, startups and shutdowns of operation units) in order to improve their profit while still fulfilling contractual requirements, such as product demand and energy rules.

Furthermore, in order to reduce the risk of uncontrolled “spot market” electricity prices, one can resort to a “futures market”, in which power purchase operations are made several months or years ahead the electricity is consumed. In this market, companies purchase electrical power blocks that will be billed at the time of

consumption at a price fixed in the present (here and now). In Spain, OMIP (Iberian Energy Derivatives Exchange, 2016) is the main operator responsible for the management of trading operations in the electricity “future market”. Contracts in this market constitute a means of managing the risk of facing future high electricity prices, which would result in extremely large operating costs and therefore low profitability. Companies in the chemical industry, *inter alia*, need accurate prices forecasts to make optimal plans. For this reason, they hire part of their electrical consumption at a fixed price in this market to minimize the exposure to “spot market” prices volatility (*i.e.*, the greater power blocks purchased in the “future market”, the less exposure to “spot market” fluctuations).

Furthermore, all the hours in a year are grouped into six tariff periods (P1 to P6) in terms of energy and also power available, where higher tariff periods show lower electricity prices (*i.e.*, P1 is the most expensive tariff and P6 is the cheapest). This causes that in one single day, several tariff periods with great pricing differences between them may apply. Users must then select the amount of energy to contract in each period according to their energy needs.

In practice, the electricity cost is subjected to the variability of both “spot” and “future” markets, which can significantly increase the production cost unless proper actions are put in place in order to hedge against the associated risk. The effect of these dynamic tariffs has been widely studied in the context of both domestic (see Gaiser *et al.* (2014); Gutiérrez-Alcaraz *et al.* (2016); Labeeuw *et al.* (2015); Widén (2014) and Finn *et al.* (2013)) and non-domestic users (see Kamilaris *et al.* (2014)). In particular, the benefits that the industry sector could attain from dynamic tariffs have already been acknowledged (Granell *et al.*, 2016). Note that this problem is even more complex in industrial scenarios, since the remarkable number of customers placing orders (*i.e.*, nitrogen, oxygen and argon) and the diversity of sectors they may come from (*e.g.*, industrial, medical and food industry) makes it hard to forecast the electricity needs precisely. This forecasting, however, is essential for boosting competitiveness and maintaining income stability. In order to deal with this volatility, planning and scheduling tools based on mathematical programming arise as a promising alternative, as they provide a sound basis for the rational operation of plants under dynamic tariffs

(Kostin *et al.*, 2011; Mele *et al.*, 2009; Cristóbal *et al.*, 2012a; Cristóbal *et al.*, 2012b). In a pioneering work, Daryanian *et al.* (1989) showed the economic benefits of studying the demand response in air separation plants. This methodology was later extended by Karwan *et al.* (2007) and Pulkkinen and Ritala (2008) by incorporating discrete operating decisions. Ierapetritou *et al.* (2002) developed a two-stage stochastic programming approach to determine the optimal schedule that minimizes the operating cost in an energy-intensive air separation plant depending on the power costs. Miller *et al.* (2008) undertook an operating analysis to determine the conditions under which intermittent operation of air separation systems is economically feasible considering peak and off-peak power prices. Zhu *et al.* (2011a) presented a model to determine optimal operating strategies while considering demand and contractual obligations, assuming instantaneous switching time between different operating conditions and constant electricity prices across the operating cycle. Later Zhu *et al.* (2011b) developed a daily multiperiod model where operating conditions under variable electricity pricing as well as nonzero transition times were taken into account. Mitra *et al.* (2012), improved previous works by incorporating accurate discrete decisions (*e.g.*, equipment shutdowns and startups) and corresponding operational constraints to better depict the model behavior. The size of the network analyzed was increased in Puranik *et al.* (2016), who studied the best configuration to supply products from different air separation sources to a set of customers through pipelines, determining which compressors and cold boxes should be into operation in each period so as to cover the global demand. These works relied on two main simplifications in order to keep the mathematical models at a manageable size. The first concerns the modeling of the tariff patterns, which were typically aggregated into fewer lumped periods. This is for instance the case of Zhu *et al.* (2011b), where a single day was split into four different power prices periods and the same pattern was repeated for all the days of the year. Similarly, in Mitra *et al.* (2012) a seasonal electricity prices forecast for a typical week was considered. The second simplification concerns the modeling of the cryogenic separation system itself, where two approaches are typically used: relying on simplified linear models, or reducing the scope of the simulation by leaving some process units out of the analysis. This is the case in Puranik *et al.* (2016), where only pipeline

demand satisfaction is considered and liquid production, product storage, etc. are omitted. Furthermore, the majority of the aforementioned works were developed assuming ideal thermodynamic calculations and making strong assumptions about the demand pattern and power pricing.

In this work we extend previous research in two different ways. On the one hand, we increase the granularity in the modelling of the electricity price pattern in order to account for hourly variations. The proposed formulation defines an accurate production schedule considering not only spot market prices but also power blocks bought in advance in “future market”. Furthermore, the boundaries of the system under study are expanded compared to previous research by including the entire network: production, treatment and conditioning (*i.e.*, compression and liquefaction), storage and loading of delivery tankers. Therefore, both gas and liquid demand are taken into account when optimizing the production schedule. The model is further enhanced by considering the option of outsourcing, that is, of covering part of the demand by purchasing products from an external supplier (*i.e.*, a second air separation unit). This is done by means of contracts that assign an energy amount to the external unit (energy needed to produce and supply the product), which has to be paid to the external supplier. The possibility to cover the pipeline demand from these two different sources (*i.e.*, main air separation unit and external one) offers great flexibility, thereby leading to significant reductions in operational costs if properly managed. The model also considers idle times occurring during equipment start-ups (until the desired product loads and purities are reached).

This systematic approach provides planning alternatives that can result in significant economic benefits and which could be hard to identify otherwise by using standard heuristics or rules of thumb. Furthermore, this approach provides an accurate prediction of the electricity hourly demand of the company. This piece of information plays a key role in the plant profitability, as energy-intensive companies must send forecasted consumption (hours or days in advance) to both the operator and distributor of the electrical system and will be compensated or penalized depending on the error of the forecasting. The capabilities of the proposed strategy are demonstrated by means of a series of case studies based on real data from an existing industrial air separation

plant. In them, we show how the process operation is affected by varying power pricing and limitations as well as by product demand fluctuations.

This article is organized as follows. We first describe the industrial network under study and formally define the problem of interest in Section 2.2. Next, the mathematical formulation used to simulate the problem is presented in Section 2.3. We then demonstrate in Section 2.4 the usefulness of the proposed approach by means of its application to different case studies. In Section 2.5 the conclusions of the work are drawn.

2.2. Problem Statement

2.2.1. Process Description

We address the economic optimization of the industrial network shown in Figure 2.1. The process contains a set of units that convert air, which is the main raw material, into six final products: oxygen gas (GOXP), nitrogen gas (GANP), industrial liquid oxygen (ILOXP), medical liquid oxygen (MLOXP), liquid nitrogen (LINP) and liquid argon (LARP). Final products GOXP and GANP are delivered directly to customers without intermediate storage via pipelines (*i.e.*, GOX and GAN pipelines, respectively). Conversely, final products LARP, MLOXP, ILOXP and LINP are stored in tanks T1, T2, T3 and T4 respectively, where a certain stock must be maintained. Storage tank T5 contains LINP, which allows re-directing a certain amount of this product in scenarios where GANP demand cannot be satisfied by normal operation. In such case, the LINP stored in T5 can be gasified and sent to the GANP pipeline.

Streams are mixed and divided using mixers and splitters, denoted by diamonds and circles, respectively, in Figure 2.1. The topology of the process is as follows. Before entering the main section of the process, the atmospheric air is fed to the pretreatment unit (PTU), where it reaches the input requirements, namely composition, temperature and pressure. The operation of unit PTU includes compression, refrigeration and elimination of impurities, such as solids in suspension or moisture in the raw material. The PTU output stream is sent to the distillation column (DCU) where four intermediate products (*i.e.*, GOXIP, GANIP, LOXIP, LARIP) with different composition, temperature and pressure are obtained. These intermediate products

require further treatment to achieve the customer quality specifications. LOXIP is produced by feeding nitrogen reflux stream from T4 to the DCU. GOXIP and GANIP are treated in compressors CU1-CU3a and CU3b-CU5, respectively, where pressure and temperature conditions are modified to achieve the final requirements in the outlet streams. Compressors CU3a and CU3b correspond indeed to a single compressor (*i.e.*, CU3), which can operate either with GOXIP or GANIP, but not with both at the same time. Note that the definition of two separate units here will allow us to avoid the definition of a disjunction later during the modelling task (see Section 2-3).

The compressor's outputs include final products GOXP and GANP, which can either be directly sent to customers or mixed with other product streams before reaching the pipeline. One alternative for both products is to merge them with externally purchased streams OGOX and OGAN. This is used to cover the high demand needs and also to guarantee the supply in case of incident or accident. OGOX and OGAN are oxygen and nitrogen in gas phase with the same specifications and qualities as the products obtained in the main process, but produced by an external supplier using a distillation column (EDCU) and external compressors ECU1 and ECU2. These units are managed by an external supplier and therefore we only include here the contracts that determine the quantities and prices of their products. OGOX is the only alternative stream that can be used to increase the production of GOXP, while the production of GANP can be complemented not only with OGAN but also with two more alternatives. One is the nitrogen gas produced in the conversion unit CBU, which transforms liquid nitrogen from the storage tank T4 and compressed oxygen gas from CU1-CU3 into nitrogen gas with GANP specifications and liquid oxygen with ILOXP quality, respectively. The second option is to use the output of the vaporizer unit (VU), which transforms the liquid nitrogen stored in the backup tank T5 into GANP, as a result of the vaporization process. This unit operates only when the demand of GANP is very high or when electrical fault or unexpected plant shutdown occur and compromise the product supply to the pipeline in emergency circumstances. LOXIP from DCU can be used to produce MLOXP, ILOXP or both at the same time, depending on their demands. Splitters SP4 and SP9 and mixers MX7 and MX8 are handled to select the final LOXIP service. LQU1 and LQU2 are two liquefiers with

different capacities, which can be used to convert gas nitrogen into liquid nitrogen. The output streams from these units are directly sent to tank T4 as LINP. PU1, PU2, PU3 and PU4 are pumps.

Storage tanks T1-T5 may receive streams in liquid phase coming from several units. When the level in these tanks T1-T4 reaches the upper limit, a certain amount of product can be sent to external tanks ET1-ET4, which are used as an additional storage station to avoid interruptions in the production. The product stored in these tanks, can also be used as final product supply.

The products ILOXP, MLOXP, LINP, LARP are sent to customers in road tankers according to a predefined planning which is known one week in advance, while the remaining are supplied via pipeline.

Due to the nature of the products, in some cases process streams can be safely released to the atmosphere (see for instance vents in SP1, SP2).

Process units consume three main utilities. Electricity (UE) is, by far, the main utility consumed in the process and is used for the operation of a large number of process units (PTU, CU1-CU5, LQU1, LQU2, EDCU, ECU1, ECU2, and PU1-PU9). Gasoil (UGO) is used only to operate VU. Cooling water (UCW) is employed in the refrigeration system of PTU, CU1-CU5, LQU1, LQU2, EDCU, EDCU1, EDCU2 and VU in order to curb the temperature increases in these equipment units and avoid operation failures, but it is not considered in our model since it only represents a 0.5% of the overall cost of utilities. All utilities are purchased from external suppliers.

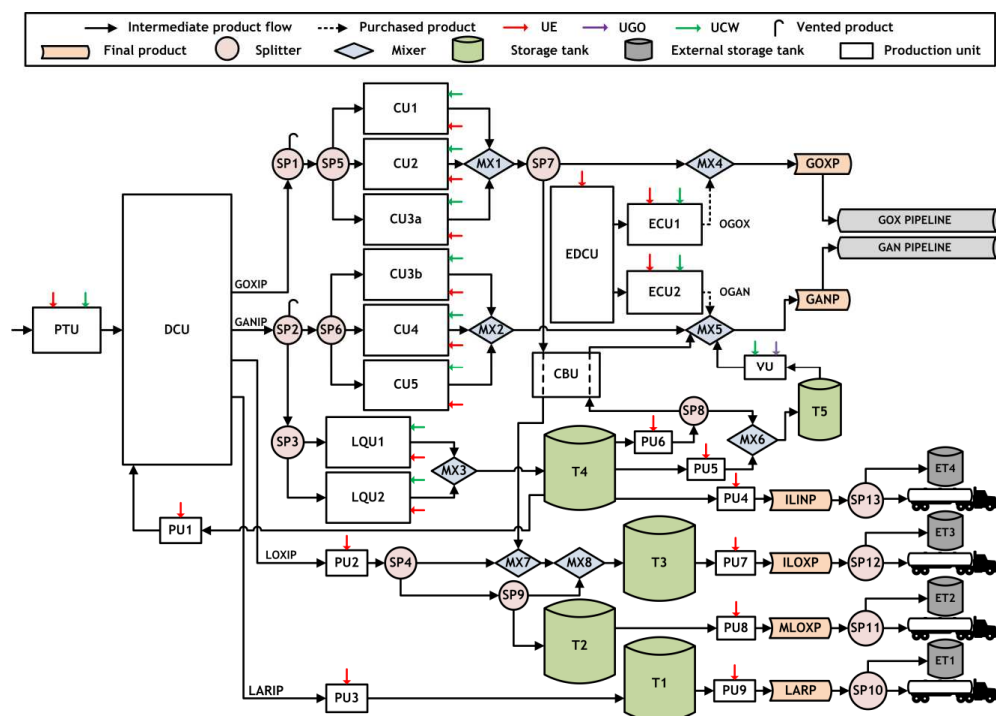


Figure 2.1. Process network studied. Raw material is separated into six final products which are distributed to customers through pipelines and road tankers. Three utilities are used in the process, although cooling water (UCW) is not included in the mathematical model since it only accounts for a marginal share of utilities cost.

2.2.2. Problem Definition

Based on the process network described above, we define the problem of interest. We are given the demand of the final products GANP, GOXP, ILOXP, MLOXP, LARP and LINP, and the economic data associated with the operation of the network (*i.e.*, products prices and utilities costs). Despite the variability in power price and product demand, we assume here that both parameters are known in advance for each time period. Two reasons support these assumptions. First, the variability of electricity prices is limited (to some extent), since only the part exposed to the “spot market” suffers from uncertainty. Second, electricity prices of the “spot market” as well as demands can, in general, be forecasted with enough accuracy in the immediate future (*i.e.*, weeks) using historical data as well as current trends. Specifically, the exact liquid demand is known by the logistic department one week in advance, whereas unexpected

orders implying large gas consumptions (*i.e.*, those that move away from the average consumption) must be warned by customers beforehand.

In this context, the aim of our study is to determine the optimal operation of the network (*i.e.*, equipment startup and shutdown times, stream flow rates, product purchases to external process, etc.) that optimizes its economic performance.

2.3. Mathematical Formulation: Deterministic Model

We have developed a deterministic multi-period optimization model to tackle the problem stated above. The mixed-integer linear programming (MILP) model (Floudas, 1995) contains continuous variables used to model stream flow rates, inventories, utility consumption and economic indicators, whereas binary variables represent logical decisions. In the ensuing subsections we describe the deterministic model, which comprises four main sets of equations: mass balance constraints; capacity constraints; equations describing utility consumption; and the objective function.

2.3.1. Mass-balance constraints

Mass balances are defined for all process units and time periods. A sketch of a generic unit and the sets defined around it is provided in Figure 2.2.

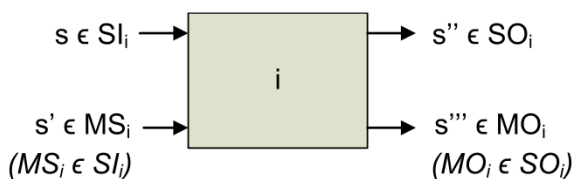


Figure 2.2. Generic process unit.

Let, SI_i and SO_i be the sets of input and output streams of unit i , respectively. In some process units with several input (output) streams, we also define set MS_i (MO_i) as the main stream into (from) that unit. Bearing this in mind, for most units that do not allow material accumulation, Eq. 2-1 applies,

$$\sum_{s \in SO_i} F_{s,t} = \sum_{s' \in SI_i} F_{s',t} \quad \forall t \quad \text{Eq. 2-1}$$

$i \in CBU, CU1 - CU5, ECU1, ECU2, MX1 - MX8, PTU, PU1 - PU9, SP1 - SP14, VU$

where $F_{s,t}$ is a continuous variable denoting the volumetric flow rate of stream s in time period t . Note that equations for mass balances still hold even when using the volumetric flow rate of the stream, as these are expressed in [Nm^3].

In the case of DCU, Eq. 2-2 is used to determine the different output flows.

$$F_{s,t} = \sum_{s' \in MS_i} F_{s',t} YIELDVOL_{i,s} + \sum_{s'' \in SI_i \setminus MS_i} F_{s'',t} YVC_{i,s} \quad \forall t, s \in SO_i, i = DCU \quad \text{Eq. 2-2}$$

Here, $YIELDVOL_{i,s}$ is a parameter accounting for the volumetric yield of stream s in unit i and $YVC_{i,s}$ is a parameter for the correction of the volumetric yield when there is a recycle (*i.e.*, stream from T4) into the DCU.

In the case of process unit CBU, mass balances are computed for nitrogen and oxygen streams separately, as these streams are not mixed inside the unit. To model this, we make use of sets MS_i and MO_i , which will both be defined for the same substance (*i.e.*, oxygen) regardless of the phase (*i.e.*, liquid or gas, see Eq. 2-3 and Eq. 2-4). The ratio between nitrogen and oxygen required for the appropriate operation of the CBU is given by the CF parameter, as illustrated in Eq. 2-5.

$$\sum_{s \in MO_i} F_{s,t} = \sum_{s' \in MS_i} F_{s',t} \quad \forall t, i = CBU \quad \text{Eq. 2-3}$$

$$\sum_{s \in SO_i \setminus MO_i} F_{s,t} = \sum_{s' \in SI_i \setminus MS_i} F_{s',t} \quad \forall t, i = CBU \quad \text{Eq. 2-4}$$

$$CF \sum_{s \in MS_i} F_{s,t} = \sum_{s' \in SI_i \setminus MS_i} F_{s',t} \quad \forall t, i = CBU \quad \text{Eq. 2-5}$$

For the storage tanks T1-T5, accumulation must be taken into account, as reflected in Eq. 2-6 and Eq. 2-7.

$$INV_{i,t} + TIME \left(\sum_{s \in SI_i} F_{s,t} - \sum_{s' \in SO_i} F_{s',t} \right) = INV_{i,t} \quad \forall i \in TI, t = 1 \quad \text{Eq. 2-6}$$

$$INV_{i,t-1} + TIME \left(\sum_{s \in SI_i} F_{s,t} - \sum_{s' \in SO_i} F_{s',t} \right) = INV_{i,t} \quad \forall i \in TI, t > 1 \quad \text{Eq. 2-7}$$

Here, $INV_{i,t}$ is a continuous variable representing the inventory of tank i in time period t , $TIME$ is a parameter denoting the duration of a time period, and TI is the set of units i which are tanks (*i.e.*, $TI = \{T1, T2, T3, T4, T5\}$). Note that for the first time interval, we require the definition of parameter $INV_{i,t}$, which provides the initial inventory of tank i (see Eq. 2-6).

In order to mimic real operation, the model includes the possibility of purchasing two outsourcing streams OGOX and OGAN to satisfy the demand of such products in the global network. The price of these products is given by the amount of electricity consumed in EDCU, ECU1 and ECU2 to produce them, and it is finally linked to the demanded flow via contractual arrangements. Note however that the model has no control over the operating conditions or the flows distribution in these units, which are decided by the external supplier. Nevertheless, EDCU has a limitation on the amount of OGAN which can be produced (and hence obtained) in comparison to the amount of OGOX, due to the air composition and the process design. We model this using parameter $CF2$, as shown in Eq. 2-8.

$$\sum_{s' \in SO_i \setminus MO_i} F_{s',t} \leq CF2 \sum_{s \in MO_i} F_{s,t} \quad \forall t, i = EDCU \quad \text{Eq. 2-8}$$

2.3.2. Capacity constrains

Some of the units have capacity limitations, which are determined mainly by their design features. This is for instance the case of tanks, whose level must lie between a lower and an upper bound, as described in Eq. 2-9:

$$MININV_i INVCAP_i \leq INV_{i,t} \leq MAXINV_i INVCAP_i \quad \forall t, i \in ST_l \quad \text{Eq. 2-9}$$

Here, $MININV_i$ and $MAXINV_i$ are parameters indicating the minimum and maximum inventories allowed for unit i and expressed as a percentage of the total capacity of the tank, which is given by parameter $INVCAP_i$, whereas T_I is the set of units which are tanks.

Similarly, lower and upper bounds are imposed on flowrates, as can be seen in Eq. 2-10 and Eq. 2-11.

$$y_{i,t} MINCAPVOL_i \leq \sum_{s \in MS_i} F_{s,t} \quad \forall t, i \in MINCAP \quad \text{Eq. 2-10}$$

$$\sum_{s \in MS_i} F_{s,t} \leq y_{i,t} CAPVOL_i \quad \forall t, i \quad \text{Eq. 2-11}$$

These equations make use of binary variable $y_{i,t}$ that equals 1 if the corresponding process unit is being operated in time period t and 0 otherwise. When the binary variable takes a value of 0, it enforces the input flow to that unit to be 0, whereas otherwise it allows it to take any value between the minimum and maximum flowrates that can be treated by unit i , denoted by parameters $MINCAPVOL_i$ and $CAPVOL_i$, respectively. $MINCAP$ is the set containing all units for which a minimum input flowrate must be defined. Note that while all the units have an upper limit imposed on their input flow, only those in set $MINCAP$ (*i.e.*, PTU, LQU1, LQU2, PU1, PU3, CBU, ECU1 and ECU2) have also a lower limit. Limits on output streams from EDCU are imposed via constraints on the input streams of compressors ECU1 and ECU2.

Process units LQU1 and LQU2, show a characteristic delay between the moment they are switched on and the moment in which they start producing. In practice, this means that the performance of these units in the period they are started on and in the remaining ones differ, as in the former they have an initial idle time that causes them to consume energy even when they still do not produce the desired product. This is modeled via the following disjunction:

$$\left[\sum_{s \in MS_i} F_{s,t} \leq DT \cdot CAPVOL_i \right] \vee \left[\sum_{s \in MS_i} F_{s,t} \leq CAPVOL_i \right] \quad \forall t, i = LQU1, LQU2 \quad \text{Eq. 2-12}$$

$$YON_{i,t} \in \{True, False\}$$

As shown, the effect of the idle time is computed via parameter DT , which limits the amount of product that the unit can process during the first time period it is on (*i.e.*, $DT \leq 1$). The associated disjunction makes use of Boolean variable $YON_{i,t}$ which is true if unit i is switched on in time period t and false otherwise. We reformulate the disjunction into mathematical equations by means of the convex hull reformulation (Vecchietti, 2003) using Eq. 2-13, Eq. 2-14 and Eq. 2-15. These equations have been appropriately simplified and combined with those imposing lower limits on the capacity of the input flows:

$$DT \cdot MINCAPVOL_i yon_{i,t} \leq FD_{s,t}^1 \leq DT \cdot CAPVOL_i yon_{i,t} \quad \forall t, i = LQU1, LQU2, s \in MS_i \quad \text{Eq. 2-13}$$

$$MINCAPVOL_i (yi_{i,t} - yon_{i,t}) \leq FD_{s,t}^2 \leq CAPVOL_i (yi_{i,t} - yon_{i,t}) \quad \forall t, i = LQU1, LQU2, s \in MS_i \quad \text{Eq. 2-14}$$

$$FD_{s,t}^1 + FD_{s,t}^2 = F_{s,t} \quad \forall t, i \in LQU1, LQU2, s \in MS_i \quad \text{Eq. 2-15}$$

Here, $FD_{s,t}^1$ and $FD_{s,t}^2$ are disaggregated variables and $yon_{i,t}$ is a binary variable that is 1 if unit i is started up in period t and 0 otherwise. These equations work as follows. If unit i is inactive in time period t ($yi_{i,t} = yon_{i,t} = 0$), Eq. 2-13 and Eq. 2-14 will force both $FD_{s,t}^1$ and $FD_{s,t}^2$ to be 0 and Eq. 2-15 will make $F_{s,t}$ equal to 0 as well. On the other hand, if the unit is switched on in time period t , Eq. 2-14 will force $FD_{s,t}^2$ to be 0, as both $yi_{i,t}$ and $yon_{i,t}$ will equal 1. Then, Eq. 2-13 will allow $FD_{s,t}^1$ to take any value between $DT \cdot MINCAPVOL_i$ and $DT \cdot CAPVOL_i$ and Eq. 2-15 will make $F_{s,t}$ equal to $FD_{s,t}^1$. Finally, if the unit is on but was not switched on in time period t , then Eq. 2-13 will force $FD_{s,t}^1$ to be 0 (as $yon_{i,t} = 0$), whereas Eq. 2-14 will allow $FD_{s,t}^2$ to take any value between $MINCAPVOL_i$ and $CAPVOL_i$, and Eq. 2-15 will make $F_{s,t}$ equal to that amount.

The value of $yon_{i,t}$ is set according to the value of $yi_{i,t}$ by means of Eq. 2-16, Eq. 2-17 and Eq. 2-18.

$$yon_{i,t} \geq yi_{i,t} - yi_{i,t-1} \quad \forall i, t > 1 \quad \text{Eq. 2-16}$$

$$yon_{i,t} \leq yi_{i,t} \quad \forall i, t > 1 \quad \text{Eq. 2-17}$$

$$yon_{i,t} \leq 1 - yi_{i,t-1} \quad \forall i, t > 1 \quad \text{Eq. 2-18}$$

In order to illustrate how these equations work, we will consider the four different possibilities we may face. When unit i is switched on in time period t , $yi_{i,t} = 1$ and $yi_{i,t-1} = 0$, so that Eq. 2-16 forces $yon_{i,t}$ to be 1 and Eq. 2-17 and Eq. 2-18 do not impose any additional constraints. When unit i is working in time period t but was switched on previously, $yi_{i,t} = yi_{i,t-1} = 1$, and then Eq. 2-16 forces $yon_{i,t}$ to be 0 and Eq. 2-17 and Eq. 2-18 do not impose any additional constraints. When unit i stops working in time period t , $yi_{i,t} = 0$ and $yi_{i,t-1} = 1$, and thus Eq. 2-17 and Eq. 2-18 force $yon_{i,t}$ to be 0, whereas Eq. 2-18 does not impose any additional constraint. Finally, when unit i is not working either in time period t or in $t-1$, then $yi_{i,t} = yi_{i,t-1} = 0$ and Eq. 2-17 forces $yon_{i,t}$ to be 0, whereas Eq. 2-16 and Eq. 2-18 do not impose any additional constraints.

As explained before, compressor CU3, which is modeled as two separated units CU3a and CU3b, can work with two different products. However, once the compressor stops working with a given product, several hours of maintenance work are required before it can be used again with the other product. This is modeled via Eq. 2-19, Eq. 2-20 and Eq. 2-21.

$$y_{i,d,t} + y_{i',d,t} \geq 1 \quad \forall t, i = CU3a, i' = CU3b, d = 1 \quad \text{Eq. 2-19}$$

$$yi_{i,t} \leq 1 - yi_{i',t'} \quad i = CU3a, i' = CU3b, \forall t, t' | t > t' > (t - PCHT) \quad \text{Eq. 2-20}$$

$$yi_{i,t} \leq 1 - yi_{i',t'} \quad i = CU3b, i' = CU3a, \forall t, t' | t > t' > (t - PCHT) \quad \text{Eq. 2-21}$$

Here, $PCHT$ is a parameter indicating the time (computed as the number of time periods) required to change the product in the compressor. Eq. 2-19 forces at least one of the two units CU3a or CU3b to be switched off, that is, prevents unit CU3 to be used with both products simultaneously.

In normal plant operation, changes in flow rates in a brief period of time must be smooth, as otherwise the overall process may become unstable thus increasing the risk of potential failures. In order to model this, it is necessary to impose a limit MFC_s on the increase or decrease of flows in two consecutive time periods (see Eq. 2-20, Eq. 2-21 and Eq. 2-22).

$$F_{s,t} - F_{s,t-1} \leq AV_{s,t} \quad \forall t > 1, s \in FCL \quad \text{Eq. 2-20}$$

$$F_{s,t-1} - F_{s,t} \leq AV_{s,t} \quad \forall t > 1, s \in FCL \quad \text{Eq. 2-21}$$

$$AV_{s,t} \leq yfc_{s,t} \cdot MFC_s \quad \forall t > 1, s \in FCL \quad \text{Eq. 2-22}$$

Here, $AV_{s,t}$ is the absolute value of the change (*i.e.*, increase or decrease) in the flow of a stream in two consecutive time periods (*i.e.*, $AV_{s,t} = |F_{s,t} - F_{s,t-1}|$), while FCL is a set comprising the streams on which this limitation is imposed and $yfc_{s,t}$ is a binary variable that equals 1 if the flow of stream s changes in time period t and 0 otherwise.

When a tank is reaching a high level, there is the possibility of depleting it by filling and sending road tankers to a nearby storage plant. This is illustrated in Figure 2.1 via splitters SP10-SP13, which are allocated downstream of those tanks (except in tank T5, where this is not an option). Those splitters must also act as switches, as it is not possible to fill a tanker for selling the product and a tanker to the associated storage plant simultaneously. To model this, we make use of the set MO_i , which contains the stream representing the product to be sold. Hence, equations modeling the switch behavior (Eq. 2-23 and Eq. 2-24) impose lower bounds on the streams not contained in MO_i (the other flows are constrained by the demand, see Eq. 2-32):

$$yw_{i,t}SMINCAP_s \leq F_{s,t} \leq yw_{i,t}SMAXCAP_s \quad \forall t, i \in SPW, s \in SO_i \setminus MO_i \quad \text{Eq. 2-23}$$

$$F_{s,t} \leq (1 - yw_{i,t})GSCAP \quad \forall t, i \in SPW, s \in MO_i \quad \text{Eq. 2-24}$$

Here, $yw_{i,t}$ is a binary variable that takes the value of 1 if splitter i is sending product to the storage plant and 0 otherwise, $SMINCAP_s$ and $SMAXCAP_s$ are lower and upper limits on the flow requirements for stream s (in this case, they are given by the capacity

of the tankers and the time required to fill them), *GSCAP* is a generic limit on the streams flow rate and *SPW* is a set containing the splitters which hold the possibility of sending tankers to the storage plant.

Tanks can only be used in time period t for this purpose provided the level of the previous time period, controlled via the continuous variable $INV_{i,t-1}$, is higher than a given threshold $VSINV_i$. We use the following disjunction (Van den Heever *et al.*, 1999) to model this.

$$\begin{aligned} & \left[VSINV_i INVCAP_i \leq INV_{i,t} \leq MAXINV_i INVCAP_i \right] \vee \\ & \left[MININV_i INVCAP_i \leq INV_{i,t} \leq VSINV_i INVCAP_i \right] \quad \forall t, i \in TVS \\ & YINV_{i,t} \in \{True, False\} \end{aligned} \quad \text{Eq. 2-25}$$

Here, $YINV_{i,t}$ is a Boolean variable that is true if the level of tank i in time period t is over the limit $VSINV_i$ and false otherwise, $MININV_i$ and $MAXINV_i$ are respectively the minimum and maximum inventories allowed for tank i , and TVS is the set of units i which are tanks sending products to the storage plant. We transform this disjunction into ordinary equations by means of the convex hull reformulation (Vecchiotti, 2003), which after appropriate simplifications leads to Eq. 2-26, Eq. 2-27 and Eq. 2-28:

$$VSINV_i INVCAP_i yinv_{i,t} \leq INVD_{i,t}^1 \leq MAXINV_i INVCAP_i yinv_{i,t} \quad \forall t, i \in TVS \quad \text{Eq. 2-26}$$

$$MININV_i INVCAP_i (1 - yinv_{i,t}) \leq INVD_{i,t}^2 \leq VSINV_i INVCAP_i (1 - yinv_{i,t}) \quad \forall t, i \in TVS \quad \text{Eq. 2-27}$$

$$INV_{i,t} = INVD_{i,t}^1 + INVD_{i,t}^2 \quad \forall t, i \in TVS \quad \text{Eq. 2-28}$$

Here, $INVD_{i,t}^1$ and $INVD_{i,t}^2$ are the disaggregated variables for the convex hull and $yinv_{i,t}$ is a binary variable that takes a value of 1 if the level of tank i is between the threshold value and its maximum allowable capacity, and 0 otherwise. Finally, Eq. 2-29 prevents tanks from being discharged when their level in the previous period remains below the threshold value.

$$yw_{i,t} \leq yinv_{i,t-1} \quad \forall t > 1, i \in TVS, i' \in SPTI_i \quad \text{Eq. 2-29}$$

Here, $SPTI_i$ is a set containing the splitters associated to tank i . In the case of period 1, the value of $yw_{i',t}$ is fixed to 0 in case the level in the corresponding tank (which is controlled via $SPTI_i$) is below $VSINV_i$ (that is, if $INVini_i < INVCAP_i VSINS_i$).

Splitter SP8 can only pump one output stream at a time, as it has only one single pump. Therefore, we distinguish between the output streams going to unit CBU and to tank T5 using binary variable $y_{i,t}$ (see Eq. 2-30 and Eq. 2-31, respectively).

$$\sum_{s \in ST_i \setminus MS_i} F_{s,t} \leq y_{i,t} GSCAP \quad \forall t, i = CBU \quad \text{Eq. 2-30}$$

$$\sum_{s \in SO_{i'} \setminus SI_i} F_{s,t} \leq (1 - y_{i,t}) GSCAP \quad \forall t, i = CBU, i' = SP8 \quad \text{Eq. 2-31}$$

Here, $GSCAP$ is a parameter denoting a generic limit on the streams flow rates.

The production network works to satisfy the demand which varies greatly from one time period to another and which is denoted by parameter $DEM_{s,t}$. Demand must be fully satisfied for all products and time periods:

$$F_{s,t} = DEM_{s,t} \quad \forall t, s \in FP \quad \text{Eq. 2-32}$$

FP is the set of streams which contain a final product.

A product inventory level can be enforced for the last period by means of parameter $INVfin$:

$$INV_{i,t} + \partial_{i,t}^+ + \partial_{i,t}^- = INVfin_i \quad \forall t = tfin, i \in ST_I \quad \text{Eq. 2-33}$$

$$0 \leq \partial_{i,t}^+ \leq UB_i \quad \forall t = tfin, i \in ST_I \quad \text{Eq. 2-34}$$

$$-UB_i \leq \partial_{i,t}^- \leq 0 \quad \forall t = tfin, i \in ST_I \quad \text{Eq. 2-35}$$

Here, $\hat{\delta}_{i,t}^+$ and $\hat{\delta}_{i,t}^-$ are variables used to account for the deficit or excess of product compared to $INVfin$, and UB_i is an upper bound on both variables $\hat{\delta}_{i,t}^+$ and $\hat{\delta}_{i,t}^-$.

2.3.3. Utility consumption

As mentioned, only electricity and gasoil are considered here.

2.3.3.1. Electricity

Two main groups of units consuming electricity exist: those where the amount of electricity consumed does not depend on the flow rate processed, which are contained in set EC (*i.e.*, $EC = \{LQU1, LQU2, P1-P9\}$), and those where the opposite occurs, contained in set EV (*i.e.*, $EV = \{CU1-CU5, ECU1, ECU2, PTU\}$). For the former, Eq. 2-36 applies:

$$UTCONS_{i,u,t} = yi_{i,t}UTRATE_{i,u} \quad \forall t, i \in EC, u = UE \quad \text{Eq. 2-36}$$

Here, $UTCONS_{i,u,t}$ is a continuous variable accounting for the consumption of utility u in unit i in time period t , $yi_{i,t}$ is a binary variable that is 1 when unit i is operating in time period t and $UTRATE_{i,u}$ is a parameter denoting the consumption of utility u by unit i when it is operating.

Conversely, to model electricity consumption when it is a function of the flow rate processed, we use a piecewise linear function (see Lin *et al.*, 2013 and Correa-Posadaa, 2014) as depicted in Figure 2-3. In this representation, the first sector (d1) indicates the case in which the unit is not operating (*i.e.*, production is equal to 0), the second interval (d2) accounts for a region in which electricity consumption is constant and finally, in the third region (d3), electricity consumption is proportional to the flow rate. Note that region d1 has been oversized to facilitate visualization, yet the upper limit of this interval (*i.e.*, $up_{i,d1}$) is indeed very small (*i.e.*, close to 0).

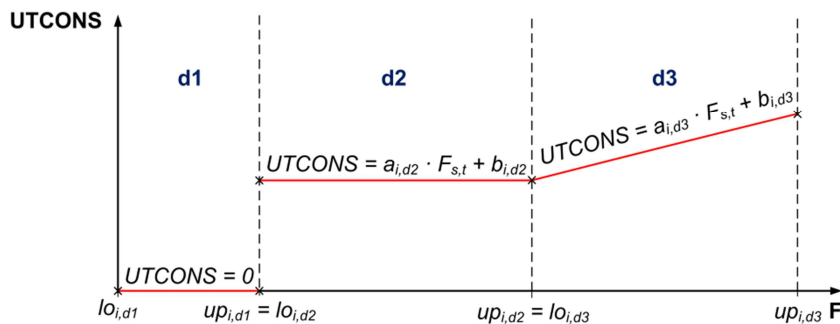


Figure 2-3. Piecewise linear approximation of utility consumption in units where the electricity consumption is a function of the flow rate processed. The first interval (d1) is oversized to facilitate visualization

This piecewise function can be modeled via the following disjunction:

$$\bigvee_d \left[\begin{array}{l} Y_{i,d,t} \\ \sum_d a_{i,d} F_{s,t} + b_{i,d} = UTCONS_{i,u,t} \\ lo_{i,d} \leq F_{s,t} \leq up_{i,d} \end{array} \right] \quad \forall t, i \in EV, u = UE \quad \text{Eq. 2-37}$$

$$Y_{i,d,t} \in \{True, False\}$$

Here, $Y_{i,d,t}$ is a Boolean variable that is true if the corresponding interval of the disjunction applies and false otherwise, $a_{i,d}$ and $b_{i,d}$ are parameters of the linear function describing the consumption of electricity of unit i in interval d and $lo_{i,d}$ and $up_{i,d}$ are respectively the lower and upper limits on that interval. The convex hull of this disjunction gives rise to the following equations:

$$\sum_d a_{i,d} Z_{i,d,t} + b_{i,d} y_{i,d,t} = UTCONS_{i,u,t} \quad \forall t, i \in EV, u = UE \quad \text{Eq. 2-38}$$

$$\sum_d Z_{i,d,t} = \sum_{s \in SI_i} F_{s,t} \quad \forall t, i \in EV \quad \text{Eq. 2-39}$$

$$lo_{i,d} y_{i,d,t} \leq Z_{i,d,t} \leq up_{i,d} y_{i,d,t} \quad \forall t, i \in EV \quad \text{Eq. 2-40}$$

$$\sum_d y_{i,d,t} = 1 \quad \forall t, i \in EV \quad \text{Eq. 2-41}$$

Here, $Z_{i,d,t}$ is the disaggregated variable for the convex hull reformulation (Vecchiotti, 2003) and $y_{i,d,t}$ is a binary variable that takes a value of 1 if the electricity consumption of unit i in period t falls in interval d and 0 otherwise. The value of this variable for internal units with variable electricity consumption and for external units is enforced via Eq. 2-42.

$$1 - y_{i,d,t} \leq y_{i,t} \leq 1 - y_{i,d,t} \quad \forall t, i \in EV, d = d1 \quad \text{Eq. 2-42}$$

Contract equations for the $UTCONS_{i,u,t}$ of ECU1, ECU2 and EDCU have been simplified to keep the model linear. The errors of these approximations are well below 2% (calculations not shown due to confidentiality issues). Note however, that external compressors ECU1 and ECU2 are embedded in the set EV , while the external distillation column EDCU is not as it requires a slightly different treatment, as illustrated in the following equations:

$$\sum_d a_{i,d} Z_{i,d,t} + b_{i,d} y_{i,d,t} = UTCONS_{i,u,t} \quad \forall t, i = EDCU, u = UE \quad \text{Eq. 2-43}$$

$$\sum_d Z_{i,d,t} = \sum_{s \in MO_i} F_{s,t} \quad \forall t, i = EDCU \quad \text{Eq. 2-44}$$

$$lo_{i,d} y_{i,d,t} \leq Z_{i,d,t} \leq up_{i,d} y_{i,d,t} \quad \forall t, i = EDCU \quad \text{Eq. 2-45}$$

$$MINCAPVOL_{i'}(1 - y_{i,d,t}) \leq \sum_{s \in SO_i \setminus MO_i} F_{s,t} \leq CAPVOL_{i'}(1 - y_{i,d,t}) \quad \forall t, i = EDCU, i' = ECU1 \quad \text{Eq. 2-46}$$

$$\sum_d y_{i,d,t} = 1 \quad \forall t, i = EDCU \quad \text{Eq. 2-47}$$

$$1 - y_{i,d,t} \leq y_{i,t} \leq 1 - y_{i,d,t} \quad \forall t, i \in EO, d = d1 \quad \text{Eq. 2-48}$$

Here, EO is the set containing the external unit (*i.e.*, $EO = \{EDCU\}$).

The overall power consumed by the process is limited in a given time period by contract requirements with energy suppliers, as illustrated in Eq. 2-49. The breach of these limitations gives rise to severe fines.

$$\sum_{i \in UPR1} UTCONS_{i,u,t} + PHTR_t + PLQ3_t \leq MAXPR1_t + MAXPR2_t \quad \forall t, u = UE \quad \text{Eq. 2-49}$$

Here, $MAXPR1_t$ and $MAXPR2_t$ are the limits on the power consumed in time period t by the process networks, which include units from the main process ($UPR1$) and units from the external supplier process ($UPR2$). $PHTR_t$ and $PLQ3$ are parameters which take into account the power consumed by machines which work in a discontinuous mode (*i.e.*, only in some time periods) and over which the model has no control.

Finally, we calculate the total electricity consumed during the simulated time (continuous variable $ECONS$) from the consumption of every unit and time period and the time length of each of the time periods, represented by the parameter $TIME$:

$$ECONS = TIME \sum_t \sum_i UTCONS_{i,u,t} \quad u = UE \quad \text{Eq. 2-50}$$

3.3.3.2. Gasoil

VU is the only unit that consumes gasoil. The gasoil consumed during time period t , accounted for in the continuous variable $UTCONS_{i,u,t}$ is proportional, via the parameter $UTRATE_{i,u}$, to the flow rate $F_{s,t}$ processed in the unit in that period, as described in Eq. 2-51.

$$UTCONS_{i,u,t} = \sum_{s \in MS_i} F_{s,t} UTRATE_{i,u} \quad \forall t, i = VU, u = UGO \quad \text{Eq. 2-51}$$

The value of the parameter $UTRATE_{VU,UGO}$ is computed from the lower heating value of the gasoil assuming a thermal efficiency η of 0.75.

Finally, the total amount of utility UGO consumed during the whole simulated time (continuous variable $GOCONS$) can be computed from $UTCONS_{i,u,t}$ and the time length of a given time period (parameter $TIME$) as follows:

$$GOCONS = TIME \sum_t \sum_i UTCONS_{i,u,t} \quad u = UGO \quad \text{Eq. 2-52}$$

Note, however, that unit VU and its associated storage tank T5 are auxiliary units used only when EDCU is not used. This is modeled via Eq. 2-53, which provides the value of the binary variable $y_{i,t}$, and Eq. 2-10 and Eq. 2-11, which enforce the inner flow to the unit to be 0 in case $y_{i,t}$ is 0 as well.

$$y_{i,t} \leq y_{i',1,t} \quad \forall t, i = VU, i' = EDCU \quad \text{Eq. 2-53}$$

2.3.4. Objective function

The model seeks to maximize the economic performance of the process. For this, we compute the profit of the network, denoted by the continuous variable *PROFIT*, as illustrated by Eq. 2-54:

$$PROFIT = SALES + DISC - EEC - GOC - MAINTC \sum_{i \in MCI} YON_{i,t} \quad \text{Eq. 2-54}$$

Here, *SALES* is a continuous variable denoting the revenues obtained from products, *DISC* is a continuous variable accounting for a discount obtained from the external supplier when products from the EDCU are purchased and which is specified in the associated contract, and *EEC* and *GOC* are continuous variables assessing the cost of electricity and gasoil, respectively. *MAINTC* is a parameter that quantifies the maintenance cost per time period when compressors from main process (embedded in set *MCI*) are operating. Longer operating times for compressors lead to higher maintenance costs. Because of this, it may be economically appealing to use compressors owned by external suppliers to cut down maintenance cost and reduce idle times during preventive maintenance tasks.

SALES are computed by means of Eq. 2-55,

$$SALES = TIME \sum_t \sum_{s \in FP} F_{s,t} PRICE_s \quad \text{Eq. 2-55}$$

where, $PRICE_s$ is the unitary price of product in stream s .

DISC is calculated according to the contract established with the provider as follows:

$$DISC = TIME \cdot DRATE \sum_t \sum_{s \in MO_t} F_{s,t} \quad i = EDCU \quad \text{Eq. 2-56}$$

where, *DRATE* is a parameter relating the discount with the amount of product obtained in the EDCU.

The electricity cost *EEC* calculation is based on the Spanish electricity market. The user of the network can buy power packages in advanced (*PCON_t*), which will be blocked for the remaining users at the appropriate time (*i.e.*, tariff period) at a fixed cost. Besides, the user can buy additional power in real time. Electricity bought in advanced (*ECONCOST_t*) and that bought in real time (*ECOST_t*) have different prices. Also, if a power package bought in advance for a given rate period is not fully used, the user has the option of selling it at the current electricity price. Eq. 2-57 models these contract options in the calculation of *EEC*:

$$EEC = TIME \sum_t \left(PCON_t ECONCOST_t + \left(\sum_i UTCONS_{i,u,t} - PCON_t \right) ECOST_t \right) \quad u = UE \quad \text{Eq. 2-57}$$

An illustrative example of how Eq. 2-57 works is shown in Figure 2.4. The three power packages (*PCON_t*) in grey color correspond to the power bought in advance at fixed price (*ECONCOST_t*) in three different tariff periods (*e.g.*, P1, P2 and P6). The area shaded in red color represents a shortage of power (more power consumed than the one originally agreed), whereas the area shaded in green color shows the excess in electricity (more electricity bought beforehand than the amount consumed). In the first scenario, the power exceeding *PCON_t* is paid at the daily electricity market price (*ECOST_t*) whereas in the second scenario the power difference is returned to the company at *ECOST_t* price.

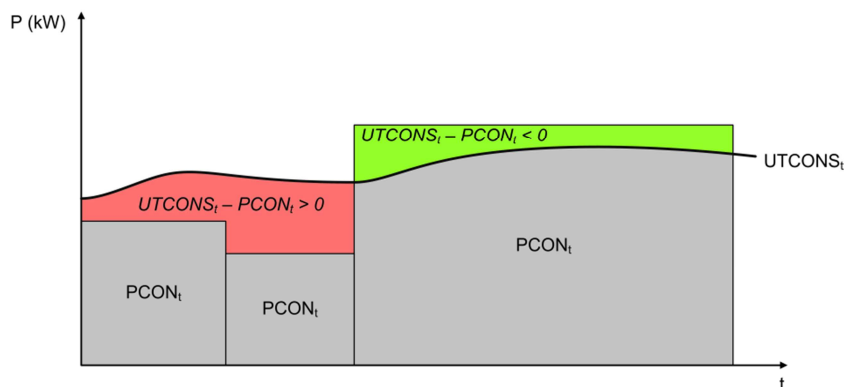


Figure 2.4. Electricity consumed (blue line) and the payments (red color) or incomes (green color) depending on the power contracted in advance (grey color).

In particular, the term $TIME \sum_t PCON_t ECONCOST_t$ considers the price of the power packages bought in advance, whereas the term $TIME \sum_t (\sum_i UTCONS_{i,u,t} - PCON_t) ECOST_t$ accounts for the difference between power packages and real consumption, regardless of whether this consumption is lower or higher than the power packages.

The cost associated to the utility UGO (GOC) is determined from the unitary cost of the gasoil (parameter $GOCOST$) and the gasoil consumption (variable $GOCONS$):

$$GOC = GOCONS \cdot GOCOST \quad \text{Eq. 2-58}$$

Finally, the objective function (variable OF) is calculated from the $PROFIT$ and different terms penalizing the deviations from the ideal plant behavior, as shown in Eq. 2-59:

$$\begin{aligned} OF = & PROFIT - (PENYON \sum_t \sum_i YON_{i,t} + PENYW \sum_t \sum_{i \in SPTI_i} YW_{i,t} \\ & + PENYFC \sum_s \sum_t YFC_{s,t} \\ & + PENINV (\sum_i \sum_t \partial_{i,t}^+ - \sum_i \sum_t \partial_{i,t}^-)) \end{aligned} \quad \text{Eq. 2-59}$$

There are five terms which are penalized. The number of times units are started is penalized via parameter *PENYON*. This prevents unnecessary switches between units (*e.g.*, some process units have the same design and technical characteristics, and the model prevents switches between these units in two consecutive time periods) as well as abnormal operating situations (*e.g.*, start and stop one machine instead of keeping it running in continuous). Parameter *PENYW* is used to control the product sent to external tanks ET1-ET4, which avoids interruptions in the production. In normal operation, the amount of product sent to these tanks must be as small as possible. Parameter *PENYFC* is used to control the maximum flow change allowed in some streams in a time period. Finally, parameter *PENINV* penalizes the deficit or excess of product stored in the last period compared to the target inventory *INVfin*. The value of these penalties is tuned beforehand and reflects a proper balance between economic performance and realistic behaviors. Note that higher penalties will result in more realistic plans, but at the expense of lower profits. A trained engineer can assess this trade-off, and play with the penalties until finding an acceptable solution. Larger penalties are applied to parameters *PENYON* and *PENYFC*, as the smoothness in the operation is of utmost importance.

The overall multiperiod model can be finally posed as follows:

$$\begin{array}{ll} (ASUOPT) & \min \quad OF \\ & s. t. \quad Eqs. (1 - 11), (13 - 26), (28 - 38), (40 - 61) \end{array}$$

Model ASUOPT is a mixed-integer linear programming (MILP) model whose size (*i.e.*, number of equations and variables) depends on the number of time periods simulated.

2.4. Case studies

To illustrate the capabilities of the model, different scenarios were solved using real data retrieved from the existing industrial facility. The first case study illustrates the optimal response of the network operation when we compare months with different electrical tariff periods. This case demonstrates as well how the process can be adjusted

when restrictive power consumption limitations are considered. In the second case study, the variability in customers' demand is studied.

To this end, model ASUOPT is implemented in GAMS and solved using CPLEX 12.6.2.0 in a WEI x86 64bit/MS Windows computer with Intel® Core™ i5-3210M CPU @ 2.50GHz processor and 4.00 GB RAM. Note that the size of the model varies from one case study to another.

2.4.1. Case study 1: Electrical periods

There are six tariff periods in terms of energy and power for intensive consumers in Spain (>450 kW) (BOE, 2001). As can be seen in Figure 2.5, these tariff periods vary from one month to another and, even, from one fortnight to another (in June). Prices of the greatest periods (*i.e.*, P3, P4, P5 and P6) are lower than those for the lower periods (*i.e.*, P1 and P2), being P1 the most expensive period and P6 the cheapest. The distribution of periods throughout the year attempts to encourage the hiring of power in periods with low saturation in the electrical networks and discourage it during periods of demand peaks with higher saturation.

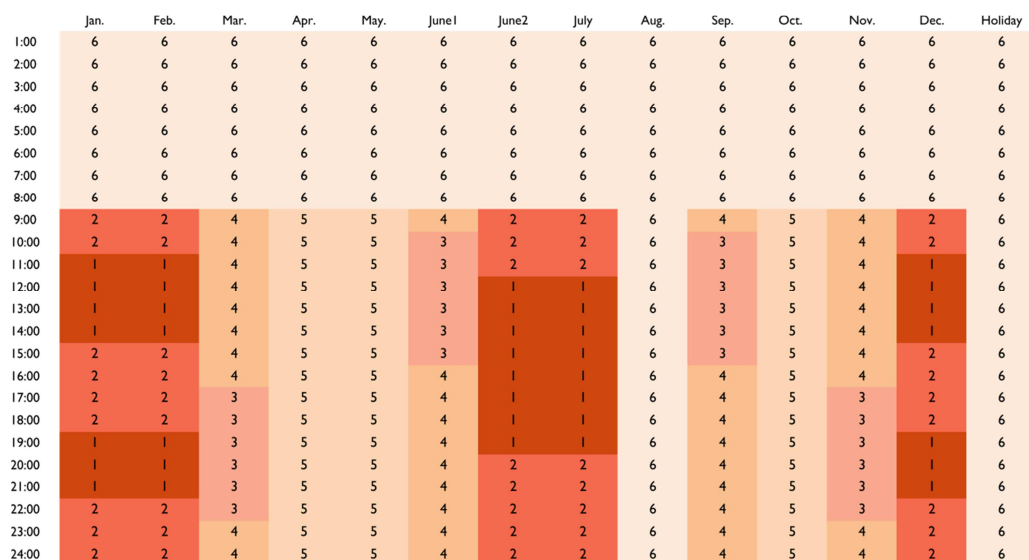


Figure 2.5. Distribution of electrical tariff periods throughout the year and their application in a day time. June1 and June2 are referred to the first and second half of June, respectively. Tariffs below months apply to weekdays (*i.e.*, Monday to Friday), while weekends (*i.e.*, Saturday and Sunday) and national holidays are always affected by P6.

The power contracted by the company in the “future market” in each period usually covers around 30-40% of the average consumption, while the extra amount is billed at the “spot market” price. The volatility of the “spot market” prices (OMI-Polo Español, 2016) is shown in Figure 2.6.

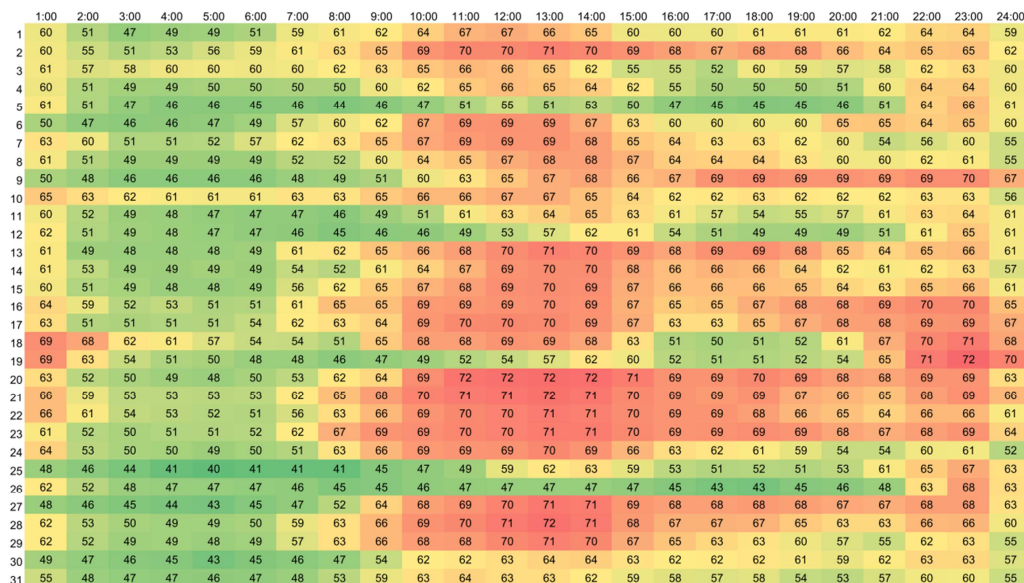


Figure 2.6. Heat map representing the evolution of electricity daily market prices for a complete month. Bright red corresponds to expensive prices while bright green corresponds to cheapest prices.

In Table 2.1 we compare the amount and price of power purchased in each tariff period beforehand (“future market”). Data is expressed as a percentage taking P6 tariff period as reference, which is characterized by higher demands and lower electricity prices. Table 2.2 displays the energy prices of the “spot market” which are applied in this case study taking into account real data compiled from historical records.

Table 2.1. Amount of purchased power and electricity price in “future market”.

	Power bought in “future market”	Electricity price in “future market”
P6	Base case	Base case
P5	-31%	+21%
P4	-38%	+23%
P3	-46%	+32%
P2	-46%	+36%
P1	-46%	+46%

Table 2.2. Electricity prices (€/MWh) for “spot market” considered in Case Study 1.

	Month													Avg.
	Jan.	Feb.	Mar.	Apr.	May	June1	June2	July	Aug.	Sep.	Oct.	Nov.	Dec.	
P1	97.25	86.87					76.25	87.13					106.98	90.90
P2	80.37	71.74					65.31	75.86					90.45	76.75
P3			55.51			68.37				77.16		68.51		67.39
P4			41.45			62.00				69.75		58.39		57.90
P5				35.59	58.11							69.09		54.26
P6	46.41	44.00	26.58	17.24	47.12	42.06	42.06	53.10	55.66	50.78	52.52	44.02	64.55	45.08
Avg.	74.67	67.53	41.18	26.41	52.61	57.47	61.21	72.03	55.66	65.89	60.80	56.97	87.32	

In this case study, we simulate one standard week in every month in order to illustrate to which extent process operation is affected by electricity prices. That is, model ASUOPT is solved for one week considering four scenarios (a-d): case (a) represents a month with expensive energy periods (*i.e.*, P1 and P2 tariff rates) such as February; case (b) represents a month in which P3 and P4 apply, such as March; case (c) represents a month with cheaper rates such as April (where P5 dominates); and finally, in case (d), August is simulated as proxy for P6 periods. In all these cases, the model contains 100123 equations, 37628 binary variables and 97936 continuous variables and takes on average 273 CPU seconds to be solved to global optimality.

The electricity consumed by the liquefaction units (*i.e.*, LQU1 and LQU2) represents approximately 45% of the overall process energy consumption. For this reason, forecasting with accuracy how both liquefiers will operate is key for avoiding mismatches with the electricity contracted and increasing the total profit. Figure 2.7 shows the time periods in which liquefiers are operated in each of the four cases described before.

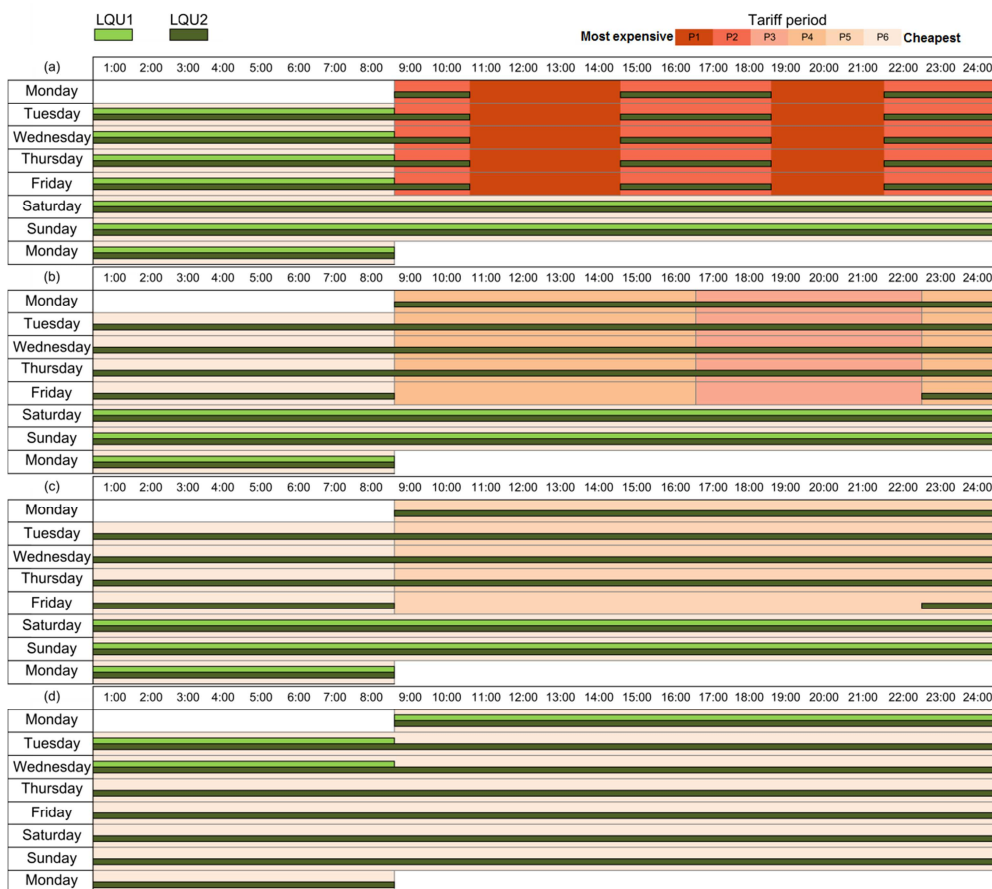


Figure 2.7. Liquefiers operation times in different scenarios. LQU1 is represented using light green bars and LQU2 is represented with dark green bars. The different tariff periods are represented using different colors so that the darker the color the higher the electricity price.

In the four cases (a-d), LQU2 is used more than LQU1, since its specific consumption is lower (14% better). Both liquefiers are operated preferably during P6 hours due to lower electricity prices (yet, different trends are followed for the same product demand). In scenario (a), liquefiers cannot be operated in P1 because the power contracted in this tariff period (very low, due to its high price) is not enough to operate these machines. In the same case (a), we note that only one liquefier can be operated in P2 tariff period (also due to power constraints). In this case, LQU2 is used in all P2 times to cover demand requirements. The optimal solution for scenarios (b) and (c) involve the same operation for liquefiers, despite the differences in the tariff periods applying in each simulation. This is because LQU1 is operated during the

weekend, when P6 applies, in order to avoid recurrent start-ups and associated idle times. LQU2 is operated in a continuous mode except in some time periods during Friday, where production is adjusted to the demand pattern and storage availability. In case (d), LQU2 is operated continuously because P6 applies during all tariff periods. LQU1 is used here to cover the demand needs.

Figure 2.8 depicts the profit and the electricity cost in each case. The worst performance for both energy cost and profit correspond to case (a), where the most expensive tariffs periods and stringent power limitation rules apply. This worst performance is taken as reference (*i.e.*, 100%) to compare with the remaining cases.

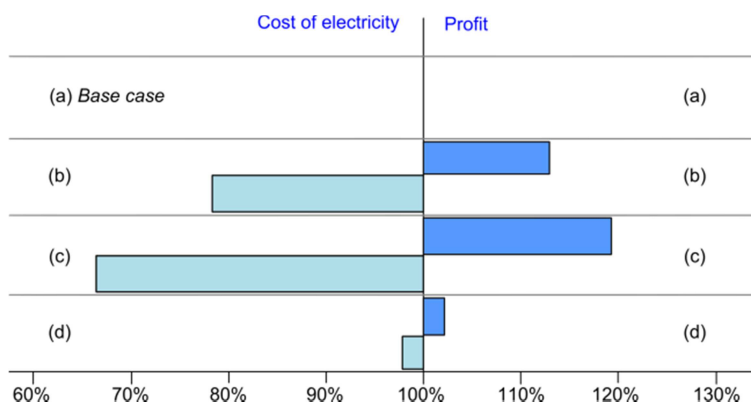


Figure 2.8. Comparison between the cost of electricity and the profit in each scenario.

The link between electricity cost and profit (scenarios with cheaper energy prices lead to higher profits, *i.e.*, simulation (c) with the lowest electricity prices has the maximum profit) is illustrated in Figure 2.8. The difference of 4.5% in profit between scenarios (b) and (c) can be explained by the 14% difference in energy costs between both months. Interestingly, the profit in case (d) is the second lowest, even if in the whole month P6 applies. This is because, as shown in Table 2.2, the cost of electricity in P6 in August (55.66€/MWh) is higher than in any tariff period in scenarios (b) and (c) (55.51€/MWh in P3 in March and 36.59€/MWh in P5 in April, respectively).

In Figure 2-9 we show the evolution of the electricity consumed by the overall process for the four cases (a-d). We also plot the maximum power that can be consumed by the process (MAXPR1 + MAXPR2 line in Figure 2.9, which differs in

each tariff period and depends on the power contracted and billed in advanced for that period. Note that the maximum power available shows the same pattern in cases (b) and (c) because the power contracted in P3 and P4 in (b) are the same as that contracted in P5 in (c).

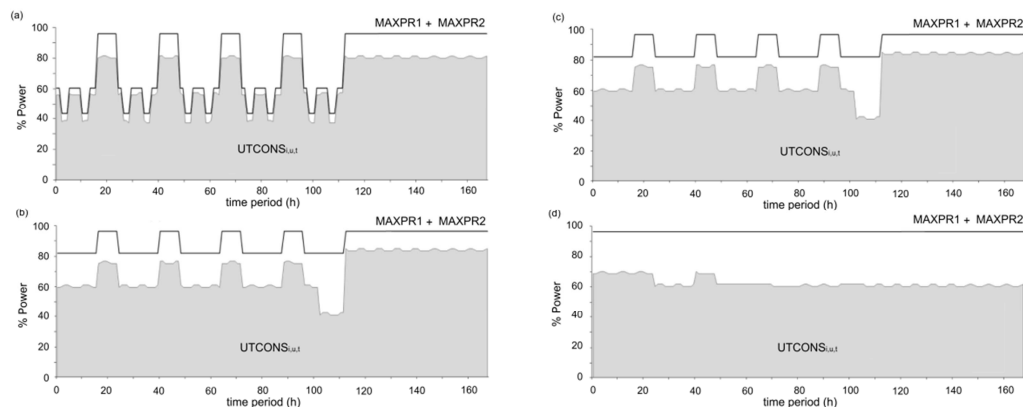


Figure 2-9. Electricity consumption of the network during a week (grey area) and maximum allowed power in each time period (black line). The amount of electricity (used and allowed) in each time period is expressed as a percentage.

The model has to adjust process operation (*e.g.*, stopping machines, reducing flows, etc.) to avoid exceeding the contracted power, since this has an associated fine. Overall, electricity consumption is optimized to take advantage of time periods in which electrical rules allow to operate the units with higher electrical consumption. This can be seen in (a), where the optimal solution relies on increasing the load on P6 periods, where the electricity is cheaper and the bound on the maximum power allowed is looser. Interestingly, cases (b) and (c) show the same trend in electricity consumption despite the differences in electricity tariffs. This suggests that the bound on the maximum power that can be consumed is a key driver of the optimal process configuration. Finally, the loose bound on the power available in (d) provides more flexibility to operate the process, thus giving rise to an almost flat electricity consumption profile.

2.4.2. Case study 2: Demand variability

Typically, the commodities involved in a highly industrialized territory can change over time as a result of variations of customers’ needs. These fluctuations have a major influence on the optimal operation of the equipment and network configuration. In order to illustrate this, we perform a sensitivity analysis by simulating replications of a week of May (*i.e.*, P5 and P6 tariff periods) with different demand needs. Specifically, the average demand retrieved from historical data is defined as the base case. Then, other replications of this week are produced by keeping the demand of all products as in the base case except for that of one product, for which we consider two scenarios: one with a low demand and one with high demand. In this case, we aggregate the demands of ILOX and MLOX and rename them as LOXP, since these demands are usually highly correlated (*i.e.*, when one increases so does the other and vice versa). Finally, we carry out two additional simulations: one in which all products are in the low demand scenario, and another one in which all products are in the high demand one. The low and high demand levels for each product are estimated from historical data (see Table 2.3). The model contains 100,123 equations, 37,628 binary variables and 97,936 continuous variables, and takes on average 670 CPU seconds to be solved. The size of the models in all simulations remains constant since they all consider one week.

Table 2.3. Demands for each product in each case study. Changes in the demand of each product are expressed as a percentage with respect to the base case. Acronyms LD and HD are used to define the low demand and high demand scenarios, respectively. ALL corresponds to the scenario in which the demand of the five products are modified simultaneously.

Base Case	GOXPS		GANPS		LOXPS		LINPS		LARPS		ALLS		
	LD	HD	LD	HD	LD	HD	LD	HD	LD	HD	LD	HD	
GOXP	-37%	+26%											
GANP			-27%	+32%									
LOXP					-29%	+22%							
LINP							-40%	+27%					
LARP									-57%	+28%			

Figure 2.10 shows how the electricity consumption of the process units is affected when the demand of one or all products is modified with respect to the base case.

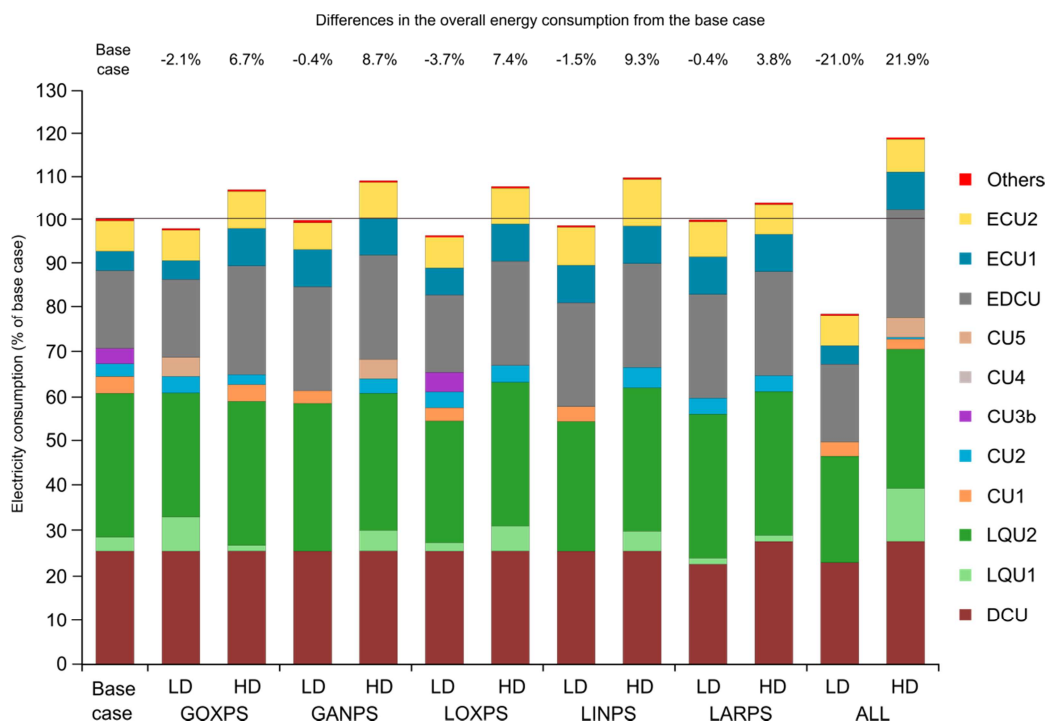


Figure 2.10. Energy consumed by process units in the different demand scenarios (*i.e.*, LD is low demand and HD is high demand). Process units with low energy consumption (*e.g.*, filling pumps) are aggregated in “Others” category. At the top of the Figure we provide the % difference in overall energy consumption with respect to the base case.

As we can see in Figure 2.10, deviations in the overall energy consumption from the base case are much higher in HD scenarios (between 3% and 9%) than in LD (between 0.4% and 4%). This is because the air composition establishes a bound on the ratio that can be obtained between the different products. Hence, in the LD scenario, products demands not modified act as bottleneck from the viewpoint of electricity consumption, thus leading to modest savings. Conversely, in HD scenarios, the product with increased demand acts as bottleneck, and thus drives the overall energy consumption. Regarding the operation of process units, notorious differences are obtained when demand requirements are modified. In all the scenarios, the DCU consumption is the same, except in the cases in which the LARP demand is modified (*i.e.*, $LARPS_{LD}$, $LARPS_{HD}$, ALL_{LD} and ALL_{HD}). This demonstrates that differences in LARP demand can entail an increase or decrease of the plant air load and, consequently, cause variations in DCU consumption (around 17% between the $LARPS_{HD}$ and $LARPS_{LD}$ cases). Differences in LD and HD scenarios for LINP and ALL are mainly

given by the use of LQU1 in the high demand scenario. This can also explain differences between LOXPS_{HD} and LOXPS_{LD}, since LOXP is obtained by thermal exchange between LINP and GOXP in CBU. Hence, in some P5 tariff periods, it is not possible to operate LQU2 without exceeding the power contracted, and therefore it is replaced by LQU1. In GOXPS, differences between LD and HD scenarios are given by an increased use of external units EDCU and ECU1 (in HD scenario), thus allowing for a reduced use of the LQU1 (see Figure 2.11). This suggests that contractual conditions for GOXP are advantageous from a given GOXP amount onwards. Note that in GOXPS_{HD}, the compressors for GANP are not used because this product is obtained from ECU2 and CBU, which in turn uses the GOXP from MX1. In GANPS_{LD}, compressors associated to GANP (*i.e.*, CU3b, CU4 and CU5) are not used neither, and the demand is satisfied by means of the GANP purchased externally from ECU2 and that obtained in CBU. Conversely, in GANPS_{HD} the need to use product from MX2 (and thus CU5) arises.

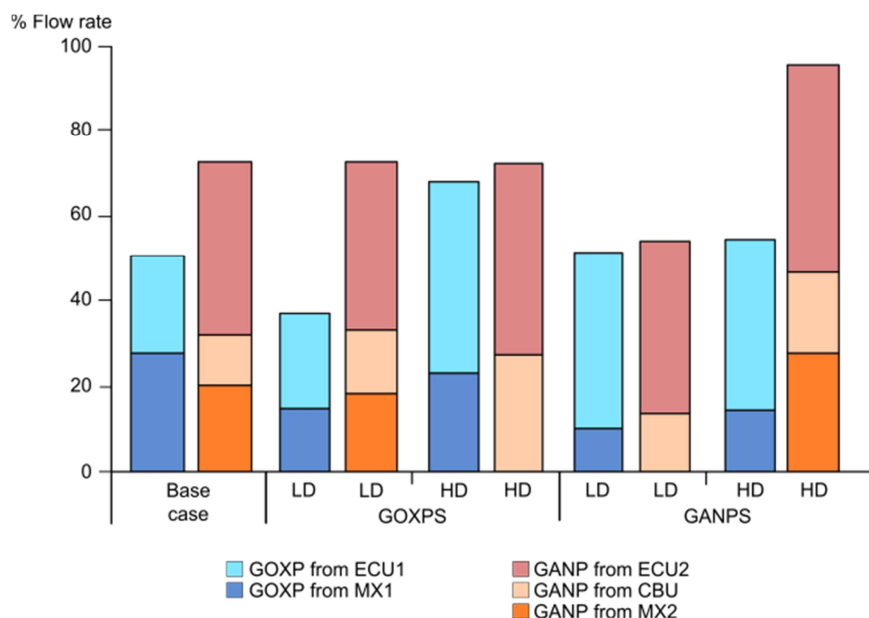


Figure 2.11. Percentage of GANP and GOXP sent to pipeline from the different production sources in the Base Case, GOXPS and GANPS. Note that VU is not an option for GANP as this unit is only used in case of emergency.

Figure 2.11 depicts the source of the gas products (*i.e.*, GOXP and GANP) distributed to the pipeline in the GOXPS and GANPS scenarios. Results reveal that most of the GANP (between 51.3% and 74.7%) is purchased from the external unit in all the scenarios, and the same holds for GOXP (between 59.0% and 79.6%) except for the base case, where outsourcing covers 43.5% of the product demand. The result is in agreement with those shown in Figure 2.10, where electricity consumption from external units (*i.e.*, EDCU, ECU1 and ECU2) represented between 28.5% and 40.6% of the total electricity consumption of the plant. This evidences the outstanding importance of properly adjusting the pipeline supply operation (*i.e.*, the balance between the amount of product purchased from the external unit versus that sent onsite).

In order to further illustrate the effect of including the external supply in the model, we depict in Figure 2.12 and Figure 2.13 how the cost of supply and the final profit of the network change (compared to the base case) with the external purchases (*i.e.*, OGOX and OGAN). The cost of supply accounts not only for the power consumed by the main process and the external unit, but also for maintenance costs (*MAINTC*) and for the discount (*DISC*) obtained when the product of *EDCU* is purchased. Specifically, in Figure 2.12, we increase the OGOX flow rate of the base case simulation (which equals the minimum that can be purchased according to contract stipulations), thus keeping constant OGAN. As can be observed, increases in OGOX can decrease the profit as much as 2.7% and increase the supply costs up to 14.5%. On the other hand, in Figure 2.13, the OGAN flow rate is varied (*i.e.*, increased or decreased) while maintaining constant the OGOX. In this case, the most negative effect is observed when OGAN is reduced by 40%, which produces a decrease in profit of 2.3% and an increase of supply costs of 12.7%. It is also noteworthy that variations in OGOX have a greater impact than those in external GAN. For instance, an increase of 30% in the external GOX flow rate increases by 8.4% the supply costs and reduces by 1.5% the overall profit, while the same increase of external GAN flow rate leads to an increase in costs of 3.6% and a decrease in profit of 0.63%. The reason behind this behavior is twofold. First, OGOX dictates the raw material load (*i.e.*, amount of air) of the external air separation unit and thus the power consumption of the external unit

(EDCU). Secondly, the discount applied when using the external units is governed by the amount of OGOX purchased, which is independent of the OGAN value.

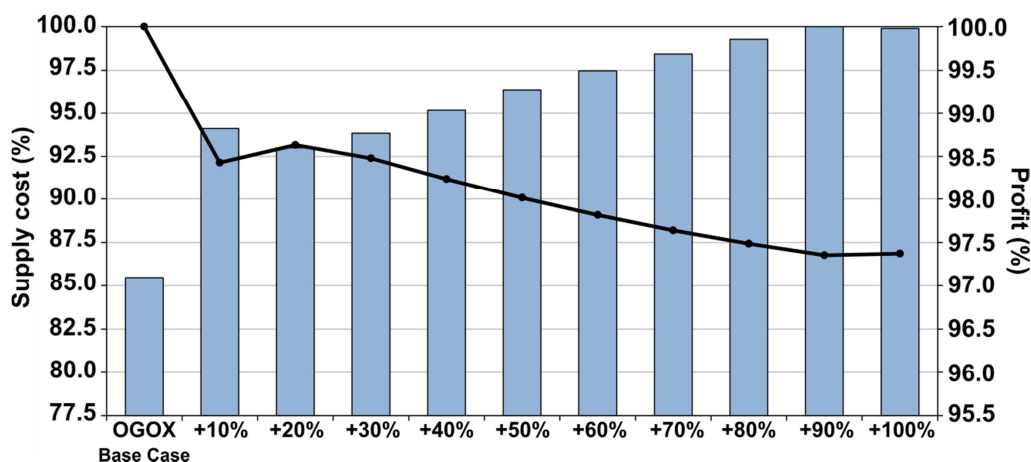


Figure 2.12. Supply costs (bars) and profit (line) allocation under different scenarios of OGOX.

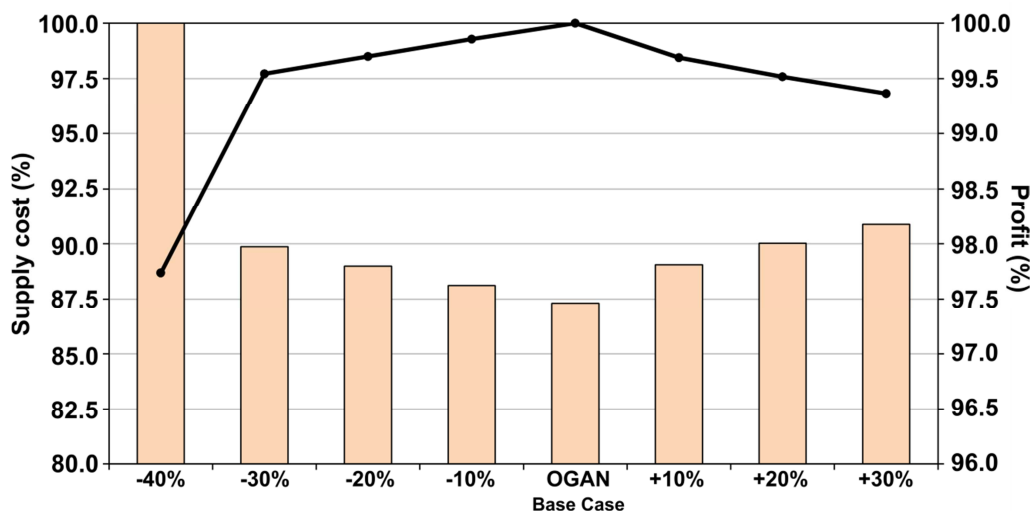


Figure 2.13. Supply costs (bars) and profit (line) allocation under different scenarios of OGAN.

In order to further illustrate the capabilities of the model for real life cases, we display in Figure 2.14 the error in the hourly electricity consumption forecasts of a real existing facility during a three-month period (October, November and December). Specifically, we compare the results obtained with the model predictions versus those obtained by applying the standard forecasting techniques previously used in the plant.

Results demonstrate that the proposed model improves the accuracy of the electricity forecasts, showing an average error of 1.5% compared to a 2.8% error with the previous methodology. Furthermore, the number of cases with “high” errors (say above 5%) has been significantly reduced (42 compared to 297, see histogram in Figure 2.14). This improvement can bring significant benefits to the company, which will be rewarded when the forecasting communicated to the electricity company is accurate enough (or otherwise penalized when the deviation is severe).

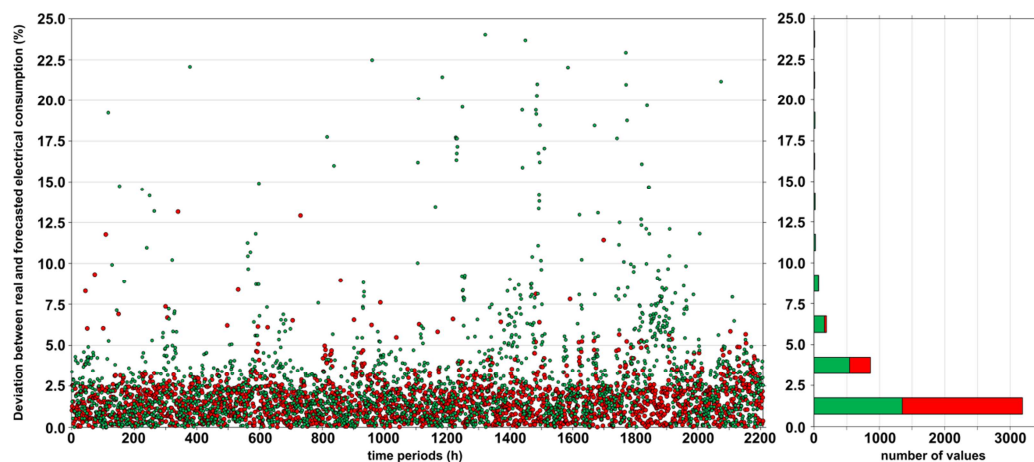


Figure 2.14. Comparison of the error in the electricity consumption forecasts between the proposed model (red circles) and the standard methodology used in a real existing facility (green circles). A histogram is depicted at the right-hand side of the figure following the same color pattern.

2.5. Conclusions

A mathematical model was developed to operate in an optimal manner cryogenic air separation networks producing oxygen, nitrogen and argon. The MILP proposed, which is based on a real industrial facility, can effectively cope with changing electricity prices, customers demand and energy rates while maximizing the plant performance. To this end, decisions on flow rates, machines starts-up and shutdowns, and purchase orders are optimized in an automatic manner according to the market needs.

Several case studies, considering realistic process scenarios (*i.e.*, demand rates, electrical tariff periods, power limitations, etc.) were presented in order to demonstrate and validate the efficacy of this MILP. The optimization was carried out for four

scenarios entailing different electricity prices, showing how these prices strongly affect the network's profit. In the face of power limitations, the model adjusts the operation to fulfill contractual and demand liabilities and hence avoid economic penalties. Furthermore, the effect of different demand patterns was also investigated.

Overall, the MILP identifies the most profitable way to operate the plant, assisting engineers in their daily activities by effectively optimizing production planning, energy rules, sales and product stocks while considering external constraints and dynamic market conditions. It is worth highlighting that all the results presented in this contribution are based on real data from an existing facility, where the proposed tool has proved extremely useful in the daily operation. Besides leading to optimized decisions, the MILP improves the electricity consumption forecasting, which helps reduce the energy costs. Therefore, our method constitutes a promising alternative for any other energy-intensive industrial process where energy savings play an important role.

Acknowledgement

The authors would like to acknowledge financial support from the Generalitat de Catalunya (2014 DI 030) in the modality of Industrial Doctoral program. Gonzalo Guillén-Gosálbez would like to acknowledge the financial support received from the Spanish "Ministerio de Ciencia y Competitividad" through the project CTQ2016-77968-C3-1-P.

2.6. Nomenclature

Process abbreviations

CBU	conversion unit
CU	compression unit
DCU	distillation column unit
ECU	external compression unit
EDCU	external distillation unit
FP	final products
GANIP	gas nitrogen intermediate product

GANP	gas nitrogen product
GOXIP	gas oxygen intermediate product
GOXP	gas oxygen product
ILOXP	industrial liquid oxygen product
LOXIP	liquid oxygen intermediate product
LARIP	liquid argon intermediate product
LARP	liquid argon product
LINP	liquid nitrogen product
LQU	liquefaction unit
MILP	mixed-integer linear programming
MLOXP	medical liquid oxygen product
MX	mixers
OGAN	purchased gas nitrogen
OGOXP	purchased gas oxygen
PU	pump unit
PTU	pretreatment unit
P1-P6	electrical tariff period
SP	splitters
T	storage tank
U	utility
VU	vaporizer unit

Sets/Indexes

I	set of process units indexed by i
P	set of properties indexed by p
S	set of streams indexed by s
T	set of time intervals indexed by t
U	set of utilities indexed by u

Subsets

EC	set of units whose electricity consumption is constant
----	--

EE	set of units with electrical consumption
EO	set of outside units whose electricity consumption is accounted for
EV	set of units whose electricity consumption is variable
FCL	set of streams with maximum switch flow limitations in a time period
FP	set of streams s which are final products
GP	set of units whose gasoil consumption is proportional to inlet flow
MINCAP	set of units with a minimum flow requirement
MO_i	main output stream of unit i
MS_i	main input stream of unit i
SI_i	set of input streams of unit i
SO_i	set of output streams of unit i
$SPTI_i$	set of units which are splitters in which one output stream can only be used if the inventory level of tank i is over $VSINV$
SPW	set of units which are SP which cannot use simultaneously both output streams
ST	set of units which are tanks
TVS	set of tanks which can send tankers to associated storage plant
UPR2	set of units which belong to supply process
UPR1	set of units which belong to main process
VS	set of streams which are tankers to storage plant

Continuous variables

$AV_{s,t}$	absolut value for flow changes in stream s in period t , Nm^3/h
$\hat{\partial}_{i,t}^+$	positive slack for inventory in unit i period t , Nm^3/h
$\hat{\partial}_{i,t}$	positive slack for inventory in unit i period t , Nm^3/h
ECONS	total electricity consumption, kWh
$F_{s,t}$	volumetric flow rate of stream s in time period t , Nm^3/h
FEP	fine when $MAXPR2_t + MAXPR1_t$ is exceeded, €
$FD_{s,t}$	disaggregated variable for death time (volumetric flow rate of stream s in time period t), Nm^3/h
GOCONS	total gasoil consumption, L

$INV_{i,t}$	inventory of unit i in time period t , Nm^3
$INVD_{i,t}$	disaggregated variable for inventory at level at which it can be depleted by means of tankers (inventory of unit i in time period t), Nm^3
PROFIT	profit, €
SALES	sales, €
$UTCONS_{i,u,t}$	consumption of utility u in unit i in time period t , kWh
$Z_{i,d,t}$	auxiliary variable for F_s in interval d of piecewise equation for electricity consumption of unit i in time period t

Binary variables

$y_{i,d,t}$	binary variable (1 if interval d in piecewise equation for electricity consumption of unit i is active in time period t , 0 otherwise)
$yfc_{s,t}$	binary variable (1 if the flow of stream s is switched in time period t , 0 otherwise)
y_i	binary variable (1 if unit i is working in time period t , 0 otherwise)
$yinv_{i,t}$	binary variable (1 if inventory of tank i in time period t surpasses the minimum required for it to be depleted by means of tankers, 0 otherwise)
$yon_{i,t}$	binary variable (1 if unit i is switched on in time period t , 0 otherwise)
$yw_{i,t}$	binary variable that equals 1 or 0 depending on which output stream s is used in SP i

Parameters

η	vaporizer efficiency
$a_{i,d}$	slope of straight line in interval d of piecewise equation for electricity consumption of unit i
$b_{i,d}$	independent term of straight line in interval d of piecewise equation for electricity consumption of unit i
$CAPVOL_i$	maximum capacity allowed for input stream of unit i , Nm^3/h
CF	corrective factor between input and output streams in unit CBU
CF2	corrective factor between OGOX and OGAN in EDCU

DEM _{s,t}	demand for product in stream s in time period t , Nm ³ /h
DISC	supplier discount on outsourcing cost, €
DT	death time in liquefiers, h
ECONCOST _t	cost of electricity bought in advance for time period t , €/kWh
ECOST _t	electricity cost in time period t , €/kWh
GOCOST	gasoil cost, €/L
GSCAP	maximum capacity for a given stream, Nm ³ /h
HVAPN2	heat of vaporization of N ₂ , kJ/Nm ³
INVCAP _i	capacity of unit i , Nm ³
INVini _i	initial inventory of tank i , Nm ³
INVfin _i	final inventory of tank i , Nm ³
LHVGO	lower heating value of gasoil, MJ/L
lo _{i,d}	lower bound of interval d of piecewise equation for electricity consumption of unit i
MAINTCOST	maintenance cost applied in unit i when it is working in time period t , €/h
MAXINV _i	maximum inventory allowed for unit i , %
MAXPR2 _t	maximum electricity that supply process can consume in time period t , kW
MAXPR1 _t	maximum electricity that can be consume in time period t by main process, kW
MFC _s	maximum flow change allowed in stream s in a time period t , Nm ³ /h
MINCAPVOL _i	minimum capacity required for input stream of unit i , Nm ³ /h
MININV _i	minimum inventory allowed for unit i , %
PCHT	product change time, h
PCON _t	power bought in advance for time period t , kW
PENINV	term to penalize the deficit or excess of stored product in the last period time
PENYFC	term to penalize flow changes in some streams
PENYON	term to penalize the numbers of times that an unit are started

PENYW	term to penalize the number of times that a tanker is sent to external storage plant
PENMB	term to penalize the breach of mass balances
PHTR _{<i>t</i>}	electricity consumption in PTU heater in time period <i>t</i> , kWh
PLQ3 _{<i>t</i>}	electricity consumption limitation in time period <i>t</i> , kWh
PRICE _{<i>s</i>}	price of product in stream <i>s</i> , €/Nm ³
PRODISC	unitary price discounted related with EDCU production, €/Nm ³
RELATION	amount of product obtained by EDCU to apply the price discount
SMINCAP _{<i>s</i>}	minimum flow requirement for stream <i>s</i> , Nm ³ /h
SMAXCAP _{<i>s</i>}	maximum flow allowed for stream <i>s</i> , Nm ³ /h
TIME	length of a time period, h
up _{<i>i,d</i>}	lower bound of interval <i>d</i> of piecewise equation for electricity consumption of unit <i>i</i>
UTRATE _{<i>i,u</i>}	consumption of utility <i>u</i> in unit <i>i</i>
VSINV _{<i>i</i>}	minimum capacity of tank <i>i</i> before it can be depleted by means of tankers, Nm ³
YIELDVOL _{<i>i,s</i>}	volumetric yield of output stream <i>s</i> of unit <i>i</i>
YVC _{<i>i,s</i>}	coefficient for corrective term for volumetric yield of output stream <i>s</i> of unit <i>i</i>

2.7. References

BOE núm. 268, de 8 de noviembre de 2001, 40618-40629

Correa-Posadaa CM, Sánchez-Martin P. Gas network optimization: a comparison of piecewise linear models. *Optimization Online*; 2014.

Cristóbal J, Guillén-Gosálbez G, Jiménez L, Irabien A. Multi-objective optimization of coal-fired electricity production with CO₂ capture. *Appl Energy* 2012a;98:266-272.

Cristóbal J, Guillén-Gosálbez G, Jiménez L, Irabien A. Optimization of global and local pollution control in electricity production from coal burning. *Appl Energy* 2012b;92:369-378.

Daryanian B, Boln RE, Tabors RD. Optimal demand-side response to electricity spot prices for storage-type customers. *IEEE Transactions on Power Systems* 1989;4:897-903.

EPEX, <http://www.epexspot.com>; 2016 (accessed 13.01.16)

European Commission, 2001. Directive 2001/77/CE of the European Parliament and Council dated 27 September 2001.

Finn P, O'Connell M, Fitzpatrick C. Demand side management of a domestic dishwasher: wind energy gains, financial savings and peak-time load reduction. *Appl Energy* 2013;101: 678–685.

Floudas, C.A., *Nonlinear and mixed integer optimization fundamentals and applications*; Oxford University Press, New York, 1995.

Gaiser K, Stroeve P. The impact of scheduling appliances and rate structure on bill savings for net-zero energy communities: application to west village. *Appl Energy* 2014;113:1586–1595.

GME, <http://www.mercatoelettrico.org>; 2016 (accessed 13.01.16)

Granell R, Axon CJ, Wallom DCH, Layberry RL. Power-use profile analysis of non-domestic consumers for electricity tariff switching. *Energy Efficiency* 2016a;9(3):825-841.

Gutiérrez-Alcaraz G, Tovar-Hernández JH, Lu CN. Effects of demand response programs on distribution system operation. *International Journal of Electrical Power & Energy Systems* 2016;74:230-237.

Iberian Energy Derivatives Exchange information available at: <http://www.omip.pt/> (accessed January 2016)

Ierapetritou MG, Wu D, Vin J, Sweeney PG, Chigirinsky M. Cost minimization in an energy-intensive plant using mathematical programming approaches. *Industrial and Engineering Chemistry Research* 2002;41:5262-5277.

Kamilaris A, Kalluri B, Kondepudi S, Wai TK. A literature survey on measuring energy usage for miscellaneous electric loads in offices and commercial buildings. *Renewable and Sustainable Energy Reviews* 2014;34:536–550.

Karwan K, Kebulis M. Operations planning with real time pricing of a primary input. *Computers & Operations Research* 2007;34:848–867.

Klaassen EAM, Kobus CBA, Frunt J, Slootweg JG. Responsiveness of residential electricity demand to dynamic tariffs: experiences from a large field test in the Netherlands. *Appl Energy* 2016;183:1065-1074.

Kopanos GM, Xenos DP, Ciccotti M, Pistikopoulos EN, Thornhill NF. Optimization of a network of compressors in parallel: operational and maintenance planning – the air separation plant case. *Appl Energy* 2015;146:453–70.

Kostin AM, Guillén-Gosálbez G, Mele FD, Bagajewicz MJ, Jiménez L. A novel rolling horizon strategy for the strategic planning of supply chains. Application to the sugar cane industry of Argentina. *Computers and Chemical Engineering* 2011;35(11):2540-2563.

Labeeuw W, Stragier J, Deconinck G. Potential of active demand reduction with residential wet appliances: a case study for Belgium. *IEEE Trans Smart Grid* 2015;6(1):315-323.

Lin M-H, Carlsson JG, Ge D, Shi J, Tsai J-F. A review of piecewise linearization methods. *Math Prob Eng* 2013;2013.

Madlener R, Stoverink S. Power plant investments in the Turkish electricity sector: areal options approach taking into account market liberalization. *Appl Energy* 2012;97:124–34.

Mele FD, Guillén-Gosálbez G, Jiménez L. Optimal planning of supply chains for bioethanol and sugar production with economic and environmental concerns. *Computer Aided Chemical Engineering* 2009;26:997-1002.

Miller J, Luyben W, Blouin S. Economic incentive for intermittent operation of air separation plants with variable power costs. *Industrial and Engineering Chemistry Research* 2008;47:1132-1139.

Mitra S, Grossmann IE, Pinto JM, Arora N. Optimal production planning under time-sensitive electricity prices for continuous power-intensive processes. *Computers & Chemical Engineering* 2012;38:171–184.

Nord Pool Spot, <http://www.nordpoolspot.com>; 2016 (accessed 13.01.16)

OMI-Polo Español S.A. Spanish market (MIBEL) regulation, <http://www.omie.es>;
2016 (accessed 13.01.16).

Pulkkinen P, Ritala R. TMP production scheduling under uncertainty: methodology
and case studies. *Chemical Engineering and Processing* 2008;47:1492-1503.

Puranik Y, Kiliç M, Sahinidis NV, Li T, Gopalakrishnan A, Besancon B. Global
optimization of an industrial gas network operation. *AIChE J* 2016;62(9):3215–24.

Smith AR, Klosek JA. Review of air separation technologies and their integration
with energy conversion processes. *Fuel Processing Technology* 2001;70(2):115-134.

Üster H, Dilaveroglu S. Optimization for design and operation of natural gas
transmission networks. *Appl Energy* 2014;133:56–69.

Van den Heever SA, Grossmann IE. Disjunctive multiperiod optimization methods
for design and planning of chemical process systems. *Computers and Chemical
Engineering* 1999;23:1075-1095.

Vecchiotti A, Modeling of discrete/continuous optimization problems:
characterization and formulation of disjunctions and their relaxations. *Computers and
Chemical Engineering* 2003;27:433-448

Widén J. Improved photovoltaic self-consumption with appliance scheduling in 200
single-family buildings. *Appl Energy* 2014;126:199-212.

Xenos DP, Ciccioiti M, Kopanos GM, Bouaswaig AEF, Kahrs O, Martinez-Botas
R, Thornhill NF. Optimization of a network of compressors in parallel: real time

Optimization (RTO) of compressors in chemical plants – an industrial case study. *Appl Energy* 2015;114:51–63.

Yan L, Yu Y, Li Y, Zhang Z. Energy saving opportunities in an air separation process. In: 12th international symposium on process systems engineering and 25th European symposium on computer aided process engineering; 2010.

Zhu Y, Legg S, Laird CD. Optimal operation of cryogenic air separation systems with demand uncertainty and contractual obligations. *Chemical Engineering Science* 2011a;66:953-963.

Zhu Y, Legg S, Laird CD. A multiperiod nonlinear programming approach for operation of air separation plants with variable power pricing. *American Institute of Chemical Engineers* 2011b;57:9

Chapter 3.
Data Envelopment Analysis and
Malmquist Productivity Index
for efficiency assessment

UNIVERSITAT ROVIRA I VIRGILI
MULTIPERIOD MODELLING PLANNING AND PRODUCTIVITY AND ENERGY EFFICIENT ASSESSMENT OF AN INDUSTRIAL GASES
FACILITY

David Fernández Linares

3. Data Envelopment Analysis and Malmquist Productivity Index for efficiency assessment

Productivity and energy efficiency assessment of existing industrial gases facilities via Data Envelopment Analysis and the Malmquist Index

David Fernández^{a,b}, Carlos Pozo^c, Rubén Folgado^a, Laureano Jiménez^b, Gonzalo Guillén-Gosálbez^{b,c}

^a *Messer Ibérica de Gases S.A.U, Autovía Tarragona-Salou, km. 3.8, 43480, Vilaseca, Tarragona, Spain*

^b *Departament d'Enginyeria Química, Universitat Rovira i Virgili, Av. Països Catalans, 26, 43007, Tarragona, Spain*

^c *Department of Chemical Engineering, Centre for Process Systems Engineering, Imperial College London, South Kensington Campus, London SW7 2AZ, United Kingdom*

Keywords: Data envelopment analysis; Energy-intensive process; Energy efficiency; Malmquist productivity index; Cryogenic air separation

3.1. Introduction

The efficient use of energy is a major challenge faced by industrial companies and the whole society in the transition towards a greener economy. Today, the industrial sector uses more energy than any other end-use sector, about one-third of the world's final energy demand (Enerdata, 2011), while predictions show that it will likely consume more than 50% of the total energy delivered in 2040. Industries are also responsible for almost 40% of the worldwide carbon dioxide emissions, a share that is expected to increase to 46% in 2040 (EIA, 2014). The use of energy in industries is

often inefficient, which creates great opportunities to reduce their energy consumption and boost their competitiveness while reducing their environmental impact.

There is a substantial literature on efficiency indicators and approaches for improving energy efficiency. As an example, various energy efficiency performance metrics were defined by Neelis *et al.* (2007); Siitonen *et al.* (2010); Saygin *et al.* (2011) and Oda *et al.* (2012), among others, with the aim to assist on how to improve the reliability and flexibility of industrial facilities and also to facilitate energy benchmarking (Chung, 2011). Along these lines, Boyd *et al.* (2008) presented a tool that can be used by plant energy managers to estimate energy efficiency, while Hasanbeigi *et al.* (2010) discussed energy-efficiency opportunities for the cement industry in the Shandong Province (China).

These energy efficiency indicators are seldom analyzed together with productivity criteria. Furthermore, they fail in identifying the sources of inefficiencies and in providing insight on how to eliminate them. Here we overcome these limitations by using a rigorous method based on DEA to diagnose whether industrial sites are operating in an efficient manner. DEA is an approach originally introduced by Charnes *et al.* (1978) in the area of economics and operations research that has recently found many applications in science and engineering. It is a non-parametric tool that objectively assesses the relative efficiency of a set of units in terms of multiple criteria by using linear programming models (Boussofiane *et al.*, 1991 and Cook *et al.*, 2009). DEA provides efficiency scores (*i.e.*, values between zero, the worst, and one, the best) for each entity being assessed and identifies in a qualitative and quantitative manner sources of inefficiency. To this end, DEA calculates an "efficiency frontier" formed by the efficient entities (*i.e.*, those with efficiency scores equal to one), which is used to establish efficiency targets and identify benchmark units that perform better than the rest.

Since its origins, DEA was used in many different contexts, from production and business firms, to non-profit agencies such as hospitals, universities, armies and countries. It was also applied to energy-intensive sectors and processes so as to enhance their level of sustainability. For instance, Azadeh *et al.* (2007) applied a DEA model to assess energy efficiency and optimize energy intensive manufacturing

sectors. Liu *et al.* (2010) used DEA to evaluate the efficiency of power-generation in thermal power plants. Han *et al.* (2014) applied DEA in the field of chemicals to assess energy efficiency in ethylene production. Blomberg *et al.* (2012) analyzed energy efficiency and energy policies in a set of pulp and paper mills using DEA. Mandal *et al.* (2011) analyzed energy use in cement companies using DEA. Ramanathan *et al.* (2000) compared energy efficiencies of different transport modes, while Zhanga *et al.* (2015) assessed the transportation sector in China. Other studies covered also minor energy users (Nassiria *et al.*, 2009 and Mousavi-Avval *et al.*, 2011). Sueyoshi *et al.* (2017) summarized previous research efforts on DEA applied to energy and the environment, concluding that DEA has been very useful in guiding large policies (Wang *et al.*, 2012 and Sueyoshi *et al.*, 2014) (*e.g.*, sustainability assessments (Galán-Martín *et al.*, 2016) related with global warming and climate change mitigation, life cycle assessments (Limleamthong *et al.*, 2016), potential CO₂ emission reductions (Choi *et al.*, 2012 and Wang *et al.*, 2014) as well as long-term business strategies. Mardani *et al.* (2017) reviewed the use of DEA models applied to energy efficiency problems, reaching similar conclusions.

In this paper we deal with the cryogenic air separation process, a mature technology that produces large amounts of technical gases with high purity standards (Smith *et al.*, 2001 and Latimer *et al.*, 1967). These pure gases are obtained by liquefying and distilling air, an energy intensive process that requires a very tight integration of heat exchangers and separation columns and which consumes large amounts of electricity (*i.e.*, tens of megawatts) to cover the high compression and liquefaction needs. In today's market place, it is crucial to adapt processes to dynamic environments (*e.g.*, location, demand, operating conditions, electricity pricing policies, etc.). In this context, assessing facilities according to predefined key performance indicators can help to identify inefficiencies and opportunities for improvement. Therefore, the most successful "best practices" can then be introduced in the plants (or, at least, in those with similar features) to finally enhance the global performance and competitiveness of the business. As will be later discussed in more detail, DEA provides an excellent framework to carry out such analysis.

While DEA has been applied to energy-intensive industries, to our best knowledge, there is a lack of research in the field of air separation technology. Energy savings opportunities in single air separation processes were discussed in (Yan *et al.*, 2010). The focus was originally on design and operational aspects, omitting comparisons with similar processes that could exploit valuable know-how on the process. In contrast to these works, ours provides an in-depth assessment of efficiency based on real data and using a rigorous method. More precisely, the methodology presented in this paper is demonstrated by studying 34 existing Air Separation Units (ASUs) from Messer, a gas company operating several plants around the world. Furthermore, an additional novelty of this work is that we study the dynamic evolution of efficiency scores, which is often neglected in the energy efficiency assessment of industrial facilities. To this end, we measure the change in efficiency over time using the Malmquist Productivity Index (MPI), first defined by Malmquist in 1953 (Malmquist, 1953) and further developed by Fare *et al.* (1992) and Fare *et al.* (1994). See also Chen *et al.* (2004) and Perez-Reyes *et al.* (2009). In the context of energy intensive processes, this approach was applied by Makridou *et al.* (2016) and Morfeldt *et al.* (2014), who assessed energy efficiency trends of energy-intensive industries in European countries, as well as in other works focused on Chinese industries. See for instance Wu *et al.* (2014), Li *et al.* (2013), Li *et al.* (2016) and Chang *et al.* (2010).

Hence, the main contribution of this work is two-fold. First, the application of DEA to real data gathered from different Air Separation Units around the world. Second, the use of the Malmquist Productivity Index to enlarge the scope of the static (“snapshot”) analysis of the ASU’s efficiencies in order to cover their evolution over time. With the proposed methodology, ASUs managers will be able to operate their facilities more efficiently.

The paper is organized as follows. In section 3.2 we describe the methodology based on DEA and MPI. In section 3.3, we present the case study dealing with a set of existing ASUs, while in section 3.4 we draw the conclusions of the study.

3.2. Methodology

Our methodology is based on DEA, which aims to identify the most efficient units among a set of comparable entities, usually referred to as decision making units (DMUs) in DEA notation (William *et al.*, 1989). This approach shows the following main advantages compared to the use of simple energy efficient indicators: (i) it allows the simultaneous analysis of multiple outputs and inputs (Charnes *et al.*, 1978); (ii) it does not require previous definition of production functions (the frontier function is estimated from empirical data on inputs and outputs rather than established beforehand according to a specific functional form describing the relationship for producing the maximal amount of outputs from a given amount of inputs); and (iii) the efficiency scores are calculate relative to the highest performance rather than to averages (Zhou *et al.*, 2008). In this section, we describe the fundamentals of DEA as applied to our case.

3.2.1. Fundamentals of DEA

DEA uses linear programming (LP) to quantitatively evaluate the relative performance of a set of units under multiple criteria. The linear optimization is applied to each single DMU. In our study, each DMU corresponds to an ASU, so DEA is used to identify the set of efficient ASUs (*i.e.*, those forming the “efficient frontier”) and ultimately establish improvement targets for the inefficient one (which if attained would make them efficient). The relative efficiency of a DMU is defined as the maximum ratio of weighted sum of outputs to the weighted sum of inputs, being the efficiency index less or equal than 1. If the efficiency index is lower than 1, then the ASU is inefficient, while otherwise it is efficient. Furthermore, the lower the value of the efficiency index, the worst the efficiency performance, which would imply that the ASU would lie far from the “efficient frontier”.

The relative efficiency score θ of a specific DMU can be evaluated by the BCC dual (*i.e.*, multiplier form) model (Banker *et al.*, 1984), which assumes variable returns to scale (VRS) (*i.e.*, increases in inputs do not imply proportional changes in outputs). The mathematical model is formulated as follows:

$$\begin{aligned}
 & \min \theta_o - \varepsilon \left(\sum_{i=1}^m S_i^- + \sum_{r=1}^s S_r^+ \right) \\
 & \text{s. t. } \sum_{j=1}^n \lambda_j x_{ij} + S_i^- = \theta_o x_{io} \quad i = 1, \dots, m \\
 & \sum_{j=1}^n \lambda_j y_{rj} - S_r^+ = y_{ro} \quad r = 1, \dots, s \\
 & \sum_{j=1}^n \lambda_j = 1 \\
 & \lambda_j, S_i^-, S_r^+ \geq 0 \quad \forall i, j, r \quad \theta_o \text{ unconstrained}
 \end{aligned} \tag{Eq. 3-1}$$

Where the notation is as follows: o , DMU being assessed; ε , non-Archimedean infinitesimal value to enforce the variables to be positive; n , number of DMUs; j , other DMUs; m , number of inputs consumed by DMU $_j$, x_{ij} , amount of input i consumed by DMU $_j$; s , number of outputs produced by DMU $_j$; y_{rj} , amount of output r produced by DMU $_j$; S_i^- , vector of slack variables representing the amount of input i that, if reduced, shifts the projection of DMU $_o$ from the weakly efficient frontier to the strongly efficient frontier; S_r^+ , vector of slack variable representing the amount of output r that, if increased, shifts the projection of DMU $_o$ from the weakly efficient frontier to the strongly efficient frontier; λ_j , linear weights assigned to every single DMU $_j$ to form a linear combination.

Note that when the efficiency of a DMU $_o$ equals one ($\theta_o = 1$) and the slacks summation is zero ($S_r^+ + S_i^- = 0$), this DMU $_o$ is considered *strongly efficient*. In the case that ($\theta_o = 1$) but ($S_r^+ + S_i^- \neq 0$) the corresponding DMU $_o$ is considered *weakly efficient*. For any inefficient DMU, it is possible to find a composite DMU (linear combination of units) that can reduce its input level maintaining the same output level.

Any inefficient DMU can become efficient by projecting it onto the “efficient frontier”, which is formed by the efficient DMUs. Note that the model stated in Eq. 3-1 follows an input-oriented approach (*i.e.*, efficiency is achieved by decreasing the input levels while outputs remain constant). In this case, the target for input i in any inefficient DMU $_o$ (TG_{io}) is calculated with the following expression:

$$TG_{io} = \sum_{j=1}^n \lambda_j x_{ij} = \theta_o x_{io} - S_i^- \quad i = 1, \dots, m \quad \text{Eq. 3-2}$$

Then, the input reduction required by a DMU to become efficient is given by the distance between the original input value and this target. Hence, the efficiency of the inefficient DMUs is improved through the reduction in inputs by moving radially toward the efficient frontier. Note that output-oriented models also exist, in which input levels are maintained and inefficient units become efficient by increasing their output levels. Note that in our case, we can manipulate inputs more easily than outputs, since the latter (*i.e.*, amount of products) are connected to the customer's demand over which we have little influence (see section 3).

3.2.1.1. DEA illustrative example

Figure 3.1 shows an illustrative example to further clarify the DEA concepts introduced above. Let us consider eight hypothetical ASUs (*i.e.*, A, B, C, D, E, F and H) consuming two inputs (*e.g.*, electricity and water) to produce the same amount of one output (*e.g.*, 1 m³ of oxygen). The axes of Figure 3.1 display the values for input 1 (x axis) and input 2 (y axis) for each DMU. Green circles (*i.e.*, A, C, E and F) show the efficient ASUs, while red circles (*i.e.*, B, D, G and H) represent the inefficient ones. The continuous line connecting the efficient ASUs denotes the “strong efficient frontier”. The extremes of this frontier (*i.e.*, A and F) are extended with lines parallel to the axes (grey lines) to build the “weak efficient frontier”. Inefficient technologies (*i.e.*, $\theta_o < 1$) are projected radially (dashed lines) in order to identify the efficiency targets (yellow circles) and the ASUs used as benchmarks (*i.e.*, DMUs corresponding to the vertexes of the facet of the frontier where the projection lies). In the case of the inefficient DMU G, its efficiency is determined by point *g*, where the efficient frontier is crossed by segment *Og*, connecting the inefficient ASU with the origin (radial projection). Thus, the efficiency of G is given by $\frac{Og}{OG}$, that is, the efficiency of this ASU is evaluated using a linear combination of ASUs A and C, as *g* is placed in the segment connecting them. Hence, ASUs A and C are the reference set for G, that is, G should

operate similar to the way A and C are run so as to improve its performance. Similarly, C and E are the reference set for ASU H. At the same time, given that many ASUs are close to ASU C, we should take C as reference ASU to improve the performance of the former units.

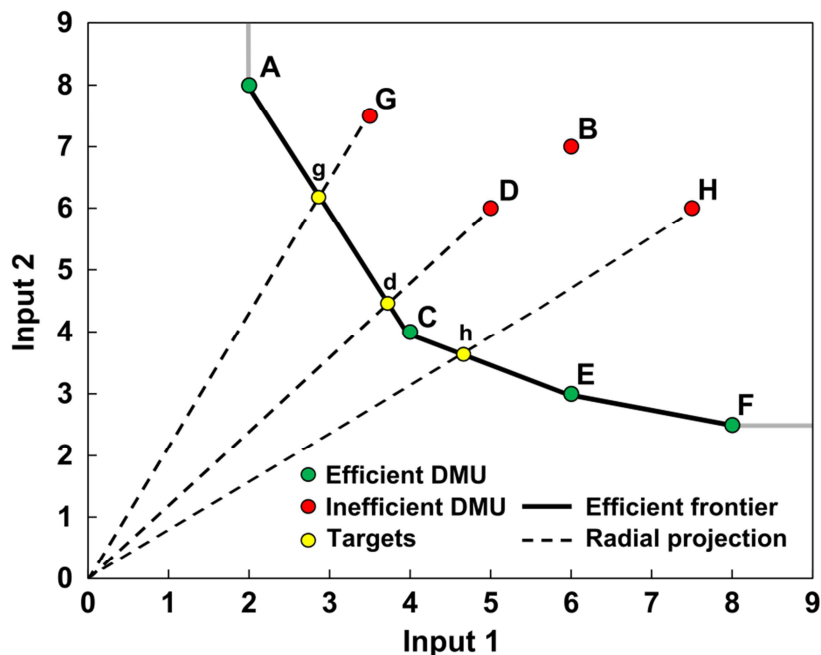


Figure 3.1. DEA illustrative example for an input-oriented case with two-input and one-output (the latter assumed constant).

3.2.1.2. Non-discretionary variables

In many DEA real applications, certain input variables are not manageable (Cooper *et al.*, 2011), that is, they cannot be controlled or modified due to production factors, design features, external constraints, etc. Hence, some input variables can be proportionally reduced (*discretionary variables*), whilst others are not subject to management control (*non-discretionary variables*), as discussed in Camanho *et al.* (2009) and Zadmirzaei *et al.* (2017). The interested reader is directed to Saber *et al.* (2011) for further information about the non-discretionary external factors that may affect a production process.

The standard DEA model presented in Eq. 3-1 is reformulated following the work by Banker *et al.* (1986) in order to accommodate non-discretionary inputs:

$$\begin{aligned}
 & \min \theta_o - \varepsilon \left(\sum_{i \in D} S_i^- + \sum_{r=1}^s S_r^+ \right) \\
 & \text{s.t. } \sum_{j=1}^n \lambda_j x_{ij} + S_i^- = \theta_o x_{io} \quad i \in D \\
 & \quad \sum_{j=1}^n \lambda_j x_{ij} + S_i^- = x_{io} \quad i \in ND \\
 & \quad \sum_{j=1}^n \lambda_j y_{rj} - S_r^+ = y_{ro} \quad r = 1, \dots, s \\
 & \quad \sum_{j=1}^n \lambda_j = 1 \\
 & \quad \lambda_j, S_i^-, S_r^+ \geq 0 \quad \forall i, j, r \quad \theta_o \text{ unconstrained}
 \end{aligned} \tag{Eq. 3-3}$$

where D and ND refer to the sets of discretionary and non-discretionary inputs, respectively. Note that inefficient DMUs are not projected in the direction of ND inputs, as these remain fixed. We also note that in the objective function of Eq. 3-3, only the input slacks related to discretionary factors appear, as discussed in Cooper *et al.*, (2006). Furthermore, in Eq. 3-2 we show the targets (TG_{i_o}) for discretionary inputs ($i \in D$), but it should be mentioned that these targets are computed differently for non discretionary inputs ($TGND_{i_o}$) and also for outputs (TGO_{r_o}), as shown in Eq. 3-4 and Eq. 3-5, respectively.

$$TGND_{i_o} = \sum_{j=1}^n \lambda_j x_{ij} = x_{i_o} - S_i^- \quad i \in ND = 1, \dots, m \tag{Eq. 3-4}$$

$$TGO_{r_o} = \sum_{j=1}^n \lambda_j y_{rj} = y_{r_o} + S_r^+ \quad r = 1, \dots, s \tag{Eq. 3-5}$$

We note that while changes in discretionary inputs to achieve (TG_{io}) are enough for *weak efficiency*, changes in non discretionary inputs and outputs to achieve ($TGND_{io}$) and (TGO_{ro}) respectively are required to attain *strong efficiency*.

3.2.1.3. DEA Super-efficiency

The standard DEA classifies the DMUs as either efficient ($\theta_o = 1$) or inefficient ($\theta_o < 1$). This classification has the limitation that it provides no ranking of efficient DMUs. Conversely, super-efficiency models allow to further discriminate among efficient ASUs. See Banker *et al.* (1988), Banker *et al.* (1989), Andersen *et al.* (1993), Wilson (1995), Ray (2004) and Seiford *et al.* (1999). In this contribution we use a VRS input-oriented super-efficiency model, as proposed by Seiford *et al.* (1998a).

$$\begin{aligned}
 & \min \theta_o^{SE} - \varepsilon \left(\sum_{i \in D} S_i^- + \sum_{r=1}^s S_r^+ \right) \\
 \text{s. t. } & \sum_{j=1, j \neq o}^n \lambda_j x_{ij} + S_i^- = \theta_o^{SE} x_{io} \quad i \in D \\
 & \sum_{j=1, j \neq o}^n \lambda_j x_{ij} + S_i^- = x_{io} \quad i \in ND \\
 & \sum_{j=1, j \neq o}^n \lambda_j y_{rj} - S_r^+ = y_{ro} \quad r = 1, \dots, s \\
 & \sum_{j=1}^n \lambda_j = 1 \\
 & \lambda_j, S_i^-, S_r^+ \geq 0 \quad \forall i, j, r \quad \theta_o^{SE} \text{ unconstrained}
 \end{aligned} \tag{Eq. 3-6}$$

Here, θ_o^{SE} is the super-efficiency score ($\theta_o^{SE} \geq 1$, where the higher the better), and o is the efficient DMU for which the super-efficiency model is applied.

Super-efficiency can be interpreted in two different ways. On the one hand, it represents the degree of efficiency stability, that is, how much can discretionary inputs worsen while the DMU is still deemed efficient. On the other hand, super-efficiency denotes the surplus of savings achieved by an efficient DMU in its discretionary inputs

(*i.e.*, the DMU would still be efficient even if some of its discretionary inputs showed worse values, thereby implying extra savings). In this contribution, we focus on this second interpretation of super-efficiency. This is because our aim is to identify best-practices regarding discretionary inputs, which can be modified at will to improve the efficiency of the ASUs (rather than outstanding performance in outputs or non-discretionary inputs).

Note that the super-efficiency model in Eq. 3-6, which is based on projecting the DMU under analysis to the efficient frontier resulting when this DMU is removed from the pool, can sometimes render infeasible (see Seiford *et al.* (1998a) and Zhu (2001)). This infeasibility has a different meaning in each of the two possible super-efficiency interpretations. In the case of efficiency stability, the infeasibility of the dual (*i.e.*, multiplier) problem means that the DMU will remain efficient regardless of the changes in discretionary inputs. Hence, it implies that such DMU shows the highest super-efficiency (*i.e.*, $+\infty$). Conversely, in the context of inputs savings, the infeasibility of the dual model implies that the DMU analyzed does not show any extra savings in its discretionary inputs (*i.e.*, its super-efficiency is given by its outputs or by non-discretionary inputs). In such case, we follow the algorithm proposed by Chen (2005) (see section 3.3 and Figure 3.3) in order to assign super efficiency value to DMUs for which problem in Eq. 3-6 is infeasible.

3.2.2. Fundamentals of Malmquist Productivity Index

To study how the efficiency of a DMU changes over time we make use of the MPI (denoted by M_o), which is defined as the ratio between the efficiency scores of the same production unit in two different time periods t and $t+1$ ($t < t + 1$), as follows:

$$M_o = \left[\frac{D_o^t(x_o^t, y_o^t)}{D_o^t(x_o^{t+1}, y_o^{t+1})} \frac{D_o^{t+1}(x_o^t, y_o^t)}{D_o^{t+1}(x_o^{t+1}, y_o^{t+1})} \right]^{1/2} \quad \text{Eq. 3-7}$$

The interpretation of the MPI is as follows: $M_o > 1$ means efficiency loss from t to $t + 1$; $M_o = 1$, means no efficiency changes from t to $t + 1$ and $M_o < 1$, means an efficiency gain from t to $t + 1$. The calculation of the MPI requires two single period

and two mixed period measurements. The two single period measurements are obtained as follows. In time period t :

$$\begin{aligned}
 D_o^t(x_o^t, y_o^t) &= \min \theta \\
 \text{s. t. } \sum_{j=1}^n \lambda_j x_{ij}^t &\leq \theta x_{io}^t \quad i \in D \\
 \sum_{j=1}^n \lambda_j x_{ij}^t &\leq x_{io}^t \quad i \in ND \\
 \sum_{j=1}^n \lambda_j y_{rj}^t &\geq y_{ro}^t \quad r = 1, 2, \dots, s \\
 \sum_{j=1}^n \lambda_j &= 1 \\
 \lambda_j &\geq 0 \quad j = 1, 2, \dots, n \quad \theta \text{ unconstrained}
 \end{aligned}
 \tag{Eq. 3-8}$$

where x_{io}^t and y_{ro}^t are the i^{th} input and the r^{th} output for DMU_o in time period t , and θ is the technical efficiency score determining the inputs reduction to produce the given output level. In the same way, we can obtain the technical efficiency score for DMU_o in time period $t + 1$ ($D_o^{t+1}(x_o^{t+1}, y_o^{t+1})$) by using the inputs and outputs in period $t + 1$ instead of t .

$$\begin{aligned}
 D_o^{t+1}(x_o^{t+1}, y_o^{t+1}) &= \min \theta \\
 \text{s. t. } \sum_{j=1}^n \lambda_j x_{ij}^{t+1} &\leq \theta x_{io}^{t+1} \quad i \in D \\
 \sum_{j=1}^n \lambda_j x_{ij}^{t+1} &\leq x_{io}^{t+1} \quad i \in ND \\
 \sum_{j=1}^n \lambda_j y_{rj}^{t+1} &\geq y_{ro}^{t+1} \quad r = 1, 2, \dots, s \\
 \sum_{j=1}^n \lambda_j &= 1 \\
 \lambda_j &\geq 0 \quad j = 1, 2, \dots, n \quad \theta \text{ unconstrained}
 \end{aligned}
 \tag{Eq. 3-9}$$

The technical efficiency for the first mixed period ($D_o^t(x_o^{t+1}, y_o^{t+1})$) is obtained by solving:

$$\begin{aligned}
 & D_o^t(x_o^{t+1}, y_o^{t+1}) = \min \theta \\
 & \text{s. t. } \sum_{j=1}^n \lambda_j x_{ij}^t \leq \theta x_{io}^{t+1} \quad i \in D \\
 & \quad \sum_{j=1}^n \lambda_j x_{ij}^t \leq x_{io}^{t+1} \quad i \in ND \\
 & \quad \sum_{j=1}^n \lambda_j y_{rj}^t \geq y_{ro}^{t+1} \quad r = 1, 2, \dots, s \\
 & \quad \sum_{j=1}^n \lambda_j = 1 \\
 & \lambda_j \geq 0 \quad j = 1, 2, \dots, n \quad \theta \text{ unconstrained}
 \end{aligned} \tag{Eq. 3-10}$$

whereas the model for the second mixed period ($D_o^{t+1}(x_o^t, y_o^t) = \min \theta$) is as follows:

$$\begin{aligned}
 & D_o^{t+1}(x_o^t, y_o^t) = \min \theta \\
 & \text{s. t. } \sum_{j=1}^n \lambda_j x_{ij}^{t+1} \leq \theta x_{io}^t \quad i \in D \\
 & \quad \sum_{j=1}^n \lambda_j x_{ij}^{t+1} \leq x_{io}^t \quad i \in ND \\
 & \quad \sum_{j=1}^n \lambda_j y_{rj}^{t+1} \geq y_{ro}^t \quad r = 1, 2, \dots, s \\
 & \quad \sum_{j=1}^n \lambda_j = 1 \\
 & \lambda_j \geq 0 \quad j = 1, 2, \dots, n \quad \theta \text{ unconstrained}
 \end{aligned} \tag{Eq. 3-11}$$

Note that this formulation corresponds to a VRS input-oriented MPI, which is consistent with what we have discussed so far.

One of the advantages of using the MPI instead of the mere inspection of the efficiency values over time is that the former can be decomposed into two components, one measuring the change in technical efficiency (TEC_o) and the other one measuring the change in the frontier technology (FS_o) between time periods t and $t + 1$. Specifically,

$$M_o = TEC_o FS_o \quad \text{Eq. 3-12}$$

$$\text{with } TEC_o = \frac{D_o^t(x_o^t, y_o^t)}{D_o^{t+1}(x_o^{t+1}, y_o^{t+1})}, FS_o = \left[\frac{D_o^{t+1}(x_o^{t+1}, y_o^{t+1})}{D_o^t(x_o^{t+1}, y_o^{t+1})} \frac{D_o^{t+1}(x_o^t, y_o^t)}{D_o^t(x_o^t, y_o^t)} \right]^{1/2} \quad \text{Eq. 3-13}$$

The meaning of this decomposition is as follows. The term TEC_o measures the change in the technical efficiency relative to the other DMUs. $TEC_o > 1$ indicates a decline in technical efficiency (*i.e.*, $\theta_o^t > \theta_o^{t+1}$), $TEC_o = 1$ no improvement or decline, and $TEC_o < 1$ an improvement (*i.e.*, $\theta_o^t < \theta_o^{t+1}$). On the other hand, the term FS_o measures the frontier shift between time period t and $t + 1$. In this case, $FS_o > 1$ indicates a regress of the frontier, $FS_o = 1$ no shift, and $FS_o < 1$ a progress of the frontier.

Note that problems in Eqs. 3-10 and 3-11 can be infeasible. The reason for this is analogous to that causing infeasibilities in super-efficiency models (see section 3.2.1.3.): the efficient frontier of these problems is built without the DMU analyzed (note the difference in time periods between the left-hand side and the right-hand side of the constraints). In the case of super-efficiency, infeasible problems have clear implications on the DMU being analyzed. However, in the context of the MPI, obtaining a numerical solution for problems in Eqs. 3-8, 3-9, 3-10 and 3-11 (*i.e.*, obtaining a numerical value for terms $D_o^t(x_o^t, y_o^t)$, $D_o^{t+1}(x_o^{t+1}, y_o^{t+1})$, $D_o^t(x_o^{t+1}, y_o^{t+1})$ and $D_o^{t+1}(x_o^t, y_o^t)$) is mandatory as otherwise the MPI cannot be determined (see Eqs. 3-12 and 3-13)). To overcome this limitation, we make use of the algorithm described in section 2.3 which assigns a numerical value to $D_o^t(x_o^{t+1}, y_o^{t+1})$ and $D_o^{t+1}(x_o^t, y_o^t)$ even when the original problems (Eqs. 3-10 and 3-11) render infeasible.

3.2.2.1. Malmquist Productivity Index illustrative example

An illustrative example of how to calculate the MPI is shown in Figure 3.2, which is based on Figure 3.1. The inputs of the eight ASUs (*i.e.*, A_t, B_t, \dots, H_t) in time period t are represented using black dots (*i.e.*, same data as in Figure 3.1), whereas white dots represent the inputs of the ASUs in time period $t + 1$ (*i.e.*, $A_{t+1}, B_{t+1}, \dots, H_{t+1}$). Figure 3.2, illustrates the changes in both TEC_o and FS_o MPI components. For example, if an ASU shows technical efficiencies of 0.4 and 0.6 in t and $t+1$ respectively, then $TEC_o < 1$ which indicates an improvement in TEC_o . The frontier between time periods t and $t + 1$ can also vary over time, thereby modifying the MPI scores. For example, ASU_D could worsen its technical efficiency scores but, as a result of the frontier change of similar ASUs ($FS_o < 1$) between t and $t + 1$, the MPI index of ASU_D becomes efficient ($M_o \leq 1$).

On the other hand, (*e.g.*, ASU_F) which is efficient in t , becomes inefficient in $t + 1$ ($M_o > 1$). The relative movement of any given DMU over time will therefore depend on both its position relative to the corresponding frontier (technical efficiency) and the position of the frontier itself (technology change). If inefficiency is not noticed, then productivity growth over time will be unable to distinguish between improvements that derive from DMU ‘catching up’ to its own frontier, or those that result from the frontier itself ‘shifting up’ over time.

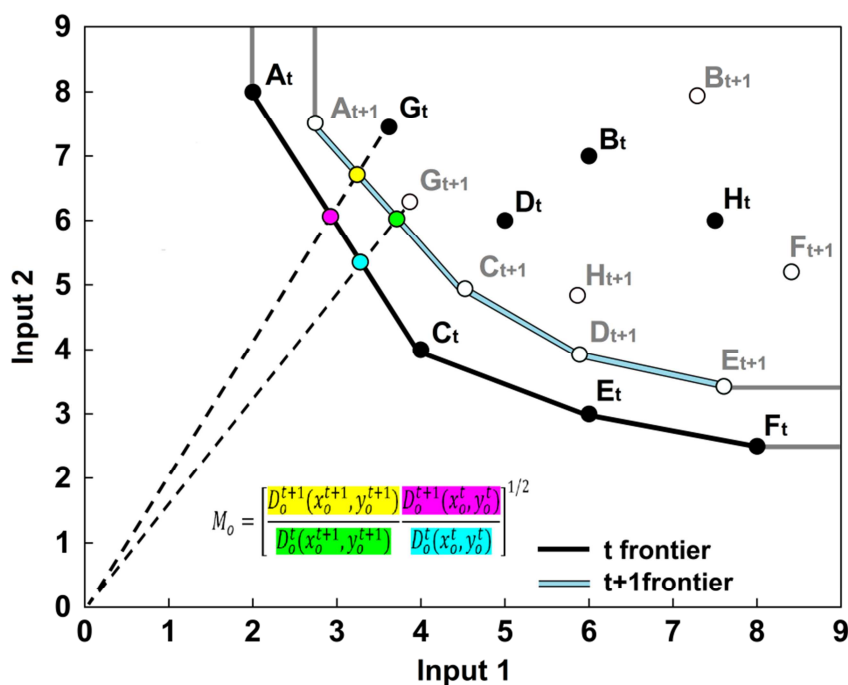


Figure 3.2. Malmquist productivity index illustrative example for period t and $t + 1$.

3.2.3. Infeasibilities in DEA models

Infeasibilities can arise in super-efficiency models (see section 3.2.1.3) as well as in the sub-problems required to compute the MPI (section 3.2.2.). In order to obtain numerical values for the (super) efficiency in both cases, we follow the approach by Seiford *et al.* (1999). In essence, we first solve an output-oriented model and then use the resulting projected output values ($\hat{y}_{ro} = \phi_o^* y_{ro}$, with ϕ_o^* being the output-oriented super-efficiency) to define a new input-oriented (super) efficiency model. If the latter still remains infeasible, we assign a value of one to the (super) efficiency. Figure 3.3 summarizes the approach in the case of super-efficiency models. Note we use the same overall approach to deal with infeasibilities in models in Eqs. 3-10 and 3-11.

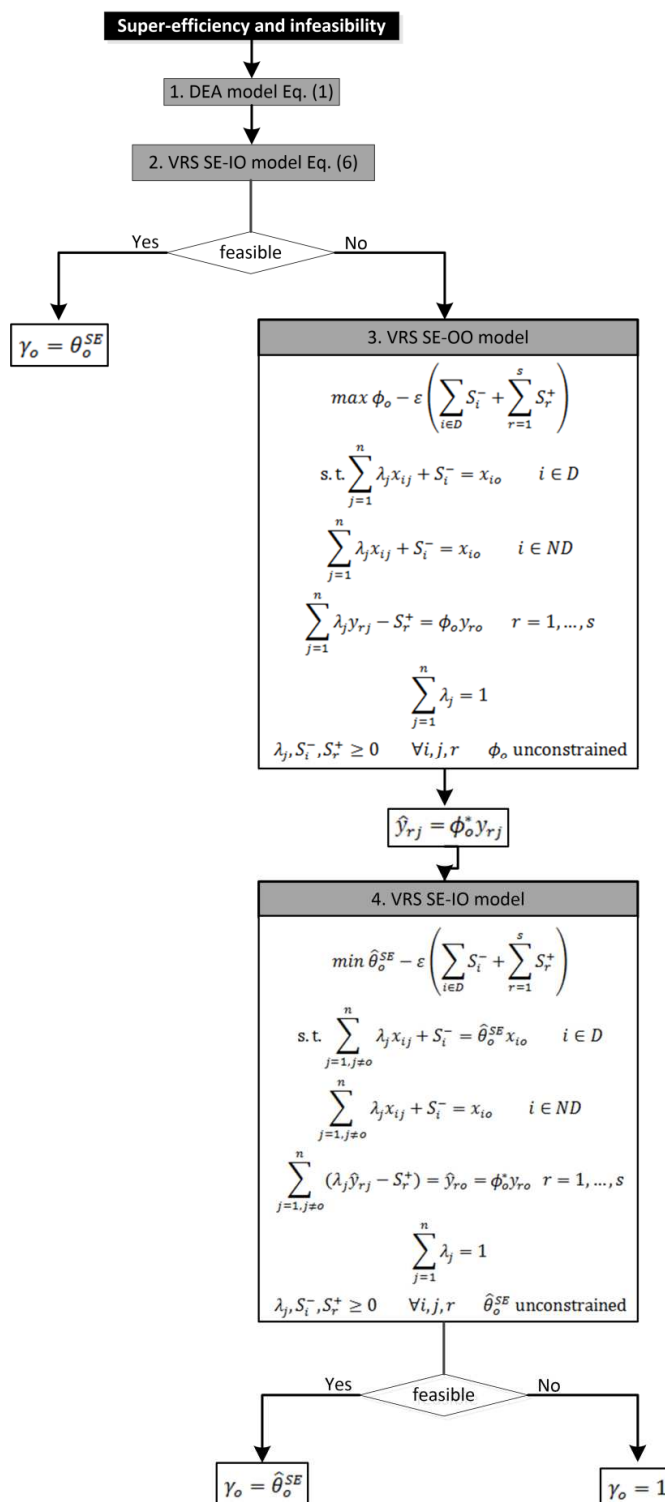


Figure 3.3. Flow diagram to fully characterize the super-efficiency by dealing with infeasibilities. SE-IO and SE-OO correspond to Input-Oriented and Output-Oriented Super-Efficiency, respectively.

From Figure 3.3, γ_o represents the score for characterizing the super-efficiency in terms of input savings. Therefore, $\gamma = \theta_o^{SE}$ if model (2) is feasible, $\gamma_o = \hat{\theta}_o^{SE}$ if model (2) is infeasible and model (4) is feasible, and $\gamma_o = 1$ if model (4) is infeasible. Note that γ_o is always greater or equal than one ($\gamma_o \geq 1$). If $\gamma_o > 1$, DMU_o has input super-efficiency, and if $\gamma_o = 1$, DMU_o does not have input super-efficiency.

3.3. Case study: industrial air separation units

We apply DEA to assess the efficiency of a set of 34 existing Air Separation Units located in Europe (19 of them) and Asia (15 of them). The ASUs operate as follows. First, the raw material (*i.e.*, ambient air) is drawn in, filtered and compressed to approximately 6 bars by a compressor. To separate air into its components, it must be liquefied at an extremely low temperature (*i.e.*, cryogenic temperatures) and, thus, as first step the compressed air is pre-cooled with chilled water. Then, impurities such as moisture, carbon dioxide or hydrocarbons are removed from the air in molecular adsorbers. Since the gases contained air only liquefy at very low temperatures, the purified air in the main heat exchanger is cooled down to approximately -175°C by means of an internal heat exchange, in which the gas flows generated during the process (*i.e.*, cold flows) cool the compressed air (*i.e.*, warm flow). Then, a rapid pressure drop causes the compressed air to cool further, and partial liquefaction takes place. Afterwards, the air is sent to the column where the separation in its components occurs. Separation of air into pure oxygen and pure nitrogen is performed in two columns, the medium and the low pressure columns, where the difference in boiling points of the air components (oxygen and nitrogen, -183°C and -196°C , respectively) is exploited for the separation process. The continuous evaporation and condensation brought about by the intense exchange of mass and heat between the rising vapor and the descending liquid produces pure nitrogen at the top of the low-pressure column and pure oxygen at the bottom. Argon is separated in additional columns and involves some extra steps in the process. Once the air components are separated and obtained at high purity, gaseous oxygen and nitrogen (GOX and GAN, respectively) are compressed until the pipeline pressure is reached in order to transport them to customers. The GOX and GAN liquefaction process is often carried out by additional

equipment that requires large amounts of energy. Note that some plants do not produce gases but only liquid products, and therefore show a slightly different design. Argon-rich stream is obtained in the medium part of the low pressure column but it needs an additional distillation process in which the impurities of nitrogen and oxygen are removed from the argon flow and, as a result, a stream of liquid argon (LAR) with high purity is obtained. Products in liquid form (LOX, LIN and LAR) are stored in tanks that are transported to customers by means of road tankers or used as a gas (*i.e.*, pipeline) backup system.

As commented in the previous description, the technologies to produce gases or liquids in ASUs are slightly different and, for this reason, it has been decided to create two DEA models, one (labelled as G) to assess the gas production technology in ASUs and another one (labelled as L) to assess the liquid production technology. By applying both models, we perform a more accurate and fair efficiency assessment. Furthermore, this allows us to analyze in greater detail those ASUs which only use one of the two technologies (*i.e.*, the ones which only produce gas or liquid). From the 34 plants under study, model G applies to 24 of them, while model L to 27 of them. We also note that 17 plants are present in both models, since they produce both gas and liquid products simultaneously. Table 3.1 summarizes the information about the ASUs to illustrate the main features of each plant.

Table 3.1. General information of the air separation units assessed. (EU: Europe; AS: Asia).

ASU	Type			Air capacity (x 1000m ³ /h)					Liquid capacity (x 1000m ³ /h)				Age (years)				
	G	L	G + L	≤ 50	> 50 & ≤ 100	> 100 & ≤ 150	> 150 & ≤ 200	> 200	≤ 10	>10 & ≤ 20	>20 & ≤ 30	> 30	≤ 5	> 5 & ≤ 10	> 10 & ≤ 15	> 15 & ≤ 20	> 20
EU_1	x			x											x		
EU_2	x			x										x			
EU_3	x			x									x				
EU_4	x			x									x				
EU_5	x				x										x		
EU_6		x							x						x		
EU_7		x								x				x			
EU_8		x								x					x		
EU_9		x								x					x		
EU_10		x							x						x		
EU_11		x							x							x	
EU_12			x	x					x				x				
EU_13			x	x						x							x
EU_14			x			x					x				x		
EU_15			x	x					x								x
EU_16			x				x		x								x
EU_17			x	x						x					x		
EU_18			x				x		x						x		
EU_19			x					x		x					x		
AS_1	x				x												x
AS_2	x							x							x		
AS_3		x								x				x			
AS_4		x							x					x			
AS_5		x										x			x		
AS_6		x							x					x			
AS_7			x				x		x								x
AS_8			x	x					x								x
AS_9			x					x				x			x		
AS_10			x				x		x						x		
AS_11			x		x							x			x		
AS_12			x					x	x					x			
AS_13			x						x						x		
AS_14			x	x						x							x
AS_15			x		x				x						x		

An important aspect in DEA analysis is how to properly identify the parameters considered as inputs and the ones considered as outputs. Here, air separation units are viewed as production systems consuming specific amounts of inputs to produce the desired outputs. Inputs and outputs are therefore defined as in Table 3.2 and Table 3.3 and Figure 3.4 and Figure 3.5 (for G and L models, respectively). We note that since our DEA analysis focuses on energy efficiency, we considered as inputs those related with electricity consumption. Other utilities (water, gasoil, etc.) represent less than 5% of the total utilities cost and therefore were omitted in the current analysis.

Table 3.2. Input/output definition of the air separation units which produce gaseous products (G).
 (ND: non-discretionary input).

Item	Description	Units
<i>Inputs</i>		
1. Electricity for air separation	Electricity used in the steps to separate the air in its components	kWh
2. Electricity for GOX compression	Electricity used in compressors to send GOX to customers	kWh
3. Electricity for GAN compression	Electricity used in compressors to send GAN to customers	kWh
4. Air capacity ^(ND)	Maximum feed air capacity of the ASU	m ³ /h
5. GOX pressure ^(ND)	Oxygen supply pressure	bar
6. GAN pressure ^(ND)	Nitrogen supply pressure	bar
<i>Outputs</i>		
1. GOX	Amount of oxygen produced in gas phase	m ³ /h
2. GAN	Amount of nitrogen produced in gas phase	m ³ /h

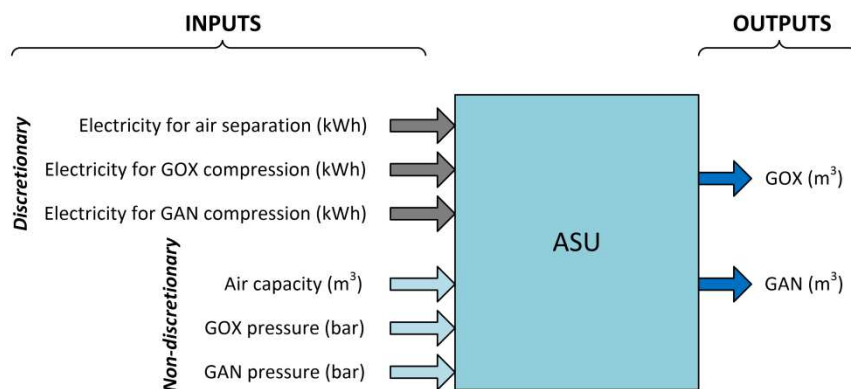


Figure 3.4. Flow diagram representing inputs and outputs in G model.

Table 3.3. Input/output definition of the air separation units which produce liquid products (L). (ND: non-discretionary input).

Item	Description	Units
<i>Inputs</i>		
1. Electricity for liquefaction	Electricity used in liquefiers to produce LOX and LIN	kWh
2. Liquid capacity ^(ND)	Maximum amount of liquid that can be produced in the ASU	m ³ /h
3. LAR capacity ^(ND)	Maximum amount of LAR that can be produced in the ASU	m ³ /h
<i>Outputs</i>		
1. LOX	Amount of oxygen produced in liquid phase	m ³ /h
2. LIN	Amount of nitrogen produced in liquid phase	m ³ /h
3. LAR	Amount of argon produced in liquid phase	m ³ /h

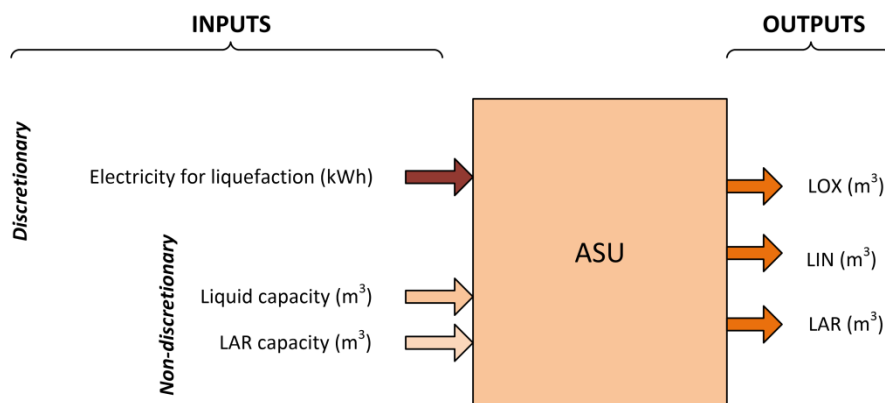


Figure 3.5. Flow diagram representing inputs and outputs in L model.

In case of model G, the non-discretionary input “Air capacity” depends on the design of the main air compressor, which was selected during the plant design taking into account the level of production (*i.e.*, demand) forecasted. In the same way, non-discretionary inputs “GOX pressure” and “GAN pressure” in model G, depend on the customers’ requirements and pipeline framework design. In the case of model L, “Liquid capacity” and “LAR capacity” are non-discretionary inputs linked to the

process design and, therefore, to structural changes or the addition of further machinery.

In Figure 3.6 and Figure 3.7, we show the relationships between inputs and outputs levels for the different air separation units in models G and L, respectively, where the percentages refer to the highest input/output value for each parameter among the whole set of air separation units assessed (*i.e.*, 100% corresponds to the largest value for each parameter). We note that the specific values for inputs and outputs of air separation units cannot be disclosed due to confidentiality issues.

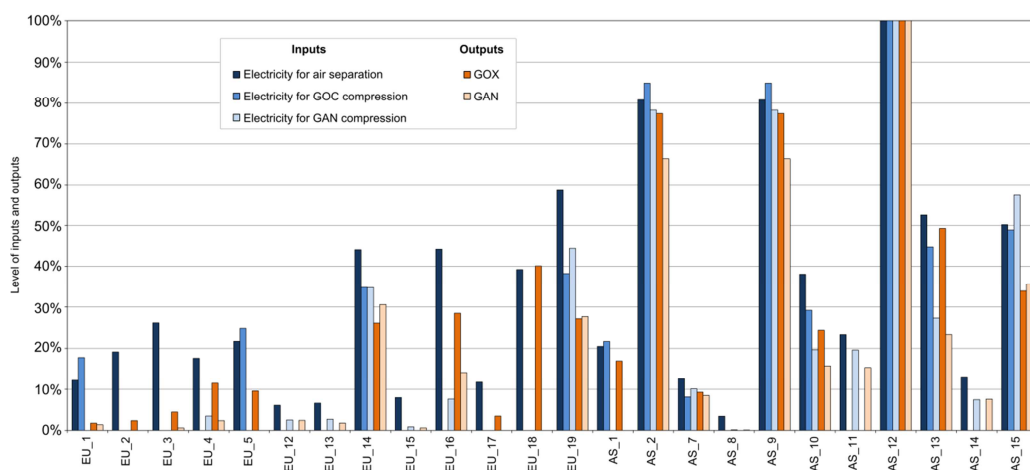


Figure 3.6. Relationship between input and output levels among the air separation plants of model G.

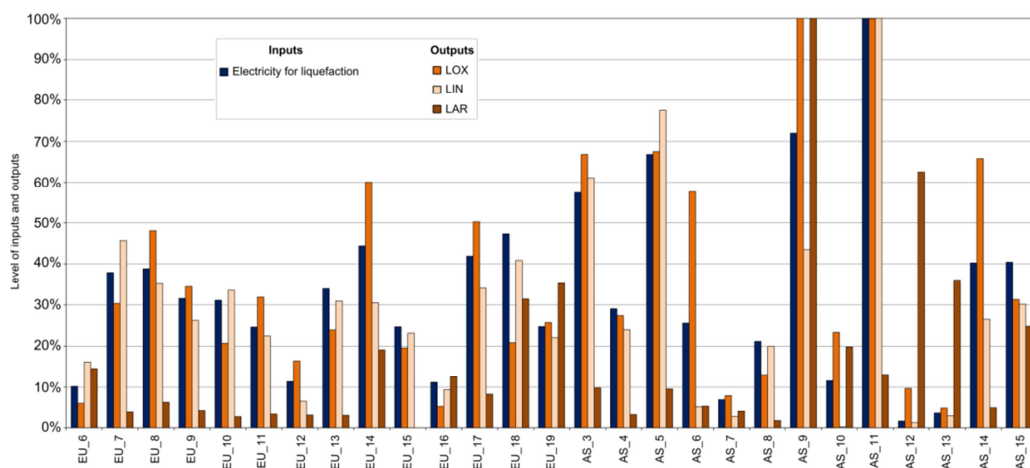


Figure 3.7. Relationship between input and output levels among the air separation plants of model L.

In order to obtain reliable results and avoid a weak discriminatory power in the DEA application, it is important to satisfy a given relationship between the number of DMUs (*i.e.*, ASUs) and the number of inputs and outputs (Cooper *et al.*, 2007):

$$\text{number of DMUs} \geq \max\{m \cdot s, 3(m + s)\} \quad \text{Eq. 3-14}$$

where m and s are the number of inputs and outputs, respectively. We note that our models G and L satisfy this rule of thumb widely use in DEA.

3.3.1. Results and discussion

Models G and L were implemented in GAMS 24.8.3 and solved with CPLEX 12.7.0.0 on an Intel® Core™ i5-3210 processor operating at 2.50 GHz (GAMS, 2015). It took around 1.6–1.8 CPU seconds to solve every instance. In the following subsections we present the main outcomes resulted from the application of both models and their subsequent assessment.

3.3.1.1. Efficiency results

When solving model G, 18 ASUs are found efficient from a total of 24 units (75% of them), as shown in Figure 3.8. Hence, six ASUs are found inefficient, with four of them showing efficiency values higher than 75% (*i.e.*, EU_19, EU_13, EU_5 and AS_10), which indicates that their distance to the efficient frontier is small. Conversely, two of these inefficient ASUs (*i.e.*, EU_15 and EU_4) show low efficiency values (58% and 53%, respectively), implying that they need larger improvements to become efficient. In model L, the results show that there are 19 efficient ASUs (70% of them), as illustrated in Figure 3.9. Among the eight inefficient ASUs, four of them show efficiency values higher than 80% (*i.e.*, EU_19, EU_10, EU_8 and EU_17). On the other hand, AS_7 shows a low efficiency value (57%).

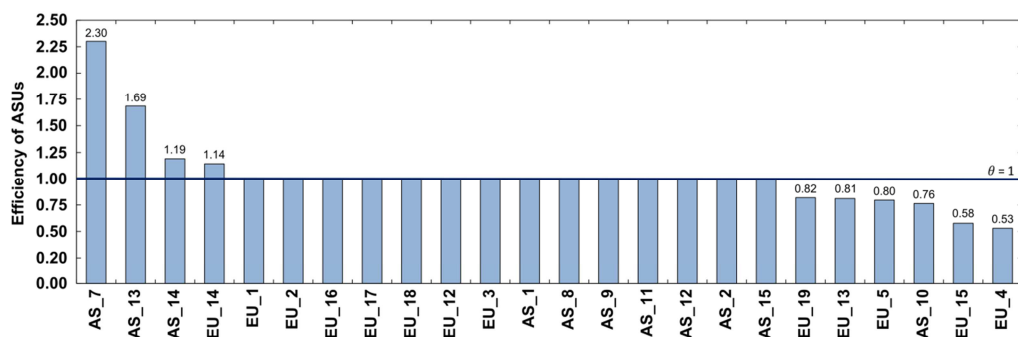


Figure 3.8. Efficiency and super-efficiency scores of the 24 ASUs in model G.

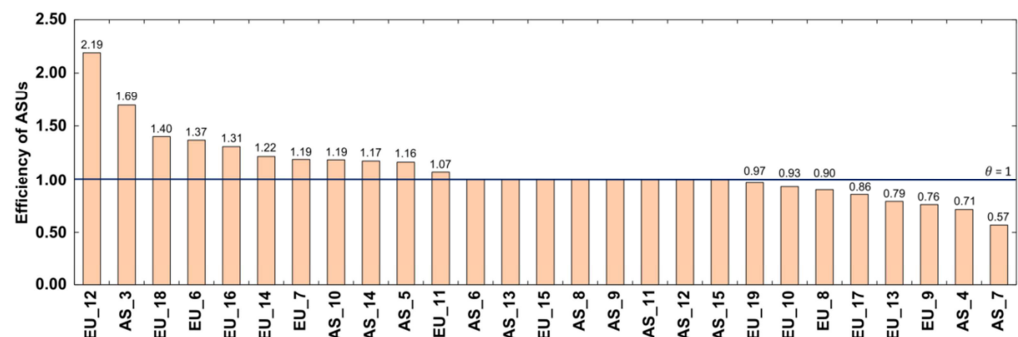


Figure 3.9. Efficiency and super-efficiency scores of the 27 ASUs in model L.

From Figure 3.8 we observe (from a location point of view) that plants located in Asia are more efficient (on average) than those in Europe. From the total of plants located in Asia, 90.9% of them are efficient, while in Europe only 61.3% of the total plants are efficient. We clarify that plants in Asia are newer than those in Europe (nearly four years newer on average), so they implement better technology. Furthermore, Asian plants have higher capacities (63.1% higher on average), so they exploit better the concept of economies of scale which results in a better use of resources. Conversely, the efficiency differences between European and Asian plants in the case of the liquid production technology (Figure 3.9) are not as significant as with the gas technology. Here, 84.6% of the Asian and 57.1% of the European plants are efficient.

From Figure 3.8 and Figure 3.9, we also note that some plants that are present in both models (*i.e.*, G and L) show different behaviors depending on the technology assessed. This can be observed in AS_7, which shows the best super-efficiency score

in model G, but is inefficient (with the worst score) in model L. The reason might be that this plant was installed to cover a high gas demand (which is its main business), whereas the liquid production is a residual business (probably oversized with respect to the current liquid demand, despite the already low liquid capacity). On the contrary, AS_10 shows high efficiency scores in model L, but low scores in model G, very likely because it recently experienced an important decrease in gas demand. We also note that some plants perform poorly in both models (EU_19 and EU_13), while others emerge as efficient in both cases (as in the case of EU_14).

3.3.1.2. Super-efficiency results

While in model G the plants located in Asia show higher super-efficiency scores (*e.g.*, AS_7, AS_13, AS_14), we find that 63.6% of the super-efficient plants in model L are located in Europe, with some of them showing particularly high super-efficiency scores (*e.g.*, EU_12). This denotes that in Europe the liquid technology is better exploited than the gas technology. This could be due to the fact that during the last years, many European ASUs have reduced their gas demand (mainly from big customers) so the production has been adapted to supply liquid customers (normally the small customers).

We note that only those ASUs with super-efficiencies strictly above one show extra savings in discretionary inputs. According to this criterion, we can rank the ASUs in model G as follow: $AS_7 > AS_{13} > AS_{14} > EU_{14}$, where AS_7 is the ASU which could achieve the largest extra savings in inputs, and EU_14 the one with the lowest ones. In model L, the ranking of ASUs showing extra savings in discretionary inputs is as follows: $EU_{12} > AS_3 > EU_{18} > EU_6 > EU_{16} > EU_{14} > EU_7 = AS_{10} > AS_{14} > AS_5 > EU_{11}$. For the rest of efficient ASUs (those with super-efficiency equal than one), super-efficiency is due to either non-discretionary inputs, outputs or a combination of the two. Hence, this is not reflected in the super-efficiency measure that we use.

3.3.1.3. Inefficiency assessment

The percentage of improvement (with respect to the current situation) required in each discretionary input to make the inefficient ASUs efficient (denoted by IMP_{ij}) is calculated as follows:

$$IMP_{ij} = \frac{x_{ij} - TG_{ij}}{x_{ij}} \cdot 100 \quad i \in D; j \text{ inefficient} \quad \text{Eq. 3-15}$$

In Figure 3.10 and Figure 3.12 we show a heat map (for G and L models) representing these improvement targets. We note that even though our main goal here is the definition of the percentage of improvement in discretionary inputs, in Figure 3.10 and Figure 3.12 we also show the percentage of improvement for non-discretionary inputs and outputs. The targets in both non-discretionary inputs and outputs correspond to slack variables S_i^- and S_r^+ , respectively, and therefore they are only required to achieve *strong efficiency*. We note that the percentages of improvement in Figure 3.10 and Figure 3.12 are expressed in absolute value without considering the corresponding sign. Therefore, in Figure 3.10 the percentage of improvement in inputs (*i.e.*, ‘Electricity for air separation’, ‘Electricity for oxygen compression’, ‘Electricity for nitrogen compression’ and ‘Air capacity’) corresponds indeed reductions (-), while the percentage of improvement in outputs (*i.e.*, ‘GOX’ and ‘GAN’) denotes increments (+). Darker colors in Figure 3.10 and Figure 3.12 imply a stronger target, and hence, the need to further reduce/increase the corresponding parameter so as to become efficient. In Figure 3.11 and Figure 3.13, we show the average percentage of improvement in each parameter. In these figures, inputs improvements are negative (since they imply reductions) and output positive (since they imply increments).

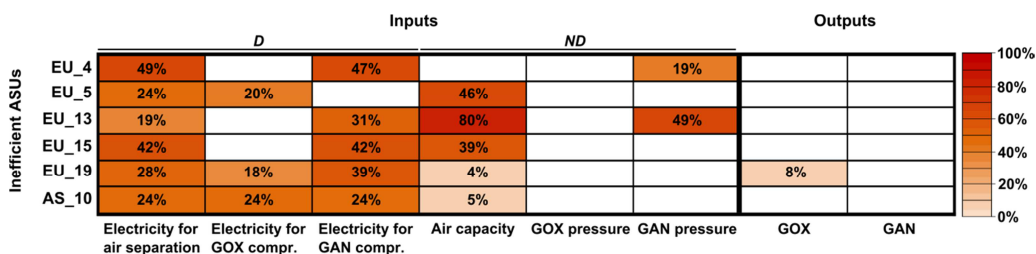


Figure 3.10. Percentage of improvement required in each inefficient ASU in model G.

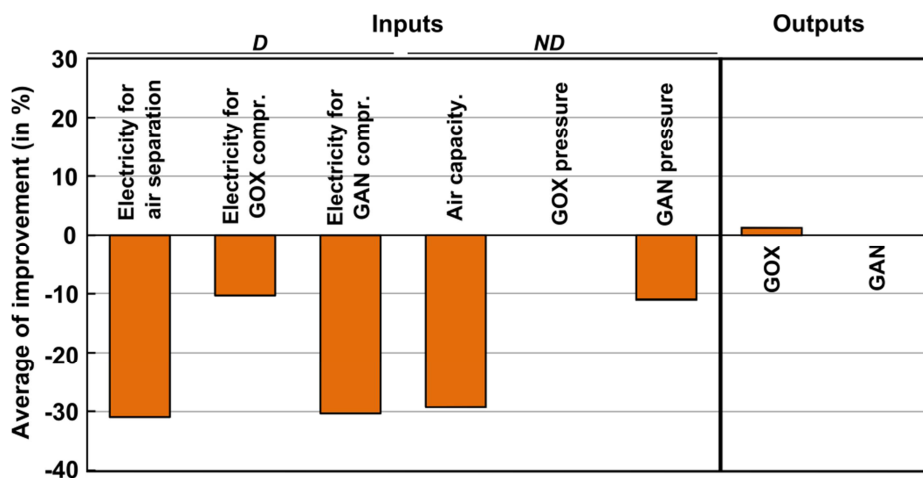


Figure 3.11. Average improvement percentage in each parameter in model G.

From Figure 3.10 and Figure 3.11, we can identify “Electricity for air separation”, “Electricity for GAN compression” and “Air capacity” as the most critical parameters of model G, which require an average reduction of 31%, 30% and 29% to become efficient, respectively. EU_13 and EU_15 are the ASUs with the largest targets in the overall set of parameters (22% and 15% on average, respectively). This is mainly due to the fact that these plants are quite old (more than 20 years), and their demand has steadily decreased over time. Therefore, their capacities are oversized. Furthermore, the processes and the machinery used in these plants are not as efficient as those more recently installed in other locations. Since “Air capacity” is a non-discretionary input, efforts should focus on reducing first both the electricity used for air separation and that used for GAN compression (note that attaining targets in discretionary inputs allows the ASU to become weakly efficient). In any case, energy consumption will always be constrained by thermodynamic limits given by the separation processes.

Finally, we note that if the inefficient ASUs from model G would operate according with the targets shown in Figure 3.10, they would reduce their overall yearly energy consumption in 300GWh.

The same approach discussed above applies to Figure 3.12 generated with model L. Here, in input categories (*i.e.*, ‘Electricity for liquefaction’, ‘Liquid capacity’ and ‘LAR capacity’) the improvement percentage represents reductions (-), whilst in the outputs (*i.e.*, LOX, LIN and LAR) it denotes increments (+).

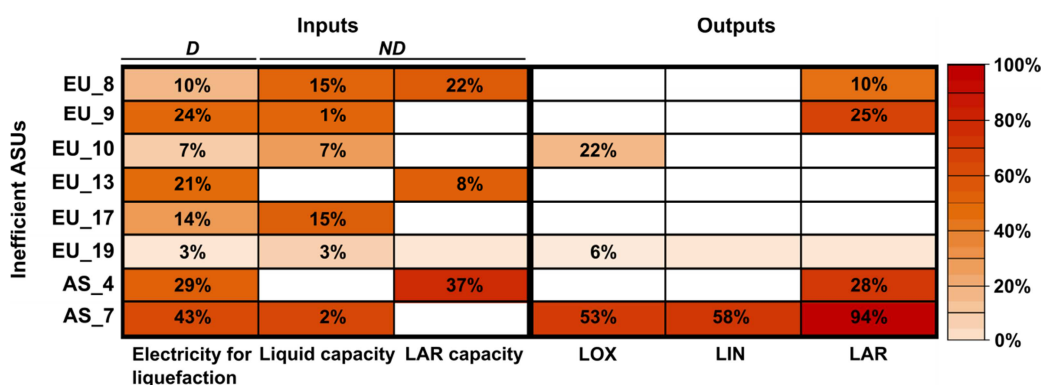


Figure 3.12. Percentage of improvement required in each inefficient ASU in model L.

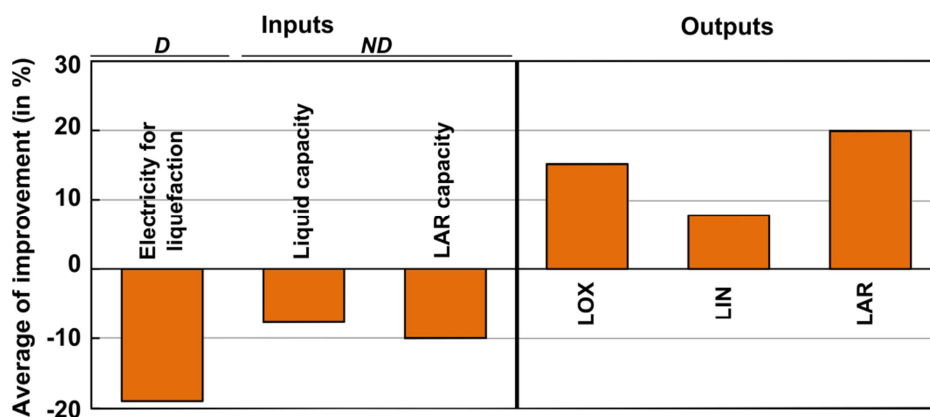


Figure 3.13. Average improvement percentage in each parameter in model L.

From Figure 3.12 and Figure 3.13, “LAR product” and “Electricity for liquefaction” emerge as the most critical parameters (on average) in model L, requiring an improvement of 20% (increasing “LAR product”) and 19% (decreasing “Electricity for liquefaction”). AS_7 and AS_4 are the ASUs with the largest targets in improving the

overall set of parameters (42% and 16% on average, respectively). This implies that higher efforts should be devoted to these processes to make them efficient. In the case of AS_7, it has experienced a strong downfall in liquid production (*i.e.*, demand) in the last years. Nowadays, only less than 5% of the liquid capacity of the plant is used, while few years ago it lied above 90%. The same occurs in LAR production, which nowadays only uses around 10% of the total LAR capacity allowed in the plant. In the case of AS_4, its liquid production takes an intermediate value (around 60% of liquefaction capacity is currently used), yet LAR production is rather low (less than 20% of LAR capacity used). Those aspects are far beyond our reach, as in some cases large industrial consumers decide to close their facilities, which results in high demand variations. As before, the main efforts should focus on reducing the electricity used for liquefaction, since “LAR product” is an output and it depends on demand requirements. Finally, if the inefficient ASUs from model L would operate according with the targets shown in Figure 3.12, they would reduce their overall yearly energy consumption in 55GWh.

Analyzing the non-discretionary inputs (as defined in Table 3.2 and Table 3.3) in both models (G and L), none of the inefficient ASUs could become strongly efficient. This is because they all have slacks in ND inputs. Nevertheless, they could improve their current efficiency level if the discretionary inputs and outputs were properly manipulated.

Figure 3.14 and Figure 3.16 show a heat map representing the linear coefficients of peers in the G and L models, respectively. Figure 3.15 and Figure 3.17 show the number of times each efficient ASU is defined as peer (*i.e.*, acts as benchmark) by the inefficient ones as well as the summation of all linear coefficients (obtained from the rows in Figure 3.14 and Figure 3.16, respectively).

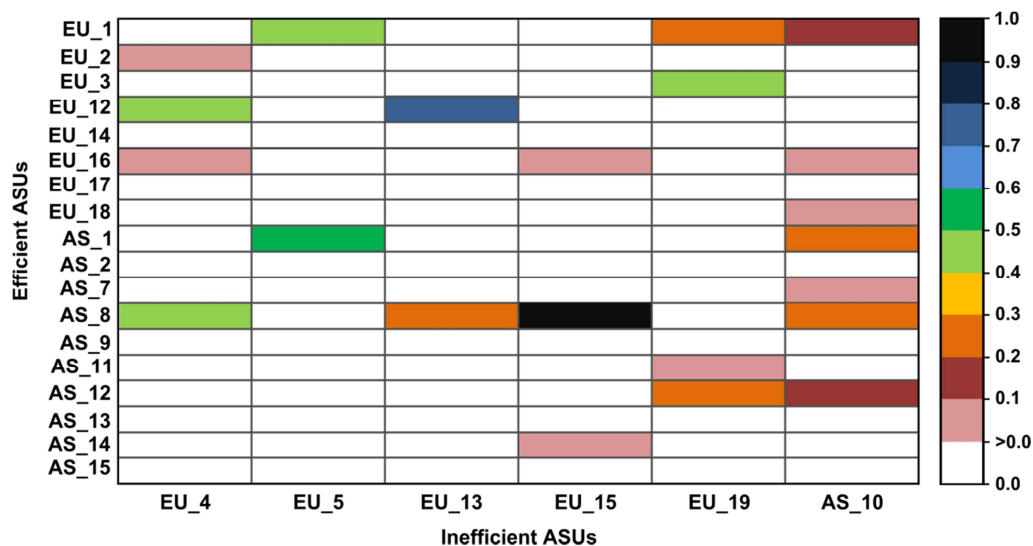


Figure 3.14. Linear weights for the benchmarks selected by each inefficient ASUs in model G.

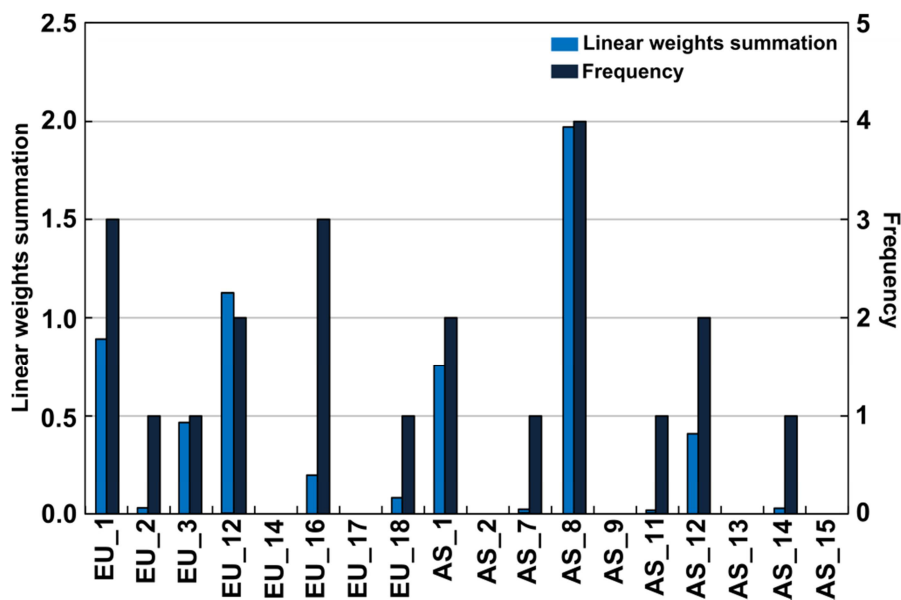


Figure 3.15. Linear weights summation in efficient ASUs and frequency to be benchmark in model G.

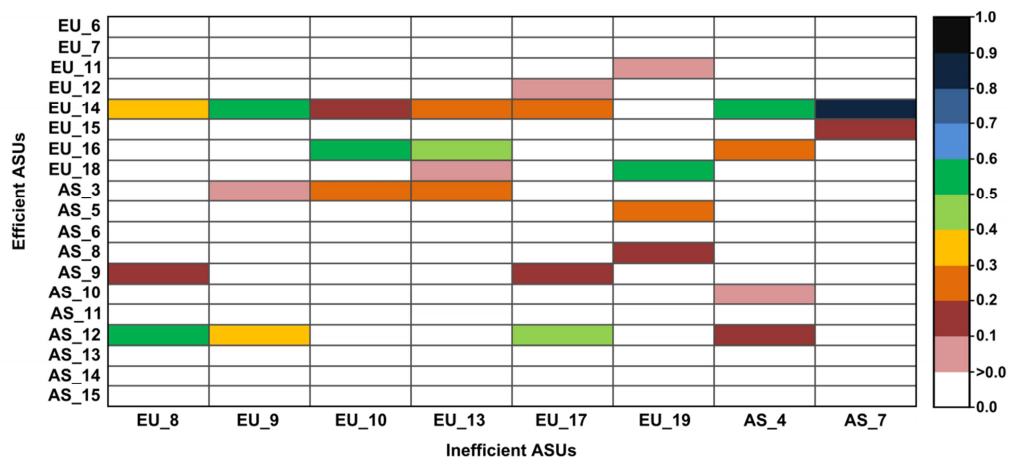


Figure 3.16. Linear weights for the benchmarks selected by each inefficient ASUs in model L.

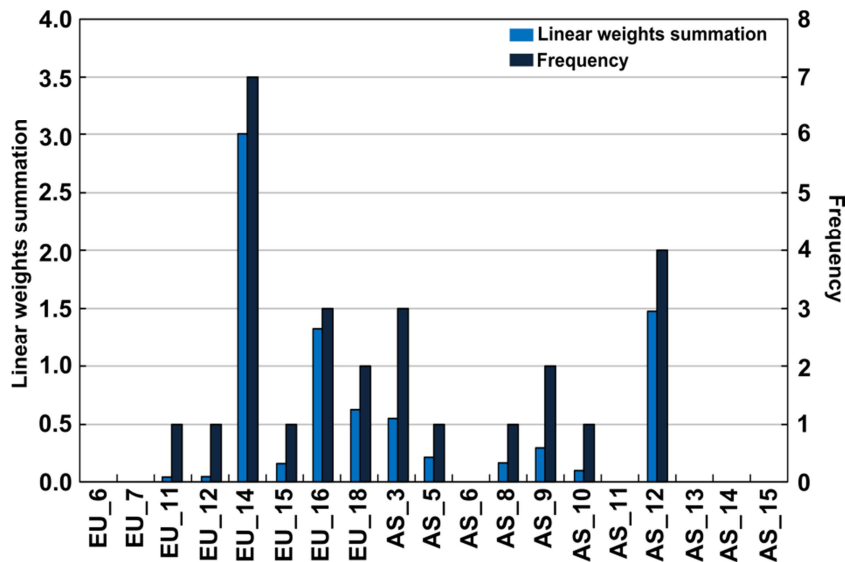


Figure 3.17. Linear weights summation in efficient ASUs and frequency to be benchmark in model L.

As an example, to facilitate the understanding of previous figures, we select EU_19 as the reference inefficient ASU in Figure 3.16. This ASU would become efficient by approaching the linear combination of its reference set formed by EU_11, EU_18, AS_5 and AS_8, with linear multipliers 0.04, 0.59, 0.20 and 0.16, respectively. This means that EU_19 should use these four ASUs as models when attempting to improve, focusing on those with higher coefficients in the linear combination.

From previous figures we observe that (in model G) AS_8 shows the highest linear coefficient summation (1.97) and the highest frequency of benchmarking (four ASUs use it as a peer). In model L, EU_14 is the preferred ASU (seven ASUs uses it as peer), showing in turn the highest linear weight summation (3.0). This means that AS_8 (in model G) and EU_14 (in model L) should be taken as reference facilities.

3.3.1.4. Malmquist Productivity Index results

The previous analysis corresponds to a snapshot for year 2016. In order to study the efficiency trends of the plants over time, we calculate the Malmquist Productivity Index (MPI) for 2013 to 2016. We have focused on this time period because some plants were recently built and their demand changed over time (*e.g.*, emergence of new customers, loss of customers, increases or decreases in demand’s flowrate, etc.). We show in Figure 3.18 and Figure 3.19, respectively, the Technical Efficiency Changes (TEC_o), the Frontier Shifts (FS_o) and the Malmquist Productivity Index (M_o) in each ASU. Colors are used to represent the intensity of improvement (green) or worsening (red) from year to year. We note that blank cells mean that the ASU did not exist in one of the corresponding years.

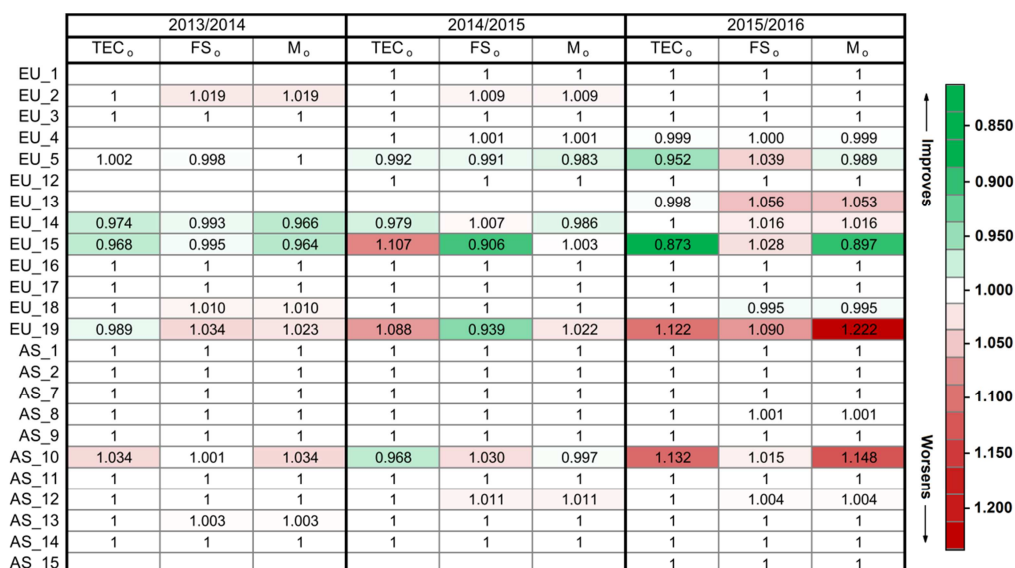


Figure 3.18. Technical efficiency changes, Frontier shift and Malmquist index in model G.

We start by analyzing the MPI in model G. The worst MPI scores are shown by EU_19 and AS_10 in the 2015/2016 time interval, with decreases of 22.2% (*i.e.*, MPI = 1.222) and 14.8% respectively. In both cases, the change is due to the combined worsening of their relative technical efficiency (TEC_o of -12.2% for EU_19 and -13.2% for AS_10) and the regression of the frontier (FS_o of -9.0% for EU_19 and -1.5% for AS_10). This means that, despite the decrease in the performance of similar ASUs from 2015 to 2016 (causing a regression in the frontier leading to FSs > 1), the technical efficiency of ASUs EU_19 and AS_10 attained even lower values in 2016 compared to 2015 (therefore, TECs > 1). In EU_19, the main factors explaining the regression in the technical efficiency between 2015 and 2016 are the worsening of 10.8% in the specific consumption (kWh/m³) of GOX compression and the decrease in the air separation efficiency (-21.7%). In AS_10, from year 2015 to year 2016, the specific consumption (kWh/m³) of GOX and GAN compression was worsened by 16.3% and 17.2%, respectively (data not shown), which were mainly caused by the reduction of both GOX and GAN demand (m³) by 14.8% and 29.4%, respectively (data not shown) occurred between both years.

Conversely, the best MPI score was attained by EU_15 with an improvement of 10.3% from 2015 to 2016. Despite the regression of the frontier (FS_o of -2.8% for EU_15) from 2015 to 2016, the high improvement in its relative technical efficiency (TEC_o of 12.3%) allowed ASUs to obtain the greatest MPI improvement. This is mainly due to the improvements of 9.1% and 8.8% (data not shown) in GAN compression and air separation, respectively.

Overall, we note that in model G MPI suffers very few changes from year to year (-0.100% in 2013/2014, -0.055% in 2014/2015 and -1.409% in 2015/2016), since the plants worsening were compensated by others improving their performance.

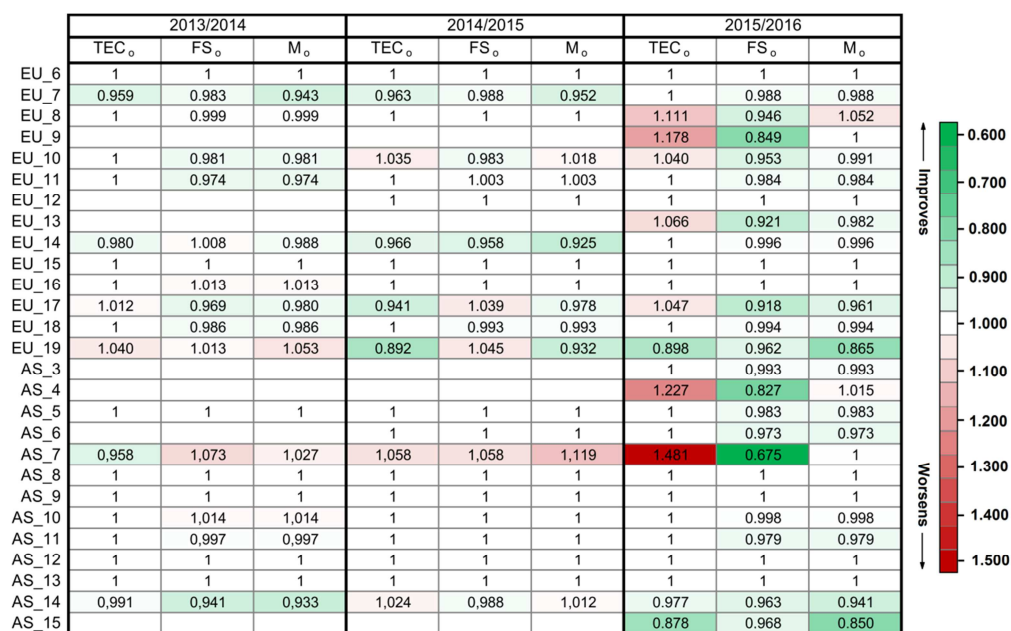


Figure 3.19. Technical efficiency changes, Frontier shift and Malmquist productivity index in model L.

The MPI in model L, shows that the worst score is obtained in AS_7 from 2014 to 2015, with a decrease of 11.9%. The result is due to the combined worsening of their relative technical efficiency and the regression of the frontier (-5.8% in both TEC_o and FS_o components). This is due to the significant losses in product demand from 2014 to 2015. In this period LOX, LIN and LAR demand (production) were reduced by 67%, 70% and 82% respectively (data not shown). In Figure 3.19, we can also observe how AS_7 behaved from 2015 to 2016. The technical efficiency of ASU_7 decreased from 2015 to 2016 (TEC_o = 1.481) due to decreases of 89.5% and 99.2% in LOX (kWh/m³ LOX) and LIN (kWh/m³ LIN) production, respectively, yet the frontier improved (FS_o = 0.675) due to the increase in the performance of similar ASUs, resulting in a MPI = 1.

On the other hand, AS_15 and EU_19 (both from 2015 to 2016) showed the best Malmquist Productivity Index with improvements of 15.0% and 13.5%. AS_15 reduced its liquefaction specific consumption by 3.2%, which was due to an increase of 42.4% in LIN production (despite a 20.1% reduction in LOX). Also, LAR production was significantly improved (37.9%) between 2015 and 2016. The good results of EU_19 in 2014/2015 resulted from the improvement (3.7%) in its liquid production.

We note that, as in model G, MPI showed very few changes from year to year (0.565% in 2013/2014, 0.308% in 2014/2015 and 1.691% in 2015/2016).

3.4. Conclusions

With the growing trend of improving industrial processes to optimize energy management, there is a clear need to develop decision-making tools to assess the energy efficiency of industrial facilities. In this paper, we applied the non-parametric method of DEA to assess the efficiencies of a set of air separation units producing nitrogen, oxygen and argon together with their evolution over time.

This approach, implemented in GAMS, allowed us to identify efficient and inefficient ASUs considering separately gas production (model G) and liquid production (model L) facilities. From the ASUs assessed in model G, 75% of them were classified as efficient, while in model L, 70% of the assessed ASUs were efficient. Super-efficiency analysis allowed us to further discriminate among the efficient ASUs. We found that 16.7% and 40.1% of ASUs in G and L models respectively showed extra-savings in their discretionary inputs.

In terms of improvement targets, “Electricity for air separation”, “Electricity for GAN compression” and “Air capacity” were identified as the most critical parameters in model G, with an average reduction needed of 31%, 30% and 29%, respectively. In the same model, EU_13 and EU_15 were identified as the ASUs requiring the largest improvements (22% and 15%, respectively). In model L, “LAR product” and “Electricity for liquefaction” were identified as the most critical parameters (on average), requiring an improvement of 20% and 19%, respectively. AS_7 and AS_4 were found as the ASUs requiring the largest improvements (42% and 16% on average, respectively).

Our analysis was further complemented with the results of the DEA Malmquist productivity approach, finding that the worst MPI scores in model G were shown by EU_19 and AS_10 in the 2015/2016 time interval, with decreases of 22.2% and 14.8%, respectively. On the other side the best MPI score was attained by EU_15 with an improvement of 10.3% from 2015 to 2016. In model L, the worst score was obtained by AS_7 from 2014 to 2015, with a decrease of 11.9%., whereas AS_15 and EU_19

(both from 2015 to 2016) showed the best MPI scores with improvements of 15.0% and 13.5%.

Overall, the combination of DEA and the Malmquist productivity index allowed us to effectively identify inefficiency sources, assess the efficiency trend in each unit and establish quantitative targets for improvement. This method can be applied in a wide range of energy intensive industrial processes (*i.e.*, chemical, automotive, metallurgy, etc.) to minimize energy losses in the transition to a more sustainable world.

Acknowledgement

The authors would like to acknowledge financial support from the Generalitat de Catalunya (2014 DI 030) in the modality of Industrial Doctoral program. Gonzalo Guillén-Gosálbez would like to acknowledge the financial support received from the Spanish "Ministerio de Ciencia y Competitividad" through the project CTQ2016-77968-C3-1-P.

3.5. Nomenclature

Abbreviations

ASU	air separation unit
BCC	Banker Charnes and Cooper model
DEA	data envelopment analysis
DMU	decision making unit
GOX	gas oxygen
GAN	gas nitrogen
LAR	liquid argon
LIN	liquid nitrogen
LOX	liquid oxygen
LP	linear programming
MPI	Malmquist productivity index
VRS	variable returns to scale

Sets

i	set of inputs indexed by i
j	set of decision making units indexed by j
r	set of outputs indexed by r
t	set of time intervals indexed by t

Subsets

D	set of inputs which are discretionary
ND	set of inputs which are non discretionary

Variables

ϕ_o	efficiency score in output oriented model
FS_o	frontier technology shift in DMU_o
γ_o	represent the score for characterizing the super-efficiency in terms of input savings
IMP_{ij}	percentage of improvement required in each discretionary input to make the inefficient ASUs efficient
λ_j	linear weight for every single DMU_j to form a linear combination
M_o	Malmquist index to measure efficiency changes in DMU_o
θ	relative efficiency score in input oriented model
θ_o^{SE}	super-efficiency score
$\hat{\theta}_o^{SE}$	super-efficiency score when super-efficiency is determined by infeasibility in model (2) and feasibility in model (6)
o	assessed DMU
S_i^-	amount of input i that, if reduced, shifts the DMU_o projection until the strongly efficient frontier
S_r^+	amount of output r that, if increased, shifts the DMU_o projection until the strongly efficient frontier
TEC_o	technical efficiency change in DMU_o
TG_{io}	target for discretionary input i in any inefficient DMU_o
$TGND_{io}$	target for non-discretionary input i in any inefficient DMU_o

TGO_{ro} target for output r in any inefficient DMU_o

Parameters

ε non-archimedean value designed to enforce strict positivity on the variables

m number of inputs consumed by a DMU

n number of decision making units

s number of outputs produced by a DMU

x_{ij} amount of input i consumed by DMU_j

y_{rj} amount of output r produced by DMU_j

3.6. References

Andersen P, Petersen NC. A procedure for ranking efficient units in data envelopment analysis. *Management Science* 1993;39:1261–1264.

Azadeh MS, Amalnick SF, Ghaderi SM, Asadzadeh. An integrated DEA PCA numerical taxonomy approach for energy efficiency assessment and consumption optimization in energy intensive manufacturing sectors. *Energy Policy* 2007;35:3792–3806.

Banker RD, Charnes A, Cooper WW. Some models for estimating technical and scale inefficiencies in data envelopment analysis. *Management Science* 1984;30:1078–1092.

Banker RD, Morey R. Efficiency analysis for exogenously fixed inputs and outputs. *Operations Research* 1986;34(4):513-521.

Banker RD, Gifford JL. *A Relative Efficiency Model for the Evaluation of Public Health Nurse Productivity*. Pittsburgh: School of Urban and Public Affairs, Carnegie Mellon University. 1988.

Banker RD, Das S, Datar SM. Analysis of cost variances for management control in hospitals. *Research in Governmental and Nonprofit Accounting*. 1989;5:268–291.

Blomberg J, Henriksson E, Lundmark R. Energy efficiency and policy in Swedish pulp and paper mills: a data envelopment analysis approach. *Energy Policy* 2012;42:569–579.

Boussofiane A, Dyson RG, Thanassoulis E. Applied data envelopment analysis. *Eur. J. Oper. Res.* 1991;52:1–15.

Boyd G, Dutrow E, Tunnessen W. The evolution of the ENERGYSTARs energy performance indicator for benchmarking industrial plant manufacturing energy use. *J. Clean. Prod* 2008;16:709–715.

Camanho AS, Portela MC, Vaz CB. Efficiency analysis accounting for internal and external nondiscretionary factors. *Computers Ops Res* 2009;36:1591–1601.

Caves W, Christensen LR, Diewert WE. The economic theory of index numbers and the measurement of input, output and productivity. *Econometrica* 1982;50:1393-1414.

Chang TP, Hu JL. Total-factor energy productivity growth, technical progress, and efficiency change: an empirical study of China. *Appl Energy* 2010;87(10):3262-3270.

Charnes A, Cooper WW, Rhodes E. Measuring the efficiency of decision making units. *Eur. J. Oper. Res.* 1978;2:429-444.

Chen Y, Ali AI. DEA Malmquist Productivity measure: new insights with an application to computer industry. *European Journal of Operational Research* 2004;159(1):239-249.

Chen Y. Measuring super-efficiency in DEA in the presence of infeasibility. *European Journal of Operational Research* 2005;161:545–551

Choi Y, Zhang N, Zhou P. Efficiency and abatement costs of energy-related CO₂ emissions in China: A slacks-based efficiency measure. *Appl Energy* 2012;98:198-208.

Chung W. Review of building energy-use performance benchmarking methodologies. *Appl Energy* 2011;88:1470-1479.

Cook WD, Seiford LM. Data envelopment analysis (DEA) - Thirty years on. *Eur. J. Oper. Res.* 2009;192:1–17.

Cooper WW, Seiford LM, Tone K. Introduction to Data Envelopment Analysis and its Uses. Springer Science, p. 351. 2006

Cooper WW, Seiford LM, Tone K. Data Envelopment Analysis: a comprehensive text with models, applications, references and DEA-Solver software. Springer Science & Business Media 2007.

Cooper WW, Seiford LM, Zhu J. Handbook on data envelopment analysis 2nd ed. New York: Springer; 2011.

Enerdata and the Economist Intelligence Unit. Trends in global energy efficiency. An analysis of industry and utilities. (Report). 2011.

Fare R, Grosskopf S, Lindgren B, Ross P. Productivity changes in Swedish pharmacies 1980-1989: A non-parametric Malmquist approach. *The Journal of Productivity Analysis* 1992;3:85-101.

Fare R, Grosskopf S, Norris M, Zhang Z. Productivity growth, technical progress, and efficiency change in industrialized countries. *The American Economic Review* 1994;84(1):66-83.

Galán-Martín A, Guillén-Gosálbez G, Stamford L, Azapagic A. Enhanced data envelopment analysis for sustainability assessment: a novel methodology and application to electricity technologies. *Computers & Chemical Engineering* 2016;90:188-200.

GAMS Development Corporation, General Algebraic Modeling System (GAMS) Release 24.4.5, Washington, DC, USA, 2015.

Han Y, Geng Z, Liu Q. Energy efficiency evaluation based on data envelopment analysis integrated analytic hierarchy process in ethylene production. *Chin. J. Chem. Eng.* 2014;22:1279–128.

Hasanbeigi A, Price L, Lu H, Lan W. Analysis of energy-efficiency opportunities for the cement industry in Shandong Province, China: a case study of 16 cement plants. *Energy* 2010;35(8):3461–3473.

Limleamthong P, Gonzalez-Miquel M, Papadokostantakis S, Papadopoulos AI, Seferlis P, Guillén-Gosálbez G. Multi-criteria screening of chemicals considering thermodynamic and life cycle assessment metrics via data envelopment analysis: application to CO₂ capture. *Green Chem* 2016;18:6468-6481.

Latimer RE. Distillation of Air. *Chemical Engineering Progress* 1967;63(2):35–59.

Li Y, Sun L, Feng T, Zhu C. How to reduce energy intensity in China: a regional comparison perspective. *Energy Policy* 2013;61:513–522.

Li K, Lin B. Impact of energy conservation policies on the green productivity in China's manufacturing sector: Evidence from a three-stage DEA model. *Appl Energy* 2016;168:351-363.

Liu CH, Lin SJ, Lewis C. Evaluation of thermal power plant operational performance in Taiwan by data envelopment analysis. *Energy Policy* 2010;38:1049–1058.

Majid Zadmirzaei, Soleiman Mohammadi Limaiei, Leif Olsson, Alireza Amirteimoori. Assessing the impact of the external non-discretionary factor on the performance of forest management units using DEA approach. *Journal of Forest Research* 2017;22(3).

Mandal SK, Madheswaran S. Energy use efficiency of Indian cement companies: a data envelopment analysis. *Energy Effic* 2011;4:57–73.

Malmquist, S. Index numbers and indifference curves. *Trabajos de Estadística* 1953;4:209-242.

Mardani A, Zavadskas EK, Streimikiene D, Jusoh A, Khoshnoudi M. A comprehensive review of data envelopment analysis (DEA) approach in energy efficiency. *Renewable and Sustainable Energy Reviews* 2017;70:1298-322.

Makridou G, Andriosopoulos K, Doumpou M, Zopounidis C. Measuring the efficiency of energy-intensive industries across European countries. *Energy Policy* 2016;88:573–583.

Morfeldt J, Silveira S. Capturing energy efficiency in European iron and steel production—comparing specific energy consumption and Malmquist productivity index. *Energy Effic* 2014;7:955–72.

Mousavi-Avval SH, Rafiee S, Jafari A, Mohammad A. Optimization of energy consumption for soybean production using Data Envelopment Analysis (DEA) approach. *Appl Energy* 2011;88(11):3765-3772.

Nassiria SM, Singh S. Study on energy use efficiency for paddy crop using data envelopment analysis (DEA) technique. *Appl Energy* 2009;86(7-8):1320-1325.

Neelis M, Ramirez A, Patel M, Farla J, Boonekamp P, Blok K. Energy efficiency developments in the Dutch energy-intensive manufacturing industry. *Energy Policy* 2007;35:6112-6131.

Oda J, Akimoto K, Tomoda T, Nagashima M, Wada K, Sano F. International comparisons of energy efficiency in power, steel and cement industries. *Energy Policy* 2012;44,118-129.

Perez-Reyes R, Tovar B. Measuring efficiency and productivity change (PTF) in the Peruvian electricity distribution companies after reform. *Energy Policy* 2009;37(6):2249-2261.

Ramanathan R. A holistic approach to compare energy efficiencies of different transport modes. *Energy Policy* 2000;28(11):743-747.

Ray SC. Data Envelopment Analysis theory and techniques for economics and operations research. *Manage. Sci.* 2004;42:1180.

Saber Saati Adel Hatami-Marbini Madjid Tavana A data envelopment analysis model with discretionary and non-discretionary factors in fuzzy environments. *Int. J. Productivity and Quality Management* 2011;8(1)

Saygin D, Worrell E, Patel MK, Gielen DJ. Benchmarking the energy use of energy-intensive industries in industrialized and in developing countries. *Energy* 2011;36:6661–6673.

Seiford LM., Zhu J. Sensitivity analysis of DEA models for simultaneous changes in all the data. *Journal of the Operational Research Society* 1998a;49:1060–1071.

Seiford LM, Zhu J. Stability regions for maintaining efficiency in data envelopment analysis. *European Journal of Operational Research* 1998b;108:127–139.

Seiford LM, Zhu J. Infeasibility of super-efficiency data envelopment analysis models. *INFOR* 1999;37:174–187.

Siitonen S, Tuomaala M, Ahtila P. Variables affecting energy efficiency and CO₂ emissions in the steel industry. *Energy Policy* 2010;38:2477–2485.

Smith AR, Klosek JA. Review of air separation technologies and their integration with energy conversion processes. *Fuel Processing Technology* 2001;70(2):115-134.

Sueyoshi T, Yuan Y, Goto M. A literature study for DEA applied to energy and environment. *Energy Economics* 2017;62: 104-24.

Sueyoshi T, Goto M. DEA radial measurement for environmental assessment: A comparative study between Japanese chemical and pharmaceutical firms. *Appl Energy* 2014;115:502-513.

U.S. Energy Information Administration (EIA). World petroleum and other liquid fuels. *International Energy Outlook* 2014.

Wang ZH, Zeng HL, Wei YM, Zhang YX. Regional total factor energy efficiency: an empirical analysis of industrial sector in China. *Appl Energy* 2012;97:115-123.

Wang K, Wei YM. China's regional industrial energy efficiency and carbon emissions abatement costs. *Appl Energy* 2014;130:617-631.

William GL, Thomas LG. Assessing productivity with Data Envelopment Analysis. *Public Productivity Review* 1989;12(4):361-372.

Wilson PW. Detecting influential observations in data envelopment analysis. *J. Product. Anal* 1995;6:27-45.

Wu AH, Cao YY, Liu B. Energy efficiency evaluation for regions in China: an application of DEA and Malmquist indices. *Energy Effic* 2014;7:429-39.

Yan L, Yu Y, Li Y, Zhang Z. Energy saving opportunities in an air separation process. In: 12th international symposium on process systems engineering and 25th European symposium on computer aided process engineering; 2010.

Zhanga N, Wei X. Dynamic total factor carbon emissions performance changes in the Chinese transportation industry. *Appl Energy* 2015;146:409-420.

Zhou P, Ang BW. Linear programming models for measuring economy-wide energy efficiency performance. *Energy Policy* 2008;36:2911-2916.

Zhu J. Super-efficiency and DEA sensitivity analysis. *European Journal of Operational Research* 2001;129:443-455.

Chapter 4. Appendix

UNIVERSITAT ROVIRA I VIRGILI
MULTIPERIOD MODELLING PLANNING AND PRODUCTIVITY AND ENERGY EFFICIENT ASSESSMENT OF AN INDUSTRIAL GASES
FACILITY

David Fernández Linares

4. Appendix

4.1. Short CV

In this section is presented a brief Curriculum Vitae of the doctoral student:

Name: David Fernández Linares

Born: July 10, 1991 – Tarragona, Spain

Education

- PhD in Industrial Process Optimization, Sustainable Process Design
(February 2015 – present)
Universitat Rovira i Virgili (Tarragona, Spain)
- Master in Chemical Engineering
(September 2012 – June 2014)
Universitat Rovira i Virgili (Tarragona, Spain)
- Chemical Engineering Degree
(September 2009 – September 2012)
Universitat Rovira i Virgili (Tarragona, Spain)

Work experience

- ASU Plant Manager in Messer Ibérica de Gases S.A.U.
(January 2018 – present)
El Morell, Spain

During the course of this industrial thesis I have been promoted within the company. At the start of the thesis I was working as Production Technician in the Messer's Air Separation Unit, placed in El Morell. Then, in January 2016 I was

promoted to Plant Manager's Assistant and finally, in January 2018, I was promoted to Plant Manager of the Air Separation Unit, being the responsible of the cryogenic air separation process. Among other things, my main responsibilities are to guarantee the plant reliability and scheduling of operation; achieve all the production, efficiency, quality and safety targets; monitoring the production and energetic efficiency KPI's; draw up and review daily, monthly and annual balances and reports; support logistic staff and coordinate all the activities with bulk logistics; ensure the accomplishment of ISO's 9001, 14001, 22000, 50001; manage of the electrical energy to guarantee contract requirements; execute productivity ideas and best practices to keep plant costs down, etc.

- Plant Manager Assistant in Messer Ibérica de Gases S.A.U.
(January 2016 – January 2018)
El Morell, Spain
- Production Technician in Messer Ibérica de Gases S.A.U.
(February 2014 – January 2016)
El Morell, Spain
- Master Internship in Messer Ibérica de Gases S.A.U.
(July 2013 – February 2014)
El Morell, Spain
- Degree Internship Polymer Group Inc.
(June 2012 – September 2012)
La Selva del Camp, Spain

Awards

During the course of this thesis two important prizes have been obtained:

- 3rd price in the 14th Doctoral Day poster exhibition organized by Universitat Rovira i Virgili. (May 2017)

- Institutional Recognition Award given by Enginyers Industrials de Catalunya (EIC). (June 2016). This award was delivered to Messer Ibérica de Gases S.A.U. for its contributions in the field of energy efficiency through the contributions of this thesis which allow the development of optimization tools in the industrial gases process.

4.2. List of publications

4.2.1. Indexed journals

- D. Fernández, C. Pozo, R. Folgado, L. Jiménez, G. Guillén-Gosálbez. Productivity and energy efficiency assessment of existing industrial gases facilities via data envelopment analysis and the Malmquist index. Applied Energy 2018;212:1563-1577.
<https://doi.org/10.1016/j.apenergy.2017.12.008>. Impact Factor: 7.9. Area: Chemical Engineering, journal number 4 of 137.
- D. Fernández, C. Pozo, R. Folgado, G. Guillén-Gosálbez, L. Jiménez. Multiperiod model for the optimal production planning in the industrial gases sector. Applied Energy 2017;206:667-682.
<https://doi.org/10.1016/j.apenergy.2017.08.064>. Impact Factor: 7.9. Area: Chemical Engineering, journal number 4 of 137.

4.2.2. Other publications

- D. Fernández, C. Pozo, R. Folgado, G. Guillén-Gosálbez, L. Jiménez. Modelo matemático para optimizar la operativa de producción en un sistema de fraccionamiento de aire. Proyectos Químicos ISSN 1887 - 1992, N°1229, 46-48, 2016.
<http://www.revistapq.com/revista/reach-repsol-seguridad-crioterapia...-64056>

- D. Fernández, C. Pozo, R. Folgado, G. Guillén-Gosálbez, L. Jiménez. A multi-period model for optimal production planning in gases. *Gasworld magazine* ISSN 1755-3857 p.38-39 August 2016.
<https://www.gasworld.com/a-multi-period-model-for-production-planning/2010813.article>
- D. Fernández, C. Pozo, R. Folgado, G. Guillén-Gosálbez, L. Jiménez. Modelo matemático para optimizar la operativa de producción en un sistema de fraccionamiento del aire. *Energética XXI* N° 157, 76-77, Abril-Mayo 2016.
<http://www.energetica21.com/revistas-digitales/abril-mayo-2016>

4.3. Conferences

4.3.1. Oral communications

- D. Fernández, C. Pozo, R. Folgado, G. Guillén-Gosálbez, L. Jiménez. Data Envelopment Analysis in Air Separation Units. *Plant Manager Meeting 2018*. April 2018. Wien (Austria).
- D. Fernández, C. Pozo, R. Folgado, G. Guillén-Gosálbez, L. Jiménez. Multiperiod model for the optimal production planning for technical gases World Sustainable Energy Days 2017. March 2017. Wels (Austria).
- D. Fernández, C. Pozo, R. Folgado, G. Guillén-Gosálbez, L. Jiménez. Optimization Model for Production Planning in Messer Iberica. *Plant Manager Meeting 2016*. October 2016. París (France).

4.3.2. Poster presentations

- D. Fernández, C. Pozo, R. Folgado, G. Guillén-Gosálbez, L. Jiménez. Evaluation of the Efficiency in a Set of Air Separation Units through Data Envelopment Analysis and Malmquist Productivity Index. *2017 AIChE Annual Meeting*. November 2017. Minneapolis (USA).

- D. Fernández, C. Pozo, R. Folgado, G. Guillén-Gosálbez, L. Jiménez. Multiperiod and multiproduct model for the optimal production planning in the gases sector: application to an industrial case study. *10th World Congress of Chemical Engineering*. October 2017. Barcelona (Spain).

UNIVERSITAT ROVIRA I VIRGILI
MULTIPERIOD MODELLING PLANNING AND PRODUCTIVITY AND ENERGY EFFICIENT ASSESSMENT OF AN INDUSTRIAL GASES
FACILITY

David Fernández Linares

UNIVERSITAT ROVIRA I VIRGILI
MULTIPERIOD MODELLING PLANNING AND PRODUCTIVITY AND ENERGY EFFICIENT ASSESSMENT OF AN INDUSTRIAL GASES
FACILITY

David Fernández Linares

UNIVERSITAT ROVIRA I VIRGILI
MULTIPERIOD MODELLING PLANNING AND PRODUCTIVITY AND ENERGY EFFICIENT ASSESSMENT OF AN INDUSTRIAL GASES
FACILITY

David Fernández Linares



UNIVERSITAT
ROVIRA i VIRGILI